



**Dário Jorge
Silva Neves**

**O efeito de acumulação de piruvato em
transaminações com levedura**

**The effect of pyruvate accumulation on whole yeast
cell transamination**



**Dário Jorge
Silva Neves**

**O efeito de acumulação de piruvato em
transaminações com levedura**

**The effect of pyruvate accumulation on whole yeast
cell transamination**

Dissertação apresentada à Universidade de Aveiro para cumprimento dos requisitos necessários à obtenção do grau de Mestre em Biotecnologia, ramo Biotecnologia Molecular (2º Ciclo), realizada sob a orientação científica da Doutora Marie Gorwa-Grauslund, Professora na Divisão de Microbiologia Aplicada da Universidade de Lund, Suécia, e da Doutora Ana Maria Rebelo Barreto Xavier, Professora Auxiliar do Departamento de Química da Universidade de Aveiro, Portugal.

Thesis presented to University of Aveiro to fulfill the requirements for the degree of MSc in Biotechnology, specialization in Molecular Biotechnology, made under scientific guidance of Professor Marie Gorwa-Grauslund, Professor at the division of Applied Microbiology of Lund University, Sweden, and Professor Ana Maria Rebelo Barreto Xavier, Auxiliar Professor at Chemistry Department of Aveiro University, Portugal.

Dedico este trabalho aos meus pais e irmã tal como aos meus amigos por terem sido
fulcrais durante todo o meu percurso académico.

I dedicate this work to my parents and sister and also to my friends for being crucial
during my academic route.

O júri

Professor José António Lopes da Silva

Professor Auxiliar do Departamento de Química da Universidade da Universidade, Portugal

Doutora Marie Gorwa-Grauslund

Professora na Divisão de Microbiologia Aplicada da Universidade de Lund, Suécia

Doutora Ana Maria Rebelo Barreto Xavier

Professora Auxiliar do Departamento de Química da Universidade de Aveiro, Portugal

Doutora Ana Catarina Gomes

Investigadora Principal no Biocant – Associação de Transferência de Tecnologia, Portugal

Agradecimentos

Agradeço à Professora Doutora Marie Gorwa-Grauslund por me ter aceite no seu grupo de investigação, pela orientação científica, pela disponibilidade e todo o conhecimento que me transmitiu durante a realização do projecto de investigação.

Agradeço à Professora Doutora Ana Xavier pela disponibilidade e constante comunicação durante a finalização do projecto de investigação.

Agradeço à aluna de doutoramento Nora Weber pela sua orientação laboratorial, amizade e pelas discussões interessantes durante o desenvolvimento do projecto.

Agradeço ao investigador de pós-doc Magnus Carlquist pela sua orientação e pelas suas intervenções objectivas.

Agradeço especialmente aos meus pais e irmã pelo apoio, carinho, incentivo e força que transmitiram durante esta experiência em Lund.

Agradeço à Marita Weiss pela sua amizade como colega de residência e pelo seu incentivo, ajuda e paciência durante a realização deste projecto.

Agradeço aos alunos de doutoramento Diogo Nunes e Alejandro Muñoz pela amizade, dicas e companhia no laboratório.

palavras-chave

Omega-transaminase, *Saccharomyces cerevisiae*, piruvato, piruvato descarboxilase, feniletilamina, tiamina

resumo

O interesse na biocatálise para a síntese de aminas quirais tem aumentado durante a última década. Tal interesse deve-se ao seu potencial para síntese de fármacos cardiovasculares, anti-hipertensivos e antieméticos tal como para a síntese de ácidos carboxílicos opticamente puros.

Dois métodos têm sido reportados para a síntese de aminas quirais por ómega-transaminases: a síntese assimétrica e a resolução cinética. Durante a resolução cinética o piruvato é consumido como aceitador de amina e convertido em L-alanina. A acumulação de piruvato da via glicolítica pode fazer-se por Engenharia metabólica, originando o aumento da velocidade da reacção para a formação da respectiva cetona.

Piruvato descarboxilase (PDC) é a enzima responsável pela conversão de piruvato em acetaldeído que por sua vez é o precursor do etanol. Estudos anteriores mostram que a acumulação de piruvato é superior através da inibição ou deleção da PDC. Seguiram-se duas abordagens para inibir a PDC sendo uma a deleção de dois genes estruturais, *PDC1* e *PDC5*, e a outra a deleção do gene *THI2* que é responsável pela síntese do co-factor da PDC, tiamina.

Neste trabalho a ω -transaminase de *Capsicum chinense* foi expressa em estirpes de *S. cerevisiae* manipuladas metabolicamente, para acumulação de piruvato, de forma a melhorar a resolução cinética de uma mistura racémica de *R,S*-feniletilamina (*R,S*-PEA). Ambas as estirpes foram construídas com sucesso e confirmadas por PCR e comportamentos fenotípicos. Porém, apenas a estirpe com a deleção de *THI2* foi isolada e mantida em glicerol com sucesso. A concentração de tiamina durante a cultura pré-fermentativa demonstrou ser crucial para a acumulação de piruvato durante as fermentações. A concentração mínima de tiamina, de forma a obter um bom rácio entre obtenção de biomassa e acumulação de piruvato foi de 0.05 μ M. Realizaram-se fermentações anaeróbicas e aeróbicas em meio Verduyn, contendo 20 g/L e 50 g/L de glucose, para confirmar o fenótipo de acumulação de piruvato e para verificar o efeito da concentração de tiamina. A acumulação máxima de piruvato atingida em meio Verduyn foi de 1.31 g/L. A acumulação de piruvato aumentou 5,7 vezes em comparação a estirpe controlo durante fermentações anaeróbicas contendo células obtidas em meio com a concentração mínima de tiamina. Após confirmação do fenótipo desejado, realizaram-se fermentações anaeróbicas e aeróbicas e verificou-se a resolução cinética de *R,S*-PEA em tampão fosfato. O fenótipo de acumulação de piruvato também foi observado em tampão fosfato, contudo, a resolução cinética não foi afetada possivelmente por uma concentração inicial de aminas demasiado baixa.

keywords

ω -transaminase, *Saccharomyces cerevisiae*, pyruvate, pyruvate decarboxylase, phenylethylamine, thiamine

abstract

The interest in biocatalytic approaches for the synthesis of chiral amines has increased during the last decades due to their potential in the synthesis of cardiovascular, antihypertensive and antiemetic drugs and for the preparation of optically pure carboxylic acids.

Two methods have been reported for the synthesis of chiral amines by ω -transaminases: asymmetric synthesis and kinetic resolution. During kinetic resolution pyruvate is required as amine acceptor and is further converted into L-alanine.

Pyruvate is the end metabolite of the glycolytic pathway. In *Saccharomyces cerevisiae*, pyruvate is further catabolized using either pyruvate decarboxylase (PDC) that converts pyruvate into acetaldehyde that is the precursor of ethanol or via pyruvate dehydrogenase (PDH). The inhibition or deletion of PDC has been reported to promote pyruvate accumulation. In the present study, two approaches were followed to decrease the PDC activity: (i) deleting the major structural encoding genes, *PDC1* and *PDC5*, or (ii) deleting *THI2* which encodes the enzyme responsible for the synthesis of PDC's co-factor thiamine. Both strategies were attempted in a *S. cerevisiae* strain carrying the ω -transaminase from *Capsicum chinense* for the kinetic resolution of a *R,S*-phenylethylamine racemate (*R,S*-PEA). The desired strains were successfully constructed and confirmed through PCR and phenotypic behaviors. However, only the *THI2* deleted strain expressing the heterologous ω -transaminase was successfully isolated. The thiamine concentration during growth prior to fermentation was crucial for the pyruvate accumulation during the fermentations. The minimal thiamine concentration to achieve a good ratio between pre-growth and pyruvate accumulation was 0.05 μ M. Anaerobic fermentations and aerobic cultivations were performed in Verduyn medium to confirm the pyruvate accumulative phenotype and screen the thiamine concentration effect with 20 g/L and 50 g/L of glucose. The maximum pyruvate titer of 1.31 g/L was achieved. The pyruvate titer was improved 5.7 when compared to the control strain during anaerobic fermentations in Verduyn medium. After confirmation of the desired phenotype, kinetic resolution of *R,S*-PEA was performed in phosphate buffer under anaerobic and aerobic conditions. Despite increased pyruvate accumulation, the kinetic resolution was not improved possibly due to a low initial amine concentration. The reasons for such assumption are related with similar ethanol titers observed in kinetic resolution reactions and pyruvate accumulation fermentations and also the residual pyruvate accumulation during kinetic resolution reactions.

Contents

Abstract (Portuguese Version)	vi
Abstract (English Version).....	vii
Contents	viii
Figures index	xi
Table index	xvi
Abbreviations index.....	xviii
1. Introduction.....	1
1.1. Whole cell biocatalysts	1
1.2. <i>Saccharomyces cerevisiae</i> as whole cell biocatalyst	3
1.2.1. <i>Saccharomyces cerevisiae</i> background strain- CEN.PK 2	5
1.3. <i>Saccharomyces cerevisiae</i> central metabolism.....	7
1.3.1. Pyruvate accumulation and its industrial interest.....	9
1.4. Production of Chiral Compounds	13
1.4.1. Chiral amines and ω -Transaminases.....	14
1.5. Aims and Objectives	19
2. Material and Methods	21
2.1. Microorganisms and Maintenance	21
2.2. Media and Stock Solutions	22
2.2.1. Culture Media	22
2.2.2. Defined Media.....	22
2.2.3. Buffers.....	23
2.2.4. Transamination Solution	24
2.3. Strain Construction	24
2.3.1. Deletion fragments	25
2.3.2. Overlap Extension PCR	26

2.3.3.	Yeast Transformation.....	27
2.3.4.	Deletion confirmation	27
2.4.	Fermentations/ Cultivations	29
2.4.1.	Aerobic Cultivation for pyruvate accumulation.....	29
2.4.2.	Anaerobic fermentation for pyruvate accumulation	30
2.5.	Dry Weight measurements and OD _{620nm} /Cell dry weight calibration curve	30
2.6.	Transamination biocatalysis	31
2.6.1.	Amine and ketone extraction for HPLC analysis.....	31
2.7.	HPLC analysis	31
2.7.1.	Metabolites and substrates	31
2.7.2.	Transamination products and substrates	32
3.	Results	33
3.1.	Engineering of yeast strains for pyruvate accumulation.....	33
3.1.1.	Construction of the deletion fragments	34
3.1.2.	Construction of the integration cassettes for gene deletion	34
3.1.3.	Transformation of yeast and strain confirmation	35
3.2.	Assessment of the strain carrying a deletion of <i>THI2</i> gene	40
3.2.1.	Pyruvate accumulation during growth	40
3.2.2.	Pyruvate accumulation during incubation in phosphate buffer	43
3.3.	Transamination using the <i>thi2</i> deleted strain	50
3.3.1.	Anaerobic transamination	50
3.3.2.	Aerobic transamination	52
4.	Discussion.....	54
4.1.	Strain confirmation and selection	54
4.1.1.	Construction of the Δ <i>thi2</i> deleted strain	54
4.1.2.	Construction of Δ <i>pdc1</i> Δ <i>pdc5</i> double deleted strain	55

4.2. Pyruvate Accumulation with CEN.PK2-1C+PAMT Δ THI2	59
4.2.1. Pyruvate accumulation in Verduyn media	59
4.2.2. Pyruvate accumulation in phosphate buffer	61
4.3. Pyruvate accumulation effect in kinetic resolution of amines	63
5. Conclusions	67
6. Future Work	69
7. References	70
8. Appendix	77
I- PCR Programs	77
II- DNA sequences of PDC1, PDC5 and THI2 from CEN.PK 113-7D	79
III- DNA sequences of Up- and Downstream of PDC1, PDC5 and THI2 in CEN.PK 113-7D	81
IV- DNA sequences of auxotrophic marker	82
V- Primer list	83
VI- OD _{620nm} /Cell Dry weight regression curve	84
VII- Fermentations/Cultivations profiles	85

Figures index

Figure 1- Yeast central carbon metabolism.	8
Figure 2- Thiamine metabolism and THI regulatory system in <i>S. cerevisiae</i> . A) PDC thiamine dependence; B) thiamine metabolism in yeast; C) hypothetical model of THI regulatory system in yeast. From <i>Xu et al [69]</i>	10
Figure 3- Hexose transporters repression signalling pathway. From <i>Gancedo [74]</i>	12
Figure 4- Annual distribution of worldwide approved drugs according to chirality character (Adapted from [77])	13
Figure 5- Asymmetric hydrogenation of a Schiff base for chiral amines synthesis.	14
Figure 6- Thermodynamic favored ω -transaminases reaction (Adapted from [85, 89]).	15
Figure 7- A. Kinetic resolution and B. asymmetric synthesis of chiral amines catalyzed by ω -transaminases.	17
Figure 8- Pyruvate accumulation approaches and their expected metabolic effect.	20
Figure 9- Primer location in the final constructs. The uncolored arrows represent the primers used for amplification of each deletion fragment. The marker sequences were amplified to include the respective promoter and terminator.	25
Figure 10- Example of homology between pairs of primers (sequence alignment was performed in Clustal Omega).....	26
Figure 11- PCR fragments for $\Delta pdc1$ strain confirmation. The PCR confirmation of each deletion was performed by amplifying two fragments: a) one that included the downstream and marker sequence, which means that only clones containing the deletion could possess this amplification; b) a second that would amplify the complete <i>PDC1</i> gene, which means that clones with the deletion would amplify a fragment with different size than the control strain since the control possessed a intact <i>PDC1</i> gene and the deleted strain would amplify a fragment containing the marker sequence.	28

- Figure 12- Scheme of overall deletion cassette construction. 33
- Figure 13- Deletion fragments amplified from genomic DNA. Fragments containing ‘_ds’, represent the downstream region of the respective gene. Fragments containing ‘_us’, represent the upstream region of the respective gene. Fragments containing ‘_trp1’ or ‘_ura3’, represent the auxotrophic marker sequence flanked by homology regions for the up and downstream region of the respective gene. The expected band size is below each band and was confirmed by comparison with the ladder. 34
- Figure 14- Gel purified deletion cassettes. *PDC1_trp1c*, *PDC5_ura3c* and *THI2_trp1c* represents the final deletion cassette for the, respectively, *PDC1*, *PDC5* and *THI2* gene. The expected band size of each cassette is below each band and was confirmed by comparison with the ladder. 35
- Figure 15- Deletion confirmation of *PDC1* in selected colonies by amplifying *PDC1_trp1* and *WPDC1* fragments. The ‘Neg’ lanes represent the amplification of the deletion confirmation fragments from genomic DNA of the control strain, whereas the ‘Pos’ lanes represent the amplification of the deletion cassettes. Successful transformed clones represent bands with the same size as the positive amplifications. 36
- Figure 16- Deletion confirmation of *PDC5* in selected colonies by amplifying *PDC5_ura3* and *WPDC5* fragments. The ‘Neg’ lanes represent the amplification of the deletion confirmation fragments from genomic DNA of the control strain, whereas the ‘Pos’ lanes represent the amplification of the deletion cassettes. Successful transformed colonies represent bands with the same size as the positive amplifications. 37
- Figure 17- Amplification of *PDC1_trp1* and *WPDC1* fragments from glycerol stocked strain. The Neg lanes represent the amplification of the deletion confirmation fragments from genomic DNA of the control strain, whereas the Pos lanes represent the amplification of the deletion cassettes. Successful transformed colonies represent bands with the same size as the positive amplifications. Successful transformed clones represent bands with the same size as the positive amplifications. 38

Figure 18- Confirmation of desired genotype through amplification of *THI2_trp1* from CEN.PK2-1C+PAMT $\Delta thi2$ clone 34 genomic DNA. The ‘Neg’ lane represents the amplification of the deletion confirmation fragments from genomic DNA of the control strain, whereas the ‘Pos’ lane represents the amplification of the deletion cassette. Genomic DNA of *thi2* deleted clone 34 was extracted and *THI2_trp1* fragment was amplified. The amplified band possessed the same size as the positive control. 39

Figure 19- Anaerobic fermentation of CEN.PK2-1C+PAMT $\Delta thi2$ clone 34 and its control in Verduyn medium pre grown in 3.32 μ M thiamine. 41

Figure 20- Anaerobic fermentation of CEN.PK2-1C+PAMT $\Delta thi2$ clone 34 and control in Verduyn medium pre grown in 0.05 μ M thiamine. 41

Figure 21- Aerobic cultivation of CEN.PK2-1C+PAMT $\Delta thi2$ clone 34 and its control in Verduyn medium pre grown in 3.32 μ M thiamine. 42

Figure 22- Aerobic cultivation of CEN.PK2-1C+PAMT $\Delta thi2$ clone 34 and its control in Verduyn medium pre grown in 0.05 μ M thiamine. 42

Figure 23- First experiment of CEN.PK2-1C+PAMT $\Delta thi2$ 34 aerobic cultivation in phosphate buffer containing 50 g/L glucose. 45

Figure 24- Representative aerobic pyruvate accumulation of CEN.PK2-1C+PAMT $\Delta thi2$ in phosphate buffer containing 20 g/L glucose 45

Figure 25- Representative aerobic pyruvate accumulation of CEN.PK2-1C+PAMT $\Delta thi2$ in phosphate buffer containing 50 g/L glucose 45

Figure 26- Comparison of pyruvate titers achieved during aerobic pyruvate accumulation in Verduyn medium and phosphate buffer. The * represent the unreliable pyruvate titer result of the control strain in phosphate buffer containing 20 g/L due to HPLC analysis issues. 47

Figure 27- Representative anaerobic pyruvate accumulation of CEN.PK2-1C+PAMT $\Delta thi2$ clone 34 and its control in phosphate buffer containing 20 g/L glucose. 47

Figure 28- Representative anaerobic pyruvate accumulation of CEN.PK2-1C+PAMT $\Delta thi2$ clone 34 and its control in phosphate buffer containing 50 g/L glucose.	48
Figure 29- Comparison of pyruvate titers during anaerobic fermentations in Verduyn and phosphate buffer for the control strain and <i>thi2</i> deleted clone 34. The grey bars represent the second experiments in which the pre-growth duration was optimized as described in 3.2.2.	49
Figure 30-Representative anaerobic kinetic resolution of <i>R,S</i> -PEA with CEN.PK2-1C+PAMT $\Delta thi2$ clone 34 and its control strain in phosphate buffer containing 20 g/L glucose. Cells were pre-grown in Verduyn medium containing 20 g/L of glucose and 0.05 μ M thiamine.	50
Figure 31- Representative anaerobic kinetic resolution of <i>R,S</i> -PEA with CEN.PK2-1C+PAMT $\Delta thi2$ 34 in phosphate buffer containing 50 g/L glucose. Cells were pre-grown in Verduyn medium containing 20 g/L of glucose and 0.05 μ M thiamine.	51
Figure 32- Aerobic kinetic resolution of <i>R,S</i> -PEA with CEN.PK2-1C+PAMT $\Delta thi2$ 34 in phosphate buffer containing 20 g/L glucose.	52
Figure 33- Aerobic kinetic resolution of <i>R,S</i> -PEA with CEN.PK2-1C+PAMT $\Delta thi2$ 34 in phosphate buffer containing 50 g/L glucose.	52
Figure 36- Possible mechanism for false positive colonies in Δ PDG strains. The high similarity between the marker sequence of the deletion cassette and the disrupted marker of the strain allows the homologous recombination between the two marker sequence and restore the expression of the amino acid biosynthetic gene.	56
Figure 35- Aerobic cultivation of Δ THI2 colonies in Verduyn medium pre-grown in medium containing 3,32 μ M thiamine.	85
Figure 36- Anaerobic fermentation of Δ THI2 colonies in Verduyn medium pre-grown in medium containing 3,32 μ M thiamine.	85
Figure 37- Aerobic cultivation of Δ THI2 colonies in Verduyn medium pre-grown in medium containing 0,05 μ M of thiamine.	86

Figure 38- Anaerobic fermentation of Δ THI2 colonies in Verduyn medium pre-grown in medium containing 0,05 μ M of thiamine. 86

Table index

Table 1- Features of the perfect yeast cell factory strain (from <i>van Dijken et al</i> [39])	5
Table 2- Reported pyruvate accumulation approaches. The theoretical maximal pyruvate yield (g pyruvate/ g glucose) is 0.98 g/g.	9
Table 3- Asymmetric synthesis and Kinetic resolution of chiral amines.	18
Table 4- Strains used and constructed in the present study	21
Table 5- Yeast Extract Peptone Dextrose[99]	22
Table 6- Yeast Nitrogen Base (aminoacids concentration followed by Pronk[100])	22
Table 7- Verduyn Mineral Medium [101]	23
Table 8- Verduyn Salt Solution	23
Table 9- YNB Buffer	24
Table 10- Transamination Solution	24
Table 11- Primer list for final amplification of the fragments obtained through Overlap Extension PCR	26
Table 12- PDC1_trp1, PDC5_ura3 and THI2_trp1 deletion confirmation fragments primer set. Each primer set is composed by an end primer of the downstream sequence and a primer located at the junction of the marker and upstream sequence.	27
Table 13- Medium for pre- fermentation growth	29
Table 14- Pyruvate titer and yield (g pyruvate/g glucose) for CEN.PK2-1C+PAMT Δ thi2 construct and its control in Verduyn medium, as a function of thiamine concentration during pre-cultivation. The theoretical maximal pyruvate yield (g pyruvate/ g glucose) is 0.98 g/g.	42
Table 15- Pyruvate titers and yields obtained in phosphate buffer containing 20 g/L or 50 g/L of glucose under aerobic conditions. Pyruvate accumulation results in 20 g/L of glucose with the control strain were unreliable due to issues in HPLC analysis. The theoretical maximal pyruvate yield (g pyruvate/ g glucose) is 0.98 g/g.	46
Table 16- Pyruvate titers and yields obtained in phosphate buffer containing 20 g/L or 50 g/L of glucose under anaerobic incubations. Control 1 and Δ THI2 1	

columns represent the first experiment whereas Control 2 and $\Delta THI2$ 2 columns represent the second experiment in which pre-growth duration was optimized as described in 3.2.2. The theoretical maximal pyruvate yield (g pyruvate/ g glucose) is 0.98 g/g. 48

Table 17- Ethanol titers and yields obtained in phosphate buffer containing 20 g/L or 50 g/L of glucose under anaerobic incubations. Control 1 and $\Delta THI2$ 1 columns represent the first experiment whereas Control 2 and $\Delta THI2$ 2 columns represent the second experiment in which pre-growth duration was optimized as described in 3.2.2. The theoretical maximal ethanol yield (g ethanol/ g glucose) is 0.51 g/g. 48

Table 18- Anaerobic transamination, comparison of conversion and enantiomeric excess in phosphate buffer containing 20 or 50 g/L of glucose. Control 1 and $\Delta THI2$ 1 columns represent the first experiment whereas Control 2 and $\Delta THI2$ 2 columns represent the second experiment in which pre-growth duration was optimized as described in 3.2.2. 51

Table 19- Aerobic transamination, comparison of conversion and enantiomeric excess in phosphate buffer containing 20 or 50 g/L of glucose. In this table only the second experiment results were presented since during the first experiment no transamination reaction was observed. 53

Abbreviations index

ADH1- gene encoding alcohol dehydrogenase 1

CC- ω TA- putative aminotransferase from *Capsicum chinense*

HIS3- gene encoding imidazoleglycerol-phosphate dehydratase

LEU2- gene encoding β -isopropylmalate dehydrogenase

NAD⁺/NADH- nicotinamide adenine dinucleotide oxidized/reduced

NADP⁺/NADPH- nicotinamide adenine dinucleotide phosphate oxidized/reduced

PDC- gene encoding pyruvate decarboxylase

PDH- gene encoding pyruvate dehydrogenase

PYC- gene encoding pyruvate carboxylase

PLP- pyridoxal-5'-phosphate

PMP- pyridoxamine-5'-phosphate

R,S-PEA- kinetic R,S-phenylethylamine

SUC2- gene encoding invertase

THI2- thiamine biosynthetic gene

TRP1- gene encoding phosphoribosylanthranilate isomerase

URA3- gene encoding orotidine 5-phosphate decarboxylase

YNB- yeast nitrogen base

YPD- yeast extract peptone dextrose

1. Introduction

1.1. Whole cell biocatalysts

The application of cells as biocatalysts started in the ancient Egypt (3100 to 332 B.C.) through the production of beer and bread [1]. However, the discovery of microorganisms, and specially yeast as the responsible agent for fermentation, only occurred 200 years ago by Antoine Lavoisier, pioneer in fermentation research [2].

Whole cell biocatalysts have advantages over systems with purified enzymes, such as the availability of co-factors and their regeneration through metabolic pathways as well as the use of cheap carbon sources as co-substrates. Whole cell biocatalysis also provides a natural intracellular environment for the enzymes which results in higher activities due to higher stability. Additionally, whole cell biocatalysis avoids expensive protein purification, reducing the overall cost [3]. However, whole cell biocatalysis holds also drawbacks such as mass transfer problems of substrates from the media to the cytoplasm. This results in lower reactions rates since the substrates have to pass through the cell membrane [4]. Low reaction yields constitute another limitation for whole cell biocatalysis. Since cells harbor several enzymes with overlapping substrate specificity, the number of undesired side reactions can be higher, leading to lower yields. Also the need for sterile conditions and scale-up problems are major challenges for the development of successful industrial whole cell biocatalysis processes.

The use of microorganisms as biocatalysts can be divided into two categories, fermentation and bioconversion. Fermentation starts with inexpensive carbon and nitrogen sources through which natural products are obtained as a result of the microorganism's complex metabolism. Bioconversion is described as a one or few step conversion of a complex substrate that does not require living cells [5].

Improvement of whole cell biocatalysis was attempted after microorganisms were recognized to be responsible for fermentation by Buchner in 1907 [6]. In the early stage of fermentation technology such attempts consisted mainly in manipulating the process conditions such as temperature, pH, oxygen and substrates concentrations. Improving biocatalysis by manipulating the microorganism began in 1930 with the discovery that microorganisms can be mutated through physical and chemical treatments [7]. Strains with

the ability to achieve higher yields, growth rate and tolerance to lower oxygen concentration were obtained. Due to lack of technology and genetic knowledge, such attempts consisted mainly in random mutagenesis followed by the screening of the best mutant. Development of genetic engineering began in 1970's due to industrial interest.

The increased knowledge about genetics, metabolic pathways and expression of heterologous enzymes led to the publication of genome databases and allowed the development of a new approach for strain improvement termed metabolic engineering. One of the first reviews about this research field was published by Bailey in 1991 [8]. At that time, metabolic engineering was described as the improvement of cellular activities through recombinant DNA technology. Metabolic engineering started as the extension or transfer of existing pathways, shifting of metabolite flows and acceleration of rate determining steps. Such outcomes were achieved mainly by expression of heterologous enzymes and deletion or overexpression of native genes. One of the first applications of metabolic engineering was the manipulation of *E. herbicola* to produce 2-keto-L-gulononic acid [9]. The traditional process consisted of two different fermentations, one with *E. herbicola* and another with a *Corynebacterium* specie. By introducing the enzyme of *Corynebacterium*, which was responsible for the last step of the process, in *E. herbicola* it was possible to obtain the same product in a single fermentation using the engineered strain [9]. However, metabolic engineering is not so simple due to intrinsic and unpredictable challenges such as appearance of new compounds, proteolysis, improperly folding, no assembly with prosthetic groups, and no suitable location for substrate access or inhibitory environments.

By comparing the early stage of metabolic engineering in the 90's with the actual status, it is possible to observe a tremendous evolution. This is mainly due to technological breakthroughs which lowered the sequencing costs contributing to the increase in genome databases, easier and more efficient genetic tools, increased knowledge about metabolic pathways and also the discovery of until then unknown regulation networks. The evolution of metabolic engineering was noticed and reviewed by Nielsen in 2001[10]. A set of tools and logical principles of the metabolic engineering approach were covered. The evolution of metabolic engineering can be related to the evolution of the several -omics (genomics, proteomics, transcriptomics and metabolomics). It is now possible to understand the metabolism and the effects of manipulations. There has been a major development after the

review of Bailey has been written, as not only deletion and expression of genes has been described, but also the manipulation of transcription levels and factors. Additionally, manipulation and selection of promoters, RNA-antisense techniques and modulation of transcription factors were identified [11, 12].

Even with the evolution of the metabolic engineering tools the principles remained the same. Such principles consist of the identification of the most probable targets, genetically construction of the corresponding strains, evaluation and characterization of the strains followed by a new round of target identification [10].

1.2. *Saccharomyces cerevisiae* as whole cell biocatalyst

Saccharomyces cerevisiae is a unicellular yeast that divides by budding and can multiply both asexually and through mating [13].

S. cerevisiae is found in nature on rotting fruit and vegetables where its preferred carbon sources, glucose and fructose, are easily accessible. It is a hypothesis that yeast produces aromatic compounds to attract wasps which thereby are used as transporters to new substrate sources [14].

S. cerevisiae is able to grow aerobically and anaerobically consuming a variety of carbon sources such as glucose, maltose, trehalose, fructose and galactose [15]. It is able to use ammonia and urea as a nitrogen source, and phosphore and sulphur are required in the growth media [16]. The doubling time is approximately 1,5-2,5 hours under its optimal growth temperature of 30°C. The main characteristic of *S. cerevisiae* is the ability to produce high titers of ethanol due to its unusual metabolism. In most eukaryotes the only factor that controls the switch from a respiratory to a fermentative metabolism is oxygen depletion [17]. However, in *S. cerevisiae* this switch also occurs when the external carbon source concentration is high [18]. *S. cerevisiae* is therefore able to produce ethanol during the first growth phase in aerobic conditions due to its respiro-fermentative behavior. Once the primary carbon source is depleted, it starts to consume the ethanol produced in the first phase. This switch is nominated diauxic shift and leads to an environmental advantage since ethanol sensitive microorganisms are inhibited once *S. cerevisiae* starts producing ethanol [19].

Saccharomyces cerevisiae is a microorganism with a lot of research, since it is non-pathogenic, inexpensive and simple to grow at a laboratorial and industrial scale. More

recently, the increasing number of sequenced genes and whole genomes [20] led to developments of bioinformatics tools and engineering techniques providing means to develop new strains of *S. cerevisiae* with desired phenotypes. *Saccharomyces cerevisiae*, as compared with other microorganisms used for biocatalysis, such as *E. coli*, presents higher robustness leading to longer glucose consumption and co-factor regeneration. This could lead to higher conversion rates compared to bacteria based biocatalysis [21].

However, there are also some drawbacks which have to be considered when using yeast as biocatalyst, for example substrates or products that are toxic to the cell, low co-substrate yield for the cofactor recycling and the existence of several enzymes with overlapping substrate specificities. Several strategies have been found to minimize such drawbacks, like substrate modification [22], different carbon sources [23], use of inhibitors [24] and biphasic systems using organic solvents or ionic liquids [25, 26].

One of the first industrial bioconversion processes in which *S. cerevisiae* was used, consisted of a biological and chemical approach where acyloin-type condensation of benzaldehyde to obtain (1R, 2S)-pseudoephedrine was developed [27]. Since then *S. cerevisiae* has been applied in several kinds of reactions, such as reduction of carbonyl bonds [28, 29] and double carbon-carbon bonds [30, 31], oxidation and racemization [32-34], hydrolase reactions [28] and formation of carbon-carbon bonds [35]. *S. cerevisiae* has also been applied for the production of functional proteins since it has the status of 'generally regarded as safe' (GRAS) assigned by the USA's Food and Drug Administration (FDA). Such proteins consist in antibody fragments and fusions [36, 37] as well as membrane protein drug targets [38].

1.2.1. *Saccharomyces cerevisiae* background strain- CEN.PK 2

Optimization of a yeast cell factory requires a multidisciplinary effort of geneticists, physiologists and biochemical engineers. To facilitate the interdisciplinary manipulations, the perfect strain would possess the features listed in Table 1.

Table 1- Features of the perfect yeast cell factory strain (from *van Dijken et al* [39])

Desired properties of a yeast laboratorial strain
Fast growth in defined mineral media without supplements other than vitamins
Wide range of carbon and nitrogen sources for growth
High biomass yield on carbon source
Fast aerobic respiratory growth in glucose-limited chemostat cultures
Growth in defined media under strictly anaerobic conditions
High sporulation efficiency, spore viability, and mating efficiency
High transformation efficiency
Genetically stable
Good production of heterologous proteins, both intra- and extracellularly

In order to find a strain family which offers an acceptable compromise between the several requirements of different research disciplines, several strains were tested focusing on standard transformation tests and cultivations under well-defined conditions [39]. The CEN.PK2 family showed during such screenings to be a strain that possesses an acceptable equilibrium between the required properties [39]. The CEN.PK2 family was constructed as part of an interdisciplinary German research project ('Stofflüsse in Mikroorganismen') by the groups of Prof. M. Ciriacy, Prof. K.-D. Entian and Dr. P. Kötter [39]. The construction of the CEN.PK2 strains began with two laboratory strains and involved a series of crosses and backcrosses. The construction of isogenic strains (same genotype which can be reproduced indefinitely) involved the introduction of the HO gene in a haploid strain which allows to induce mating type switch [40]. After loss of the plasmid, sporulation of the resulting diploid strain yielded the desired isogenic haploid strains of opposite mating types. Besides these prototrophic haploid strains and diploid strains, isogenic haploid strains with all possible combinations of the auxotrophic markers *ura3*, *his3*, *leu2* and *trp1* were constructed.

The obtained CEN.PK2 family was stored in the European *Saccharomyces cerevisiae* archive for functional analysis (EUROSCARF) [41]. One of such strains, CEN.PK2-1C is the background strain used in the present study.

CEN.PK2-1C is a haploid strain with a MATa mating type and a genotype containing the mutations *ura3-52*, *trp1-289*, *leu2-3*, *his3Δ1* and the expression of *MAL2-8^c* and *SUC2* [42]. The *ura3-52* is a non-reverting *URA3* mutation caused by a Ty insertion within the coding sequence of *URA3* gene [43]. This mutation disrupts *URA3* which encodes the orotidine 5-phosphate decarboxylase required for synthesis of pyrimidine ribonucleotides in yeast RNA and makes the strain uracil auxotrophic [44]. The *trp1-289* mutation consists of a point mutation of CAG to TAG in position 403 of the *TRP1* ORF [45]. *TRP1* encodes phosphoribosylanthranilate isomerase that catalyzes the third step of tryptophan biosynthesis [46]. A stop codon is created in the middle of the *TRP1* ORF leading to tryptophan auxotrophy. The *leu2-3* manipulation consists of several mutations such as GTC to GTT silent change at codon 56, GTT to GCT missense change at codon 69 (change from valine to alanine), G insertions at nucleotide 249 and 792 making each a frameshift, GTT to GTC silent change at codon 299 and GAC to AAC missense change modifying an aspartate to asparagine [47, 48]. *LEU2* encodes for β-isopropylmalate dehydrogenase (IMDH) which catalyzes the third step of leucine biosynthesis pathway. These mutations disrupt the activity of IMDH leading to a leucine auxotrophic strain. The *his3Δ1* manipulation consists of the 187 bp *HindIII-HindIII* internal deletion of *HIS3* [49]. *HIS3* encodes the enzyme imidazoleglycerol-phosphate dehydratase which catalyzes the sixth step in histidine biosynthesis and through its inactivation the strain becomes histidine auxotrophic [50]. The insertion of *MAL2-8^c* allows the consumption of maltose in the presence of glucose since the expression of this allele results in a constitutive and non-glucose-repressible *AGT1/MAL11* expression [51]. The insertion of *SUC2* allows the consumption of sucrose since *SUC2* encodes invertase a sucrose hydrolyzing enzyme [52].

With such genetic profile CEN.PK2-1C is a good strain to study the effect of gene deletions since it possesses mainly one copy of each gene due to its haploid nature. Also the four auxotrophic markers allow the expression/deletion of several genes without the need of marker regeneration, the use of antibiotics such as kanamycin or recombination markers like the Cre-Lox recombination technique.

1.3. *Saccharomyces cerevisiae* central metabolism

In yeast carbon metabolism, pyruvate is obtained from glucose through glycolysis. Pyruvate can be considered as the branch point in the yeast carbon metabolism because it can be redirected to different outcomes depending on the growth conditions.

The enzymes responsible for pyruvate breakdown are pyruvate dehydrogenase complex (PDH), pyruvate decarboxylase (PDC) and pyruvate carboxylase (PYC) (Figure 1) [53]. The pyruvate dehydrogenase complex is located in the mitochondrial matrix and converts pyruvate to acetyl-CoA, which is substrate of the tricarboxylic acid cycle (TCA cycle). In this pathway, a pyruvate transporter located in the inner mitochondrial membrane is required for pyruvate to be further oxidized [54]. After the oxidation of pyruvate to acetyl-CoA, the TCA cycle begins with the synthesis of citrate. Through citrate synthetase, oxaloacetate and acetyl-CoA are converted into citrate at the expense of a water molecule. Considering that oxaloacetate would only be obtained through the TCA cycle, regeneration of oxaloacetate in each turn of the cycle would be necessary. However, if oxaloacetate would only be obtained through the TCA cycle it would lead to its shortfall since TCA cycle intermediates are important biosynthetic building blocks and are withdrawn from the cycle. PYC has the assimilatory function of converting pyruvate into oxaloacetate and provide the necessary oxaloacetate to avoid such shortfall. This enzyme, such as PDH, is also located in the mitochondrial matrix [55].

Besides the PDH pathway, yeast carbon metabolism has an alternative route to obtain acetyl-CoA. This alternative pathway consists of PDC, acetaldehyde dehydrogenase and acetyl-CoA synthetase [56] where acetyl-CoA is obtained in the cytosol and can enter the TCA cycle after being transported by carnitine acetyl transferase to the mitochondrial matrix. However, the major product obtained through this pathway is ethanol, which is obtained after the reduction of acetaldehyde by the alcohol dehydrogenase 1 (ADH 1) (Figure 1). Even if this pathway is less energy efficient, this bypass is important during growth with sugars as carbon source, since cytosolic acetyl-CoA is essential for lysine and lipid synthesis [57, 58].

The carbon fluxes through these pathways are affected mainly by the presence of oxygen and by glucose concentration. Under glucose limited aerobic growth conditions, pyruvate is converted by PDH to acetyl-CoA and then completely oxidized to CO₂ (Figure 1). In the absence of oxygen, pyruvate is converted by PDC to acetaldehyde leading to the

fermentative behavior of *S. cerevisiae*. Under aerobic conditions with high glucose concentrations *S. cerevisiae* shows a respire-fermentative behavior [59]. This effect is specific to *S. cerevisiae* and termed Crabtree effect. The reason for this respiro-fermentative behavior has been reported as a selective advantage over competing organisms through ethanol production by repression of TCA cycle enzymes [60, 61] and electron chain components [62].

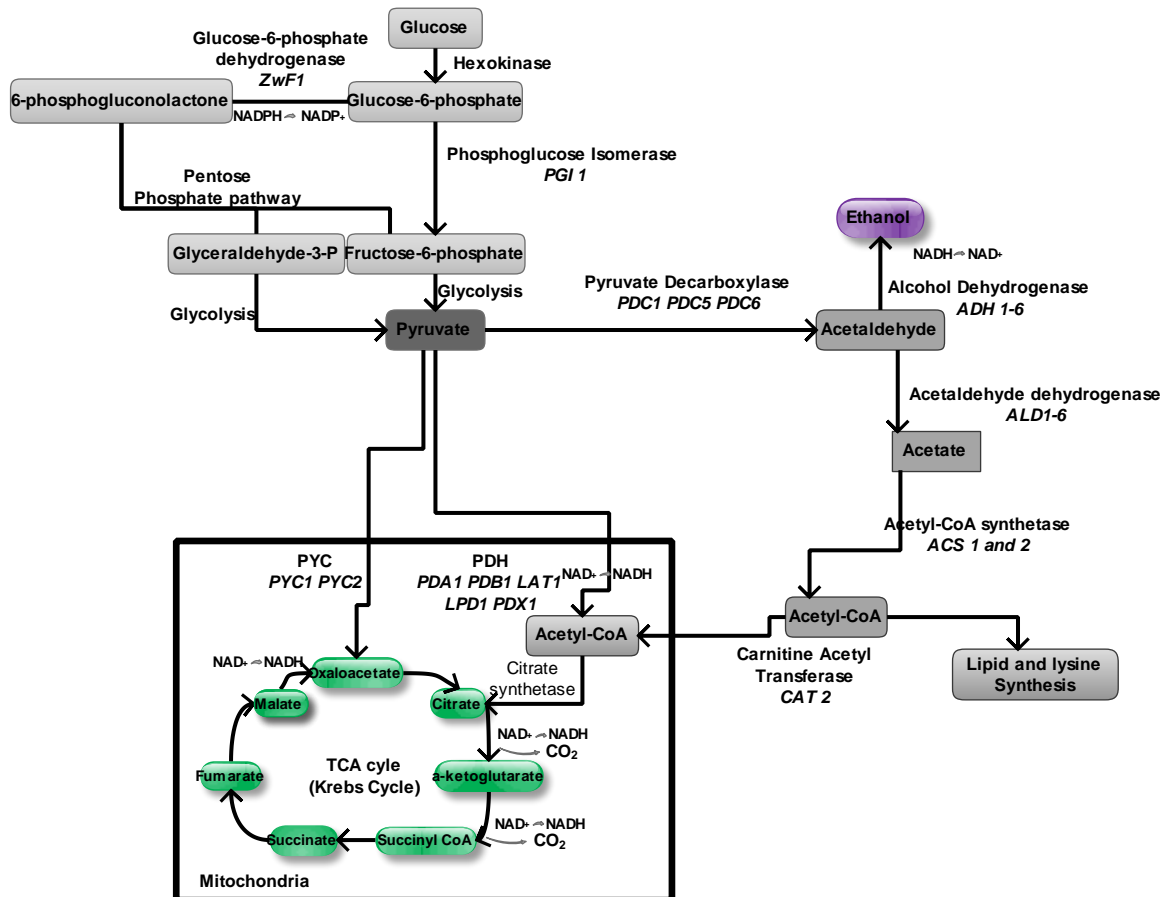


Figure 1- Yeast central carbon metabolism.

1.3.1. Pyruvate accumulation and its industrial interest

The accumulation of pyruvate in industrial processes has been studied since the late 60's [63]. Pyruvate is a precursor for drugs/agrochemicals synthesis, enzymatic production of amino acids (L-tryptophan, L-tyrosine and L-dihydro phenylalanine) and has a healthcare function as dietary supplement [64, 65].

Two strategies for pyruvate accumulation inside whole cell are higher flux through glycolysis and/or deletion of the pyruvate consuming enzymes [66]. The high fermentative potential of *S. cerevisiae* is due to the activity of PDC, which even under glucose limited conditions can consume up to 50% of the pyruvate obtained from glycolysis [67]. The inhibition of PDC is therefore the best target for pyruvate accumulation. Several approaches to inhibit PDC activity were reported and are summarized in Table 2. Pyruvate accumulation approaches can be divided into two categories: deletion of the structural genes encoding PDC or their inhibition through vitamin auxotrophy.

Table 2- Reported pyruvate accumulation approaches. The theoretical maximal pyruvate yield (g pyruvate/ g glucose) is 0.98 g/g.

Strain/Reference	Metabolic Engineering/Phenotype	Pyruvate (g/L)	Yield (g pyruvate/g glucose)	Cell Amount (OD ₆₀₀)	Obtained after (h)
<i>Torulopsis glabrata</i> [65]	Wild-type with vitamin auxotrophies	57	(Not reported)	30	59
<i>S. cerevisiae</i> [68]	ΔPDC1 ΔPDC5 ΔPDC6, selected through spontaneous mutations to grow under glucose	135	0.54	60	100
<i>Torulopsis glabrata</i> [66]	ΔPDC, pyruvate decarboxylase negative	82.2	0.55	ca 50	52
<i>S. cerevisiae</i> [69]	Δ <i>thi2</i> , thiamine biosynthetic pathway deleted and optimized C:N ratio	8.21	0.16	3.61	96

One of the first to report about pyruvate accumulation was *Yonehara et al* [65] where *Torulopsis glabrata*, a glucose repression positive yeast strain [70] auxotrophic for the vitamins thiamine, nicotinic acid, pyridoxine and biotine, was grown under specific concentrations of these vitamins in order to accumulate pyruvate. The selection of these auxotrophies is connected to their co-factor function of pyruvate consuming enzymes: 1) thiamine is a co-factor for PDC and PDH (Figure 2A), 2) nicotinic acid is a building block of the NAD⁺ co-factor for glycolytic enzymes, 3) biotin is a co-factor for PYC 4) pyridoxine is a co-factor of transaminases. The last named enzymes are not related to the

carbon metabolism but consume pyruvate as substrate. Fermentation with this strain and using 100 g/L glucose as carbon source yielded, pyruvate titer of 57 g/L after 59 hours.

The most recent development in pyruvate accumulation by vitamin auxotrophy was reported by *Xu et al* [69]. Yeast usually takes up external thiamine to synthesize ThDP, but during external privation of thiamine it is able to synthesize the co-factor *de novo* (Figure 2B). Three genes that positive regulate the synthesis and transport of thiamine were identified as *THI2*, *THI3* and *PDC2* by *Nosaka* [71]. In this work a hypothetical model of the yeast THI regulatory system was described. During thiamine starvation Thi3p, Thi2p and Pdc2p form a complex which activates the *THI* genes and results in the *de novo* thiamine synthesis. When thiamine is abundant, it binds to Thi3p inhibiting the formation of the THI activation complex (Figure 2C).

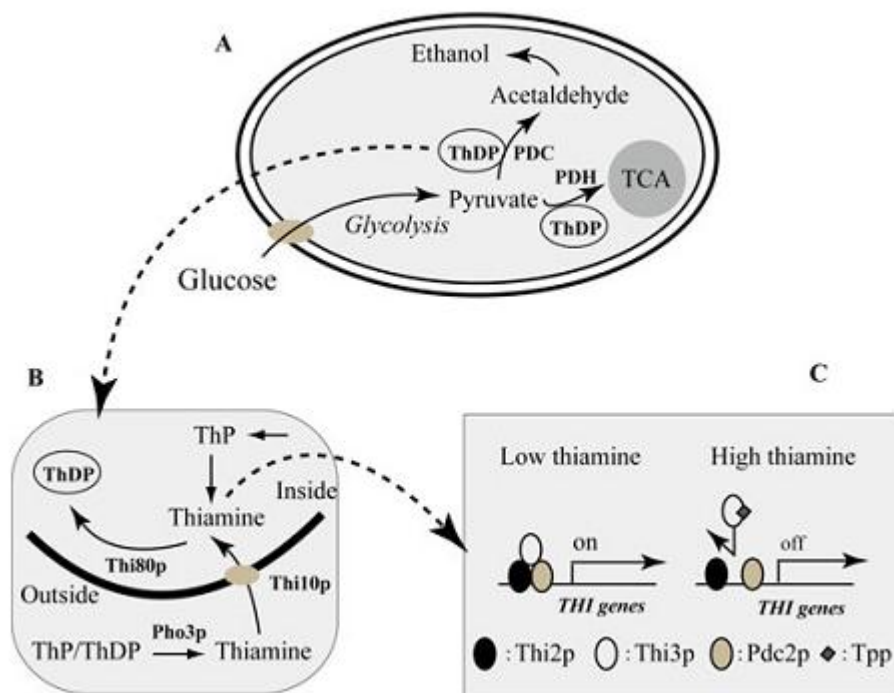


Figure 2- Thiamine metabolism and THI regulatory system in *S. cerevisiae*. A) PDC thiamine dependence; B) thiamine metabolism in yeast; C) hypothetical model of THI regulatory system in yeast. From *Xu et al* [69]

THI2 defective mutants are not able to synthesize thiamine but are fully capable of its transport. Strains with *THI3* deletion are unable to express all thiamine regulated genes, which indicates its role as a global regulator (Figure 2C). *PDC2* is not only necessary for the expression of THI genes but also for the expression of PDC structural genes (*PDC1*

and *PDC5*). In the study of *Xu et al*, it was possible to identify the best knock out mutant for pyruvate accumulation as a strain with $\Delta thi2$ deletion. The highest pyruvate titer, 8.21 g/L, was obtained after 96 hours during a batch culture in which urea and 0.04 μ M thiamine were added and C:N ratio was optimized (Table 2).

The alternative approach to accumulate pyruvate, deletion of PDC structural genes, was reported by *van Maris et al* [68]. In this work the three structural PDC genes were deleted (*PDC1*, *PDC5* and *PDC6*). As reported by *Flikweert et al* [72], the obtained strain was unable to grow under excess of glucose due to the inability to synthesize cytosolic acetyl-CoA. Another reason for such glucose sensitive phenotype is related to redox imbalances. Due to a high glycolytic activity and a limited mitochondrial respiratory chain, the reoxidation of cytosolic NAD^+ was reduced which inhibited key reactions in biosynthesis [73].

A strain without PDC genes, needs provision of C_2 carbon sources and bypass the need for PDC. To overcome this drawback an evolutionary adaptation through chemostat cultures was performed which led to the isolation of a *S. cerevisiae* C_2 independent ΔPDC control strain. Transcriptional profiling of the evolved PDC negative strain showed that the total amount of hexose transporters (HXT) was four-fold lower than the reference strain [73]. By screening possible mutations in the transcriptional regulators of HXT, a mutation in *MTH1* was identified. In the absence of glucose in wild type yeast, Mth1p forms a complex with Std1p and Rgt1p and represses the transcription of hexose transporters (Figure 3) [74]. However in the presence of glucose Mth1p/Std1p is phosphorylated and degraded, inhibiting the formation of the repression complex and thereby HXT genes are expressed and glucose is transported inside the cell.

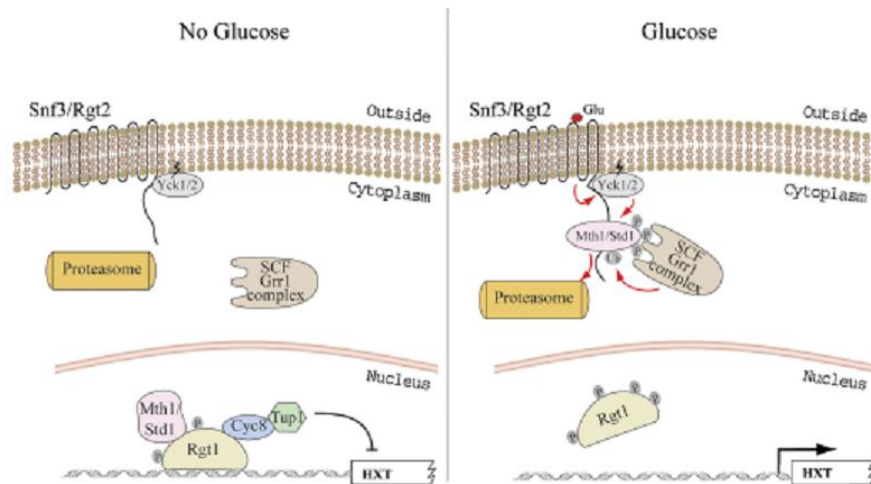


Figure 3- Hexose transporters repression signalling pathway. From *Gancedo* [74].

By mutating *MTH1* the degradation of Mth1p is decreased resulting in a lowered expression of hexose transporters. Therefore, the glycolytic activity was reduced which avoided the fast depletion of cytosolic NADH/NAD⁺ pool.

Application of the obtained strain in an aerobic batch starting with 100 g/L of glucose with two additional glucose pulses of 100 g/L, resulted in a pyruvate titer of 135 g/L. However, it is important to notice that a high amount of cells (60 OD_{660 nm}) was used during the cultivations which could explain the high pyruvate titer.

The accumulation of pyruvate through PDC deletion was also reported in *Torulopsis glabrata* by Wang et al [66]. To obtain the reported pyruvate titer of 82.2 g/L, fermentations were performed in a media containing 150 g/L glucose and 0.033 μM of thiamine. However, the need for thiamine addition in his work is unclear since the need for its addition is only during vitamin auxotrophy.

1.4. Production of Chiral Compounds

During several decades, the chirality of pharmaceutical compounds has been neglected. Pharmaceutical compounds contained a racemic mixture, which means that they consisted of equal amounts of *R* and *S* enantiomers. Enantiomers show completely identical physical and chemical properties when present in an achiral environment. However, in a chiral environment such as *in vivo*, each enantiomer possesses different chemical, biological and pharmacological behaviors. Such properties can make one enantiomer the cure for certain diseases and the other having side or no effect. Due to this, an incident occurred in the 1960s with thalidomide. This drug was sold as sleeping pill and helped pregnant women with morning sickness. However, only the *R* form acted as sedative and possessed the desired effect. The *S* form led to limb abnormalities in the newborns, such as phocomelia, dysmelia, Amelia, bone hypoplasticity and other congenital defects [75]. The discovery of such effects led to an increase in the preparation of pure enantiomers since the 1980s [76]. The worldwide market share of single-enantiomer drugs in 2002 was 39% and represented an increase of 12% since 1996. Production of pharmacological racemates decreased since the 90's because the use of enantiometric pure products allowed to reducing dosages and avoiding side effects (Figure 4) [77]. It was also reported in 2003 that the worldwide revenues from chiral production would increase from 4.8 billion dollars to 14.9 billion dollars by 2009 [78]. However the forecast was not achieved since in April 2012 a report from bcc research showed that the global chiral technology market was worth nearly 5.3 billion dollars in 2011.

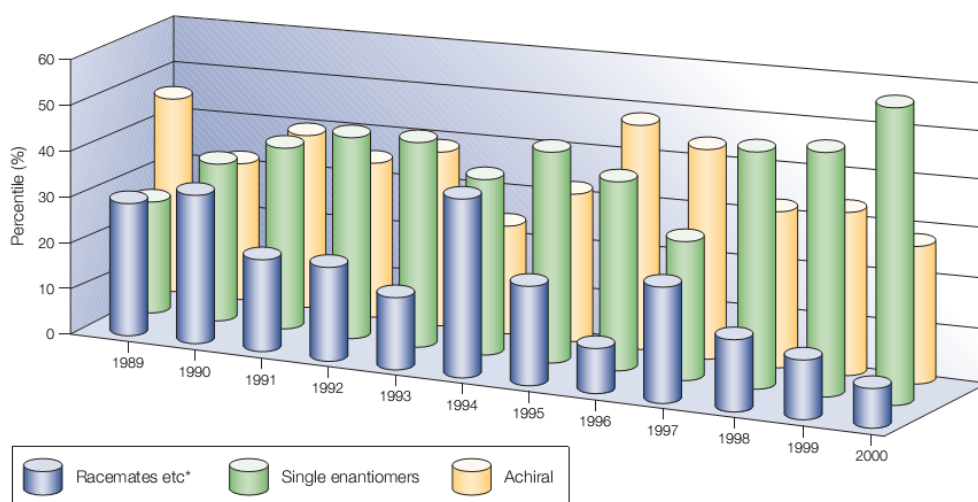


Figure 4- Annual distribution of worldwide approved drugs according to chirality character (Adapted from [77])

The most recent report on global chiral market indicates a compound annual growth rate (CAGR) of 14.2% between 2005 and 2015 [79], showing the increasing interest in developing more efficient methods to obtain pure enantiometric compounds.

In the last decade several new biological chiral synthesis reports have been published. Some of them consist in the stereoselective reduction of ketones using enzymes preparations or whole cell biocatalysis. Such examples are the kinetic resolution of racemic bicyclononane-2,6-dione [80], 5,6-epoxy-bicycloheptane-2-one [81] and asymmetric reduction of bicyclooctane-dione [21] using genetically engineered baker's yeast.

1.4.1. Chiral amines and ω -Transaminases

Chiral amines are used in the pharmaceutical and fine chemicals industries, because of their potential in the synthesis of cardiovascular, antihypertensive and antiemetic drugs and for the preparation of optically pure carboxylic acids [82].

Chiral amines can be obtained through chemical transformations, such as asymmetric hydrogenation of a Schiff base [83, 84]. However, such processes suffer from harsh reaction conditions, use of toxic transition metal catalysts and insufficient stereoselectivity since the enantiometric excess often does not exceed 60% [85, 86] (Figure 5).

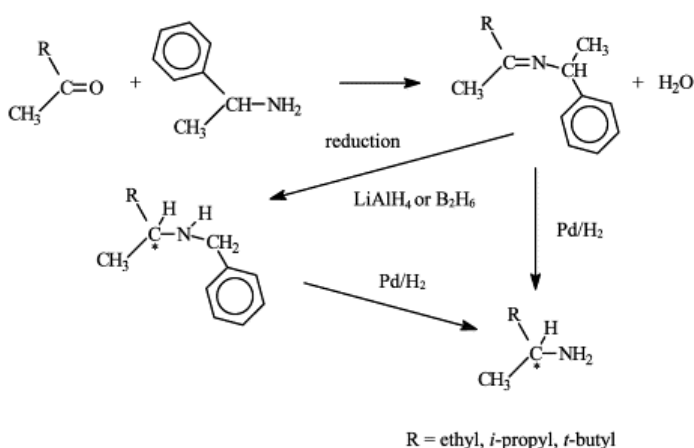


Figure 5- Asymmetric hydrogenation of a Schiff base for chiral amines synthesis.

These drawbacks do not exist with enzymatic reactions. On the contrary, they occur under mild conditions and offer stringent stereoselectivity making enzymatic approaches more sustainable.

One of these enzymes, ω -amino acid: pyruvate transaminase (ω -transaminase) has been identified and studied for the application in chiral amines production. ω -transaminases belong to the subgroup III, which are able to transfer an amino group from a non- α position amino acid (such as 4-aminobutyrate) or an amine compound with no carboxylic group (such as phenylethylamine) to an amino acceptor (such as pyruvate) needing pyridoxal-5'-phosphate (PLP) as co-factor [87]. The first attempt of using ω -transaminases for chiral amines synthesis was reported by Celgene Corporation [88].

The ω -transaminase reaction is constituted by an oxidative deamination of an amine donor and reductive amination of an amino acceptor [85]. The reaction starts by the formation of a Schiff base between PLP and a lysine of the ω -transaminase active site [85]. The amino group of the donor is transferred to the PLP-enzyme complex through the Schiff base generating a pyridoxamine-5'-phosphate (PMP) and the respective ketone (Figure 6 I.). In the last step, the amino group of the PMP is transferred to an amine acceptor and the PLP-enzyme complex is regenerated [85] (Figure 6 II.).

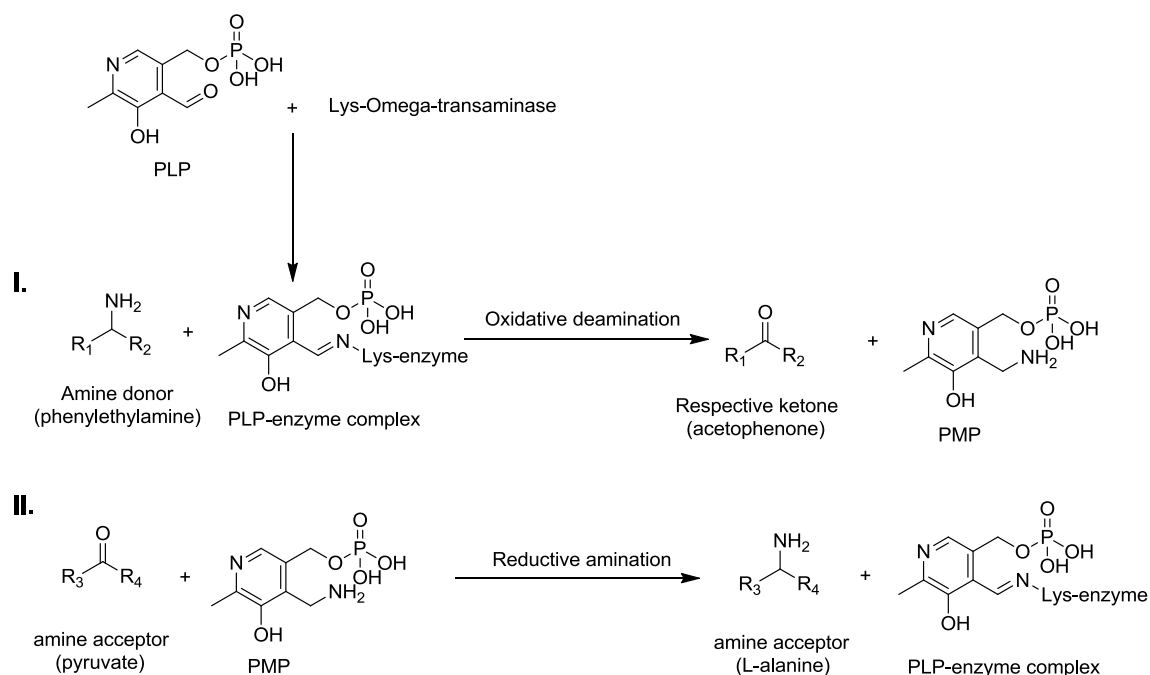


Figure 6- Thermodynamic favored ω -transaminases reaction (Adapted from [85, 89]).

ω -transaminases have the following advantages for the production of chiral amines: broad substrate specificity, high enantioselectivity and high turnover numbers. Comparing ω -transaminases to alternative enzymatic reactions, such as hydrolases and dehydrogenases, it can reach rapid reaction rates without additional co-factor regeneration dependence since its co-factor, PLP, is regenerated during the reaction (Figure 6) [82, 90].

The ω -transaminases co-factor regeneration independence could constitute a big advantage over dehydrogenases which use NAD^+ or NADP^+ as co-factors. NADP^+ and NAD^+ and their reduced forms are crucial in yeast metabolism where yeast keeps a balanced regeneration of such co-factors [91]. NADP^+ is preferentially used in assimilatory pathways such as biomass synthesis and NAD^+ is used in dissimilatory reductions such as reduction of acetaldehyde to ethanol or the reduction of the quinone pool of the respiratory chain [92]. By overexpression of a heterologous dehydrogenase, the redox balance of the required co-factor could be affected. This could result in growth issues since the affected pathways are crucial for biosynthetic precursors and energy obtainment. Transaminases do not require $\text{NAD}^+/\text{NADP}^+$ nor consume their co-factor PLP but regenerate it during the reaction. The $\text{NAD}^+/\text{NADP}^+$ independence could result in a more active metabolism since there is no competition for co-factors between the enzymes of the yeast metabolism and the transaminase.

Two approaches can be followed in order to obtain a pure chiral amine solution: kinetic resolution (Figure 7 A.) and asymmetric synthesis (Figure 7 B.).

During asymmetric synthesis of chiral amines a suitable amine donor is required, such as L-alanine (Figure 7B). On the contrary, for the kinetic resolution of racemic amines a suitable amine acceptor is needed such as pyruvate (Figure 7A) [93]. During kinetic resolution the stringent stereospecificity for one of the enantiomers is taken as advantage in order to convert only one of the chiral amines to a ketone and obtain an enantiometric pure solution of the non-reacting enantiomer. The maximum yield of a single kinetic resolution is 50% and thereby the process efficiency is hampered by a cost increase due to the requirement of a amine racemization of the obtained ketone for an additional round of kinetic resolution.

In asymmetric synthesis the pro-chiral ketone is provided and targeted to the stereoselectively aminated product [85].

Theoretically it is possible to reach a conversion of 100% by asymmetric synthesis. However, the thermodynamic equilibrium has to be overcome since ketone formation, the reverse reaction of asymmetric synthesis, is favored and also product inhibition by the amine has been observed [93].

In this way the generally faster reaction rate of the kinetic resolution compared to the asymmetric synthesis, renders the resolution approach more suitable conditions for industrial scale up, despite the lower maximal 50% reaction yield [88].

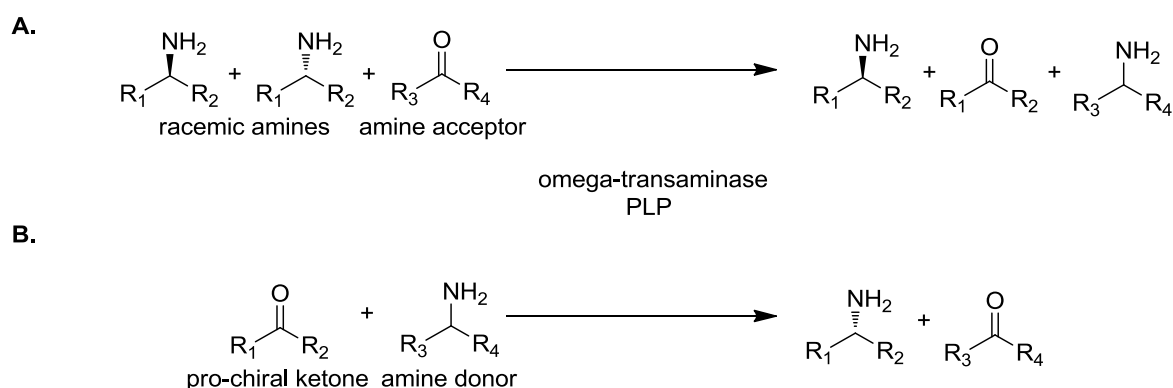


Figure 7- A. Kinetic resolution and **B.** asymmetric synthesis of chiral amines catalyzed by ω -transaminases.

Several approaches and improvements to overcome specific drawbacks of kinetic resolution and asymmetric synthesis of chiral amines were reported and are summarized in Table 3.

During kinetic resolution of chiral amines using purified enzymes, stoichiometric amounts of pyruvate are required, increasing the overall cost of the process. *Truppo et al* [93] developed a method in which the transaminase was coupled to an amino acid oxidase that catalyzes the conversion of L-alanine into pyruvate, to reduce the amount of pyruvate added to the kinetic resolution reaction and thereby also the cost. The alanine obtained after the transamination reaction is oxidized leading to regeneration of pyruvate *in situ*. The reaction with such setup achieved a conversion of 50% yielding a 99% enantiometric excess of *R*-phenylethylamine (see Table 3).

Another approach of kinetic resolution of chiral amines is using whole cells expressing the ω -transaminase. Such an approach was performed by *Bea et al* [82] that overexpressed an ω -transaminase from *Vibrio fluvialis* in *Pichia pastoris*.

To overcome the thermodynamic hindrance during asymmetric synthesis, *Koszelewski et al* [94] coupled a lactate dehydrogenase to the transaminase reaction which drove the reaction towards the amine form by converting the obtained pyruvate into lactate (see Table 3). A high amount of L-alanine is though needed since there is no co-substrate regeneration.

Table 3- Asymmetric synthesis and Kinetic resolution of chiral amines.

Strain/ Reference	Reaction	Yield (%)	Ee (%)
Kinetic Resolution			
<i>Alcaligenes denitrificans</i> intrinsic ω -transaminase [90]	<p>R-amino-n-butylamine + S-amino-n-butylamine + pyruvate \rightarrow 2-oxopentanoic acid + L-alanine + R-amino-n-butylamine</p>	56	99
Codexis ATA-117 transaminase combined with an amino acid oxidase [93]	<p>R-a-phenylethylamine + S-a-phenylethylamine + pyruvate \rightarrow L-alanine + acetophenone + R-a-phenylethylamine</p> <p style="text-align: center;">Amino acid oxidase</p>	50	99
ω -transaminase from <i>Vibrio fluvialis</i> overexpressed in <i>Pichia Pastoris</i> [82]	<p>R-a-phenylethylamine + S-a-phenylethylamine + pyruvate \rightarrow L-alanine + acetophenone + R-a-phenylethylamine</p>	52.2	99
Asymmetric Synthesis			
Codexis ATA-117 transaminase combined with a lactate dehydrogenase [94]	<p>4-phenyl-2-butanone + L-alanine \rightarrow (R)-4-phenylbutan-2-amine + pyruvate</p> <p style="text-align: right;">LDH Lactate</p>	91	99
Enzyme extract from <i>Vibrio fluvialis</i> [95]	<p>3-fluoropyruvate + S-a-phenylethylamine \rightarrow R-3-fluoroalanine + acetophenone</p>	96.2	99

1.5. Aims and Objectives

The aim of the present study was (i) to genetically engineer a *S. cerevisiae* strain in order to increase the accumulation of pyruvate and thereby increase the reaction rate of a heterologously expressed aminotransferase and (ii) to evaluate the resulting strains for the kinetic resolution of (*R,S*)-phenylethylamine.

In order to accumulate pyruvate two strategies were followed, both of them consisting in inhibiting the activity of PDC while coupling it to a lower PDH activity by high glucose concentrations or oxygen limitation [60].

The first one consisted in deleting the major structural genes encoding PDC (namely *PDC1* and *PDC5*). Pyruvate is not consumed further by cytosolic alcohol dehydrogenase and acetaldehyde dehydrogenase in such double knock-out. The fermentative behavior under anaerobic and high glucose concentration could thereby be removed, leading to the desired pyruvate accumulation.

The second strategy consisted in deleting the thiamine biosynthetic gene *THI2*, which inhibits the synthesis of ThDP, a necessary co-factor of PDC (Figure 8). The expected phenotype of this strain was to accumulate pyruvate but without completely blocking the fermentative pathway of the yeast. The two strategies differed in the viability of the cells. The transaminase expressed in *S.cerevisiae* consisted of a putative aminotransferase from *Capsicum chinense* (CC- ω TA) [96] that had been reported as responsible to catalyze the formation of vanillylamine from vanillin [97].

CC- ω TA was chosen because this transaminase was reported to be active at a broad pH range including physiological pH [98].

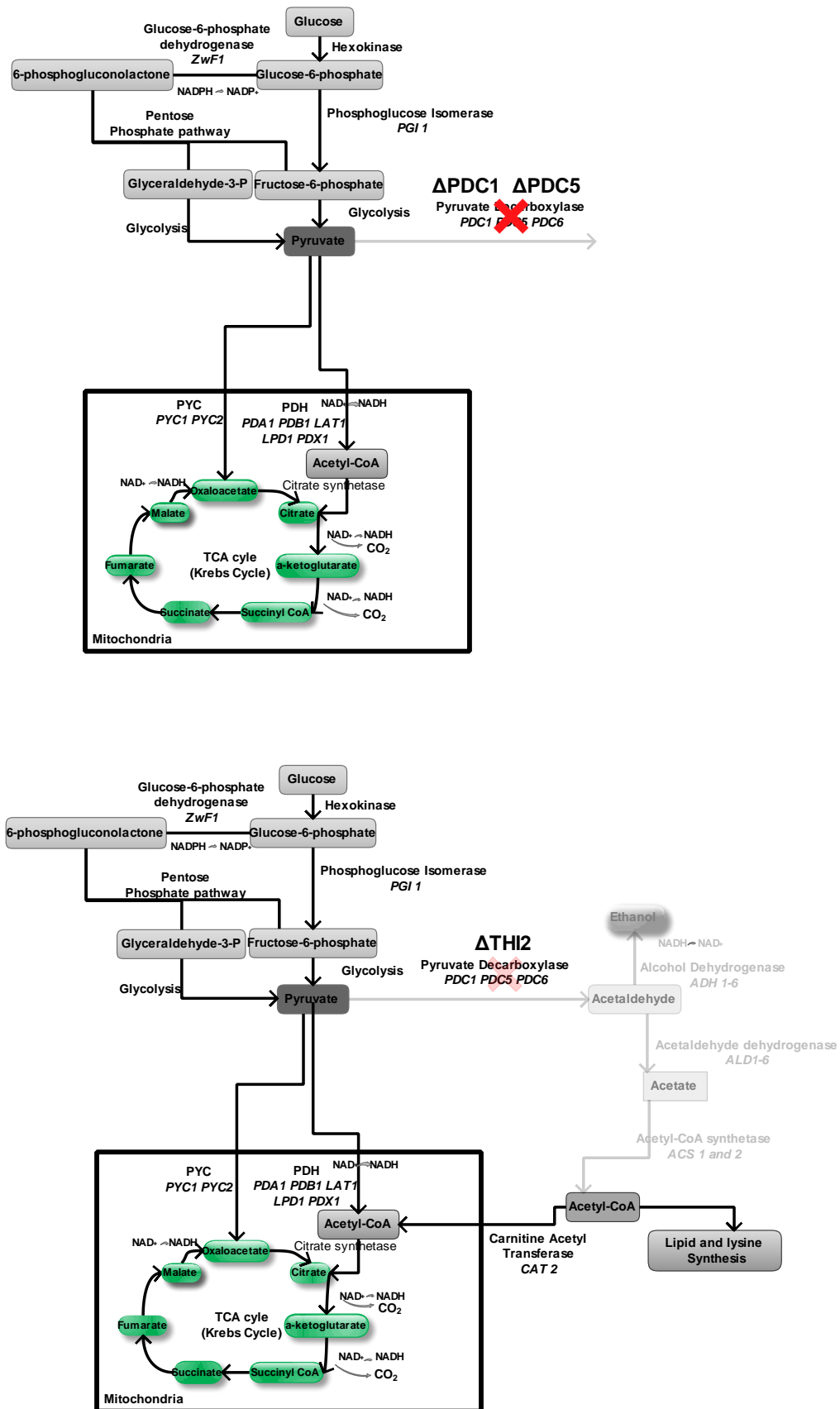


Figure 8- Pyruvate accumulation approaches and their expected metabolic effect.

2. Material and Methods

2.1. Microorganisms and Maintenance

The background strain used in the study, was CEN.PK2-1C HXT7p_PAMT_PGKt (CEN.PK 2-1C+PAMT) which possesses the genomic integrated CC ω transaminase [98]. In addition a series of strains were constructed (Table 4 and Result Section).

All strains were grown in YPD or YP EtOH, then the cell suspension was centrifuged at 3000 g for 5 minutes, and cells were washed with demineralized H₂O and resuspended in 20% glycerol with YPD or YP EtOH and stored at -80°C. All manipulated strains were grown at 30°C on YNB plates containing aminoacids and maintained at 4°C.

Table 4- Strains used and constructed in the present study

Strains	Related characteristic	Source or reference
CEN.PK2-1C+PAMT	Wild type with uracil, tryptophan and histidine auxotrophy	Weber <i>et al</i> , 2013
CEN.PK2-1C+PAMT <i>Δpdc5</i>	CC ω -TA integrated, deleted <i>PDC5</i> gene	This work
CEN.PK2-1C+PAMT <i>Δpdc1 Δpdc5</i>	CC ω -TA integrated, deleted Pyruvate Decarboxylase	This work
CEN.PK2-1C+PAMT <i>Δthi2</i>	CC ω -TA integrated, deleted thiamine biosynthetic gene	This work

2.2. Media and Stock Solutions

Acetophenone, racemic 1-phenylethylamine and pyruvate were purchased from Merck (Hohenbrunn, Germany), pyridoxal-5'-phosphate from AppliChem (Darmstadt, Germany) and all other chemicals from VWR (Leuven, Belgium).

2.2.1. Culture Media

2.2.1.1. YPD (Yeast Extract Peptone Dextrose)

Table 5- Yeast Extract Peptone Dextrose[99]

Compound	YPD Glc Liquid	YPD EtOH Liquid	YPD Plates
	g.L ⁻¹	g.L ⁻¹	g.L ⁻¹
Peptone from Casein	20	20	20
Yeast Extract	10	10	10
Glucose	20	-	20
Ethanol	-	15.8	-
Agar	-	-	15

2.2.2. Defined Media

2.2.2.1. YNB (Yeast Nitrogen Base) supplemented with aminoacids

Table 6- Yeast Nitrogen Base (aminoacids concentration followed by Pronk[100])

Compound	YNB Glc Liquid	YNB EtOH Liquid	YNB Glc or (EtOH) Plates
	g.L ⁻¹	g.L ⁻¹	g.L ⁻¹
Yeast Nitrogen Base w/o Amino acids	6.7	6.7	6.7
Potassium hydrogen phthalate	10.2	10.2	10.2
KOH	2.2	2.2	2.2
Glucose	20	-	20
Ethanol	-	15.8	(15.8)
L-Leucine	0.5	0.5	0.5
L-Histidine	0.13	0.125	0.13
Uracil	0.15	0.15	0.15
L-Tryptophane	0.075	0.075	0.075
Agar	-	-	15

*Aminoacids were added depending on auxotrophic demand of the strain

2.2.2.2. Verduyn Mineral Media

Table 7-Verduyn Mineral Medium [101]

Compound	Verduyn Mineral Media g.L ⁻¹	Compound	Verduyn Mineral Media g.L ⁻¹
(NH ₄) ₂ SO ₄	5	EDTA	0,015
MgSO ₄ · 7H ₂ O	0,5	ZnSO ₄ · 7H ₂ O	4.5x10 ⁻³
KH ₂ PO ₄	3	MnCl ₂ · 2H ₂ O	1x10 ⁻³
Biotin	5x10 ⁻⁵	CoCl ₂ · 6H ₂ O	3x10 ⁻⁴
Pantheotic acid calcium salt	1x10 ⁻³	CuSO ₄ · 5H ₂ O	3x10 ⁻⁴
Nycotin acid	1x10 ⁻³	Na ₂ MoO ₄ · 5H ₂ O	4x10 ⁻⁴
Myo-inositol	0,025	CaCl ₂ · 2H ₂ O	4.5x10 ⁻³
Thiamine · HCl	1x10 ⁻³	FeSO ₄ · 7H ₂ O	3x10 ⁻³
Pyridoxol · HCl	1x10 ⁻³	H ₃ BO ₃	1x10 ⁻³
Para-aminobenzoic acid	2x10 ⁻⁴	KI	1x10 ⁻⁴

Compound	Verduyn Mineral Media g.L ⁻¹
Glucose	20
Ethanol	(15.8)
L-Leucine	0.5
L-Histidine	0.125
Uracil	0.15
L-Tryptophan	0.075

2.2.3. Buffers

2.2.3.1. Verduyn Salt Solution

Table 8-Verduyn Salt Solution

Compound	10x Verduyn Salt Solution g.L ⁻¹
(NH ₄) ₂ SO ₄	50
MgSO ₄ · 7H ₂ O	5
KH ₂ PO ₄	30

2.2.3.2. YNB Buffer

Table 9- YNB Buffer

Compound	5x YNB Buffer
	g.L ⁻¹
Potassium hydrogen phthalate	51
KOH	11

* pH 5.5

2.2.4. Transamination Solution

Table 10- Transamination Solution

Compound	Transamination Solution
	g.L ⁻¹
Glucose	20 or 50
NaPO ₄	11.8
RS-Phenylethylamine	3.03
PLP	2.5x10 ⁻⁴

*pH 7.0

2.3. Strain Construction

The work-flow for construction of the desired strains consisted in identifying the DNA sequences and chromosomal location of the genes to be deleted, constructing the deletion cassettes and performing the respective yeast transformations.

All sequence manipulations (primer design, predicted PCR's and homology screening) were performed using the software GENTle. Primers were ordered from MWG-Biotech AG (Ebersberg, Germany). PCR mixes were prepared according to the DNA polymerase kit protocol and the thermocycler programs are listed in Appendix I-. Phusion Hot Start II High-Fidelity DNA Polymerase mix (Thermo Scientific, USA) was used to avoid non-specific amplification and primer degradation and receive extreme fidelity. PCR reactions were performed using the C1000™ Thermal Cycler (BioRad, USA), and electrophoresis run in the Mupid-exU System gel electrophoresis equipment (Clontech, USA). Gels were analyzed using Bio-Rad ChemiDoc XRS System (BioRad, USA). Genomic DNA was extracted and the PCR fragments were purified using, respectively,

Pierce* Yeast DNA Extraction Kit (Thermo Scientific, USA) and Gene Jet Purification kit (Thermo Scientific, USA). All DNA quantifications were performed using BioDrop DUO (Bio Drop, UK).

2.3.1. Deletion fragments

It was necessary to amplify the downstream and upstream regions of each gene as well as the respective auxotrophic marker to perform the targeted deletion of the genes. This required the identification of each gene locus so that primers could be designed for the respective downstream and upstream region.

After obtaining the location of the *PDC1*, *PDC5* and *THI2* ORF's in CEN.PK 113-7D (see sequences in Appendix II-), 300 to 600 bp upstream and downstream were selected for each gene (see sequences in Appendix III-). With these sequences and the sequence of the respective auxotrophic markers *TRP1* and *URA3* (see sequences in Appendix IV-), primers were designed in order to obtain and amplify those fragments (previous work performed by Ander Sandström). The up-/downstream sequences and the *URA3* marker were amplified from genomic DNA of CEN.PK 113-7D and *TRP1* was amplified from a Mumberg vector from the laboratory collection (see primer list on Appendix V-) (Figure 9). The sequences used for primer design consisted of CEN.PK 113-7D databases (<http://www.sysbio.se/cenpk/>).

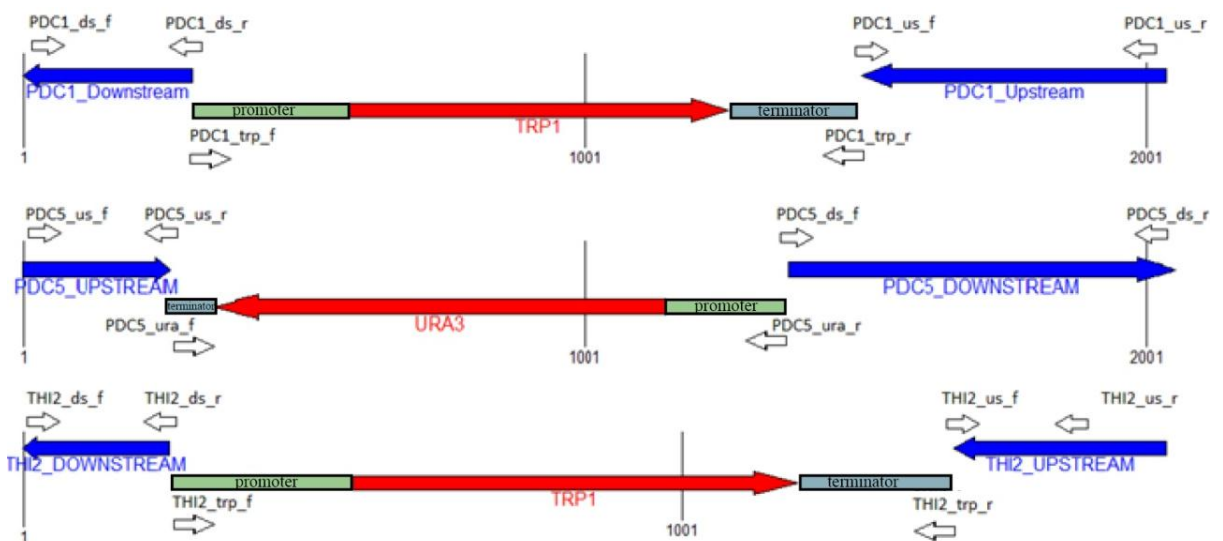


Figure 9- Primer location in the final constructs. The uncolored arrows represent the primers used for amplification of each deletion fragment. The marker sequences were amplified to include the respective promoter and terminator.

The pairs of primers PDC1_ds_r/PDC1_trp1_f, PDC1_trp1_r/PDC1_us_f, PDC5_ura_f/PDC5_us_r, PDC5_ura_r/PDC5_ds_f, THI2_trp_f/THI2_ds_r and THI2_trp_r/THI2_us_f were designed to create a minimal 30 bp homologous region which was crucial for the Overlap Extension PCR.

```

PDC1_ds_r  3'-5' CTTATAAACTTTAACTAATAATTAGAGATTAATCGCCGACATTACTATATATATA-----
PDC1_trp1_f 5'-3'-----TAATAATTAGAGATTAATCGCCGACATTACTATATATATAATAGGAAGCATTTAATAG
*****

PDC1_us_f  3'-5' GCAAAAATAACACAGTCAAATCAATCAAAAACAACACTCAACCC-----
PDC1_trp1_r 5'-3' -CAABATAACACAGTCAAATCAATCAAAAACAACACTCAACCCCTATCTCG
*****

```

Figure 10- Example of homology between pairs of primers (sequence alignment was performed in Clustal Omega).

2.3.2. Overlap Extension PCR

The deletion fragments were fused by overlap extension PCR to create the final deletion cassettes. In this type of PCR, the ≥ 30 bp homologous regions of the deletions fragments behave as ‘primers’, leading to the fusion of the several fragments.

This method is divided into two stages, the first consisting of 30 fmol of each deletion fragment in the PCR mix which leads to 30 fmol of the deletion cassette. Secondly, the respective end primers are added in order to amplify the whole deletion cassette (Table 11). The PCR products were purified and recovered with the QIAquick® Gel Extraction Kit (Qiagen, Germany).

Table 11- Primer list for final amplification of the fragments obtained through Overlap Extension PCR

Deletion	Forward Primer	Reverse Primer
<i>PDC1</i>	PDC1_ds_f	PDC1_us_r
<i>PDC5</i>	PDC5_us_f	PDC5_ds_r
<i>THI2</i>	THI2_ds_f	THI2_us_r

2.3.3. Yeast Transformation

Single yeast colonies were picked and transformed as described by *Gietz & Schiestl* [102]. The amount of DNA used per transformation was 500 ng. The cells were resuspended in dH₂O after heat treatment. CEN.PK 2-1C+PAMT $\Delta pdc1 \Delta pdc5$ cells were resuspended in YP for 3 hours to allow the cell membrane to recover in order to resist to ethanol stress.

After the transformation process, the cells were streaked on YNB plates with aminoacids and 20 g/L glucose. The CEN.PK 2-1C+PAMT $\Delta pdc1 \Delta pdc5$ strain was plated on YNB with L-histidine and 2% ethanol (15.78 g/L).

2.3.4. Deletion confirmation

Colonies from each transformation plate were picked and genomic DNA was extracted to confirm that the deletion was successful after each transformation. Two PCR reactions were performed for each colony, the first primer set was composed by an end primer of the downstream sequence and a primer located at the junction of the marker and upstream sequence (resulting in PDC1_trp1, PDC5_ura3 and THI2_trp1 fragments) (Table 12) (Figure 11 a)). The second primer set was composed by the end primers (resulting in WPDC1, WPDC5 and WTHI2 fragment), the same used for amplifying the deletion cassettes (Table 11) (Figure 11 b)). An example of the fragments that should be obtained in a $\Delta pdc1$ strain is shown in Figure 11. PCR programs are listed in Appendix I-.

Table 12- PDC1_trp1, PDC5_ura3 and THI2_trp1 deletion confirmation fragments primer set. Each primer set is composed by an end primer of the downstream sequence and a primer located at the junction of the marker and upstream sequence.

Deletion confirmation	Forward Primer	Reverse Primer
PDC1_trp1	PDC1_ds_f	PDC1_trp1_r
PDC5_ura3	PDC5_ura3_f	PDC5_ds_r
THI2_trp1	THI2_ds_f	THI2_trp1_f

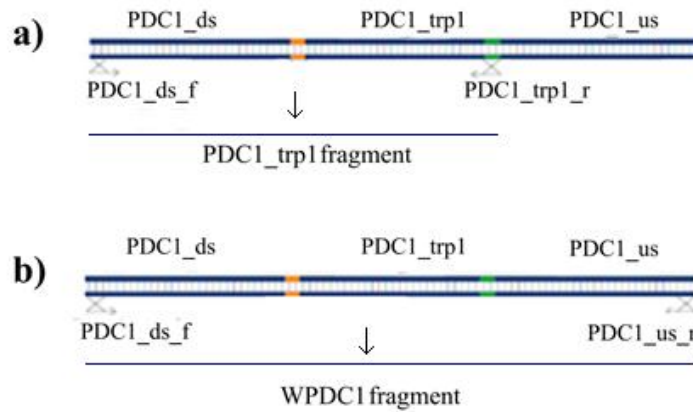


Figure 11- PCR fragments for $\Delta pdc1$ strain confirmation. The PCR confirmation of each deletion was performed by amplifying two fragments: a) one that included the downstream and marker sequence, which means that only clones containing the deletion could possess this amplification; b) a second that would amplify the complete *PDC1* gene, which means that clones with the deletion would amplify a fragment with different size than the control strain since the control possessed a intact *PDC1* gene and the deleted strain would amplify a fragment containing the marker sequence.

Besides the PCR confirmation also a phenotype screening was performed. For the $\Delta pdc1 \Delta pdc5$ strain the absence of growth in medium containing 20 g/L of glucose confirmed the double deletion. The deletion of *THI2* was also confirmed by growth absence in medium lacking thiamine.

2.4. Fermentations/ Cultivations

Biomass required for the fermentations was obtained by picking single colonies from YNB agar plates and pre-growing them in falcon tubes of 50 mL containing 5 mL of medium. After reaching an OD of 2, the cells were centrifuged and resuspended in fresh medium and inoculated in 1L shake flasks containing a final medium volume of 100 mL.

The cells were incubated in a rotary shake incubator with 180 rpm at 30°C and harvested during mid-stationary phase to start the fermentations/cultivations. During the fermentation, samples were taken and observed under the microscope to detect any contamination.

If not stated otherwise, the specific medium in which each strain was inoculated is listed in

Table 13.

All fermentations/cultivations were performed as biological duplicates.

Table 13- Medium for pre- fermentation growth

Strain	Medium for pre-fermentation growth
CEN.PK2-1C+PAMT <i>Δthi2</i>	Verduyn w/o Thiamine + 20 g/L glucose + Uracil+ L-Histidine+ 0.05 μM Thiamine
CEN.PK2-1C+PAMT <i>Δpdc1 Δpdc5</i>	YP+ 15.78 g/L ethanol

2.4.1. Aerobic Cultivation for pyruvate accumulation

After obtaining the required biomass in 1L shake flasks, the cells were centrifuged for 8 minutes at 3200 rcf and washed two times with 25 mL of dH₂O. The OD_{620nm} of the obtained solution was measured and the volume necessary to obtain a starting OD_{620nm} of 2 for the aerobic fermentation was harvested, centrifuged and resuspended in 25 mL of the fermentation medium in a 250 mL shake flask. The fermentation medium consisted of Verduyn mineral medium supplemented with aminoacids and 20 g/L of glucose. The medium for CEN.PK2-1C +PAMT *Δthi2* did not contain thiamine.

The OD_{620nm} was measured over time using Ultrospec 2100 pro spectrophotometer (GE Healthcare Life Sciences, USA). At the same time samples were centrifuged and the supernatant stored at -20°C for further analysis.

2.4.2. Anaerobic fermentation for pyruvate accumulation

Cells required for the anaerobic fermentation were obtained as described in 2.4. The anaerobic fermentation started with an initial OD_{620nm} of 20 in 10 mL medium in a small vial containing a magnetic stirrer and sealed with a rubber lid. A syringe filled with cotton was inserted in the rubber lid to avoid overpressure of CO₂. The fermentation medium was the same as described in the aerobic cultivation under 2.4.1. Samples were recovered with a syringe to avoid oxygen to enter in the vial and compromise the anaerobic environment. The OD_{620nm} was measured over time, samples were centrifuged and the supernatant stored at -20 °C for further analysis.

2.5. Dry Weight measurements and OD_{620nm}/Cell dry weight calibration curve

Pall Life Science Supor® 450 47 mm 0.45µm pore filters were dried in a microwave at 350 W for 4 minutes and cooled down inside a desiccator. After weighing the filters (W₀), they were used to filter the cell suspension with a Millipore filter holder under vacuum. Cells were washed with dH₂O three times with the volume of the filtrate. The filters were put in a microwave for 8 minutes at 350 W and cooled down inside a desiccator. The filters were weighed (W₁) and the dry weight per L of suspension was calculated through the following equation: Dry Weight/L (g/L) = $\frac{W_1 - W_0}{suspension\ volume\ (L)}$. Each dry weight measurement was performed in duplicate.

Construction of a calibration curve between the OD_{620nm} measurements during the fermentations and the respective cell dry weight was performed with the following procedure. Each strain was pre-grown and handled as described in 2.4 and 2.4.1. After obtaining a high cellular density solution (~25 OD_{620nm}) serial dilutions were performed in order to obtain the OD_{620nm} range measured during fermentations/cultivations. Duplicates of cell dry weight of each solution were measured as described before and a linear regression curve between the undiluted OD_{620nm} values of each solution and respective mean of cell dry weight measurements was constructed (Calibration Curves can be seen in Appendix VI-).

2.6. Transamination biocatalysis

Cells for the transamination biocatalysis were obtained as described in 2.4. The experiments were performed at the same conditions as described in 2.4.2. The buffer contained either 20 or 50 g/L D-glucose, 3.03 g/L of racemic RS-phenylethylamine, 0.1 μ M of PLP and 20 OD_{620nm} biomass in 100 mM NaPO₄ buffer at pH 7.0. Samples of 1 mL were taken and mixed with 100 μ L of HCl 1M to stop the reaction. The cells were discarded after centrifugation and supernatant stored at -20 °C for further analysis.

2.6.1. Amine and ketone extraction for HPLC analysis

The samples were thawed, 30 μ L of NaOH 10 M added to the sample and mixed thoroughly. After mixing, 200 μ L of n-heptane including 0.1% butylamine was added and the solution mixed thoroughly for 1 minute. The samples were centrifuged for 5 minutes under 13000 rcf and the organic phase recovered. The procedure was repeated with 400 μ L of n-heptane including 0.1% butylamine and the time for centrifugation increased to 10 minutes. The recovered organic phase was used for HPLC analysis

2.7. HPLC analysis

2.7.1. Metabolites and substrates

The metabolites pyruvate, succinate, acetate, glycerol, ethanol and the substrate glucose were quantified using two Aminex® HPX-87H Ion Exclusion columns (Bio-rad, USA) with H₂SO₄ 5 mM at 0.6 mL/min as mobile phase under 45 °C. The volume injected per sample was 20 μ L. The HPLC system consisted of a Waters 1525 Binary HPLC pump, autosampler (Waters 717 plus), CH-30 Column Heater (FIATron™ Systems Inc.), Shimadzu Refractive Index Detector RID-6A and absorbance detector (Waters 2487 Dual λ). An absolute calibration curve was performed for each metabolite covering the measured values.

2.7.2. Transamination products and substrates

The transamination product acetophenone and the substrate *R,S*-phenylethylamine were quantified using a ChiralCEL® OD-H column with 0.1 % butylamine, 15% isopropanol and 85% n-heptane at 1mL/min as mobile phase under room temperature. Each sample was injected twice with a volume of 5 μ L per injection. The HPLC system consisted of a Waters 1525 Binary HPLC pump, Waters 2707 autosampler and Waters 2485 UV/Vis detector. An absolute calibration curve was performed for each compound covering the measured values.

3. Results

3.1. Engineering of yeast strains for pyruvate accumulation

An overview of the strategy used for the construction of deletion cassette is presented in Figure 12. In short, the required deletion fragments to construct the deletion cassettes were amplified and purified in order to be fused through overlap extension PCR. The background strain was transformed with the deletion cassettes after confirming their successful construction through agarose gel electrophoresis. PCR amplification of the integrated deletion cassette in the genome of the transformed colonies and assessment of expected phenotypic behaviors were performed to confirm successful transformations. Results are presented below.

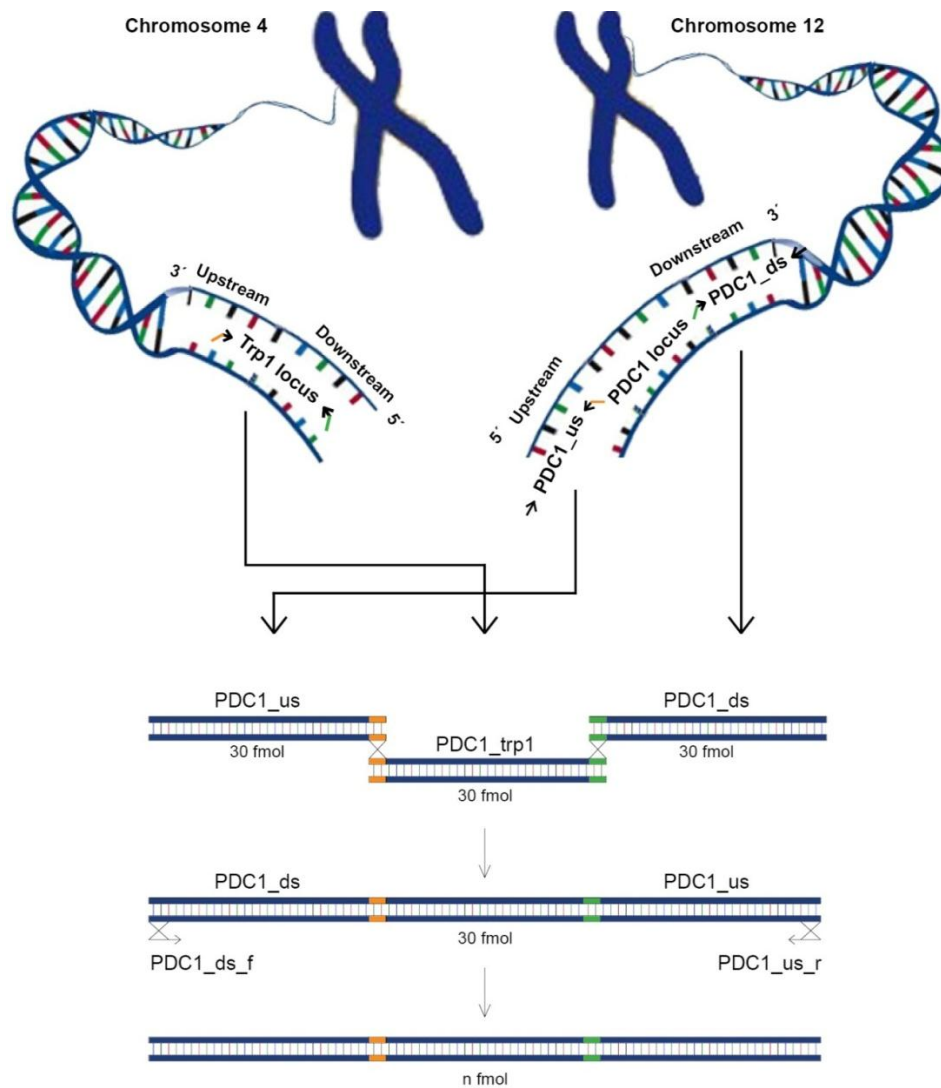


Figure 12- Scheme of overall deletion cassette construction.

3.1.1. Construction of the deletion fragments

The construction of the *THI2* and *PDC 1, 5* deleted strains began with amplification of several deletion fragments that were constituted either by the upstream and downstream sequence of each gene or the auxotrophic marker sequence flanked by homology regions for the up and downstream region of the gene to be deleted.

All of the necessary deletion fragments were successfully amplified and gel purified. The expected fragment size is shown below each band. In all cases, the size was confirmed by comparison with the ladder (Figure 13).

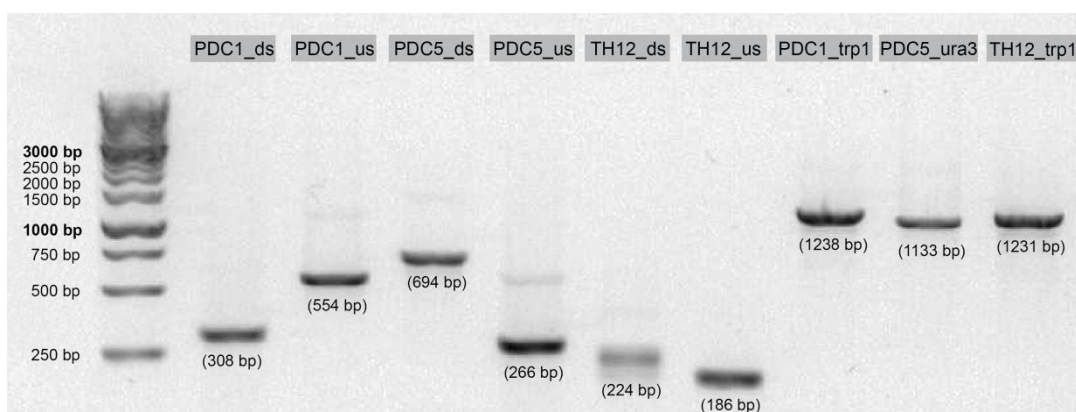


Figure 13- Deletion fragments amplified from genomic DNA. Fragments containing ‘_ds’, represent the downstream region of the respective gene. Fragments containing ‘_us’, represent the upstream region of the respective gene. Fragments containing ‘_trp1’ or ‘_ura3’, represent the auxotrophic marker sequence flanked by homology regions for the up and downstream region of the respective gene. The expected band size is below each band and was confirmed by comparison with the ladder.

3.1.2. Construction of the integration cassettes for gene deletion

An overlap extension PCR to fuse the deletion fragments was performed. After performing overlap extension PCR, the successful construction of the deletion cassettes was confirmed by electrophoresis as shown in Figure 14.

The deletion cassettes were PCR amplified to obtain the required amounts for the transformation of CEN.PK2-1C+PAMT.

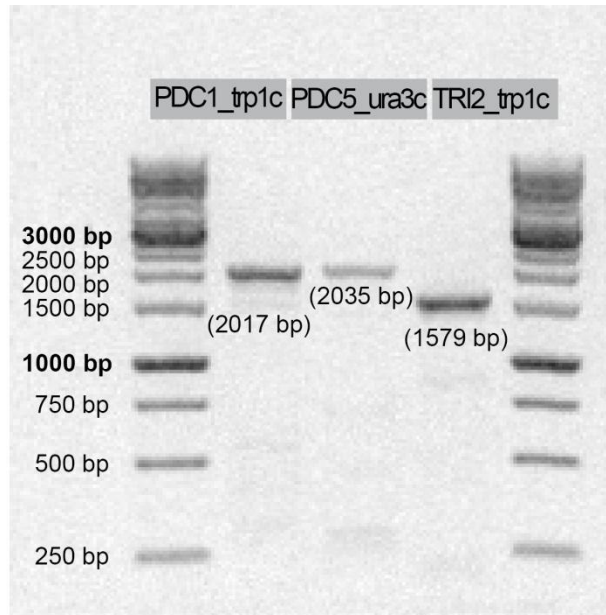


Figure 14- Gel purified deletion cassettes. PDC1_trp1c, PDC5_ura3c and TRI2_trp1c represents the final deletion cassette for the, respectively, *PDC1*, *PDC5* and *THI2* gene. The expected band size of each cassette is below each band and was confirmed by comparison with the ladder.

3.1.3. Transformation of yeast and strain confirmation

3.1.3.1. Construction of CEN.PK 2-1C+PAMT Δ PDC1 Δ PDC5

The construction of the *pdc1* and *pdc5* deleted strain started with the transformation of the control strain with the PDC1_trp1c deletion cassette. However, PCR amplification of the PDC1_trp1 and WPDC1 fragments demonstrated that the selected clone did not contain the desired *PDC1* deletion. Since no successfully transformed clone was isolated, the construction of the desired strain started by transforming the control strain with the PDC5_ura3c deletion cassette.

After transforming CEN.PK2-1C+PAMT with PDC5_ura3c deletion cassette, a strain lacking PDC5 was selected and confirmed by PCR amplification of PDC5_ura3 and WPDC5 (data not shown). The obtained Δ *pdc5* strain was transformed with PDC1_trp1 deletion cassette. Several colonies were selected for genomic DNA extraction and amplification of PDC1_trp1, WPDC1, PDC5_ura3 and WPDC5 fragments were performed (deletion confirmation fragments are described in 2.3.4). The negative bands resulted from the amplification of the fragments from genomic DNA of the control strain CEN.PK2-1C+PAMT, whereas the positive bands resulted from the amplification of the constructed deletion cassettes. The confirmation was done by comparing the band sizes with the

positive and negative bands. A successful transformation was confirmed when the colony amplification had the same band size as the positive. From the 10 selected colonies, six carried the expected deletions as shown on Figure 15 and Figure 16.

Three of those colonies were restreaked on new plates (colonies 2, 7 and 8) and new colonies were picked and grown in order to make glycerol stocks.

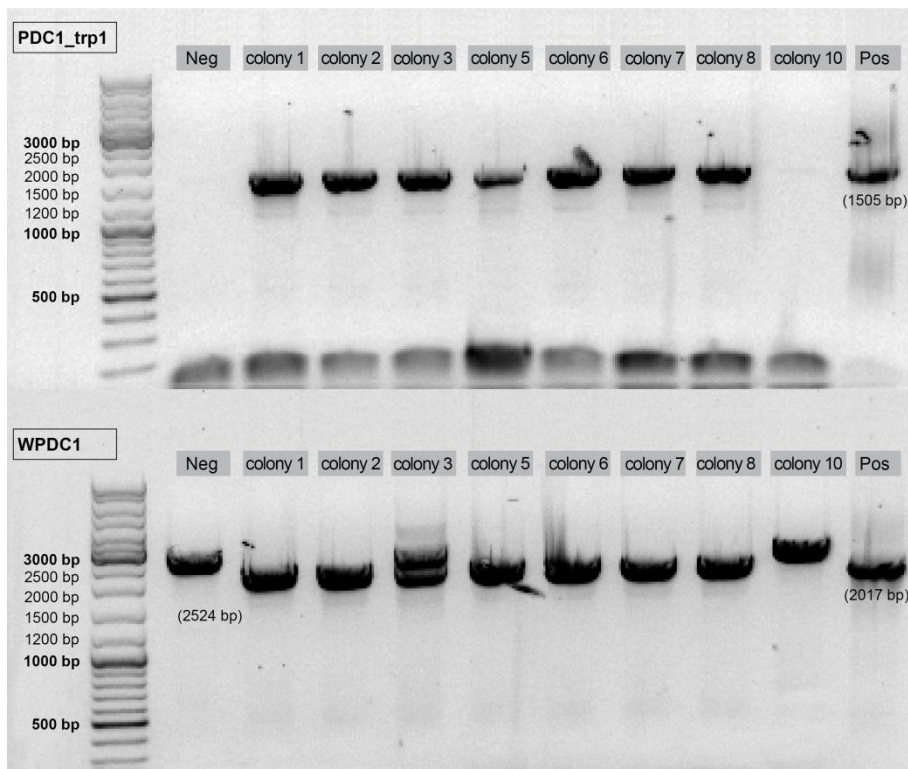


Figure 15- Deletion confirmation of *PDC1* in selected colonies by amplifying *PDC1_trp1* and *WPDC1* fragments. The 'Neg' lanes represent the amplification of the deletion confirmation fragments from genomic DNA of the control strain, whereas the 'Pos' lanes represent the amplification of the deletion cassettes. Successful transformed clones represent bands with the same size as the positive amplifications.

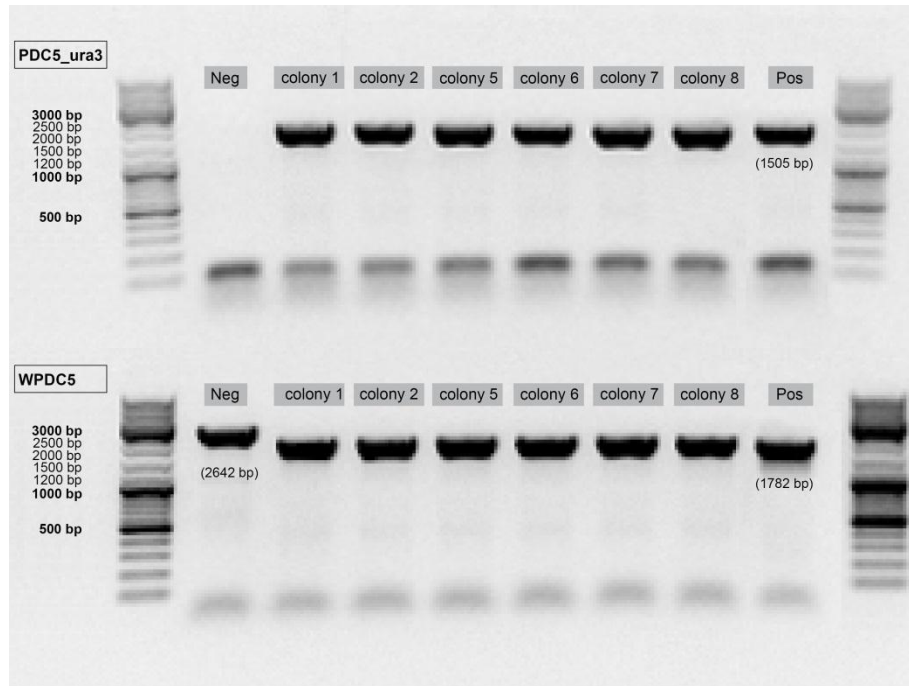


Figure 16- Deletion confirmation of *PDC5* in selected colonies by amplifying *PDC5_ura3* and *WPDC5* fragments. The 'Neg' lanes represent the amplification of the deletion confirmation fragments from genomic DNA of the control strain, whereas the 'Pos' lanes represent the amplification of the deletion cassettes. Successful transformed colonies represent bands with the same size as the positive amplifications.

At the beginning of the fermentations each of the glycerol stocked colonies were also inoculated in 20 g/L glucose containing medium to observe the predicted absence of growth in medium containing glucose. However, growth was observed after 48 hours. Genomic DNA of those cultivations was extracted and amplification of *PDC1_trp1* and *WPDC1* was performed to evaluate if growth was due to revertance of the mutation (Figure 17). The amplification of the *PDC1_trp1* fragment could lead to the conclusion that the clones still possessed the deletion, since they possessed bands with the same size as the positive control (Figure 17, *PDC1_trp1* gel). However, the amplification of *WPDC1* demonstrated that the clones did not possess the desired deletion since the obtained bands possessed the same size as the negative control (Figure 17, *WPDC1* gel). A possible reason for the amplification of *PDC1_trp1* fragments with the clone's genomic DNA could be due to the existence of two copies of the gene. However, this would result in the existence of 2 bands in the *WPDC1* amplification since there would be one band for the deleted and another for the non-deleted copy. Yet, only one band was present in the *WPDC1* amplifications of the clones, which means that the bands present in the *PDC1_trp1*

amplifications could be due to contaminations. These results demonstrated that the glycerol stocked strains did not longer possess the desired deletion.

Due to the difficulties in avoiding deletion reversion during the construction of the *pdc1* and *pdc5* deleted strain, the following part of the study focused in the second engineering strategy, based on thiamine auxotrophy.

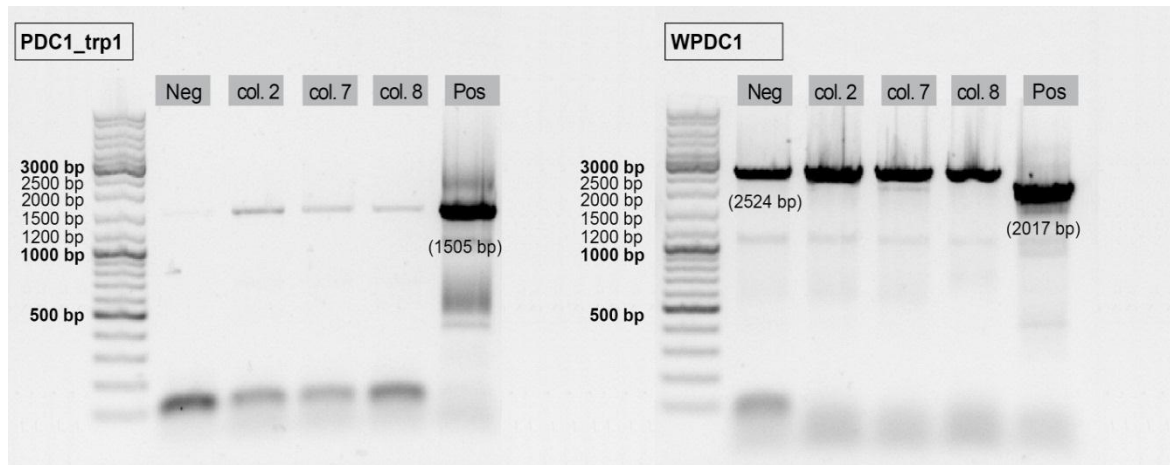


Figure 17- Amplification of *PDC1_trp1* and *WPDC1* fragments from glycerol stocked strain. The Neg lanes represent the amplification of the deletion confirmation fragments from genomic DNA of the control strain, whereas the Pos lanes represent the amplification of the deletion cassettes. Successful transformed colonies represent bands with the same size as the positive amplifications. Successful transformed clones represent bands with the same size as the positive amplifications.

3.1.3.2. Construction of *CEN.PK 2-1C+PAMT ΔTHI2*

A similar integration fragment was obtained for deleting *THI2*. After transforming *CEN.PK2-1C+PAMT*, several colonies were picked and inoculated in Verduyn medium without thiamine. The clones that did not grow were selected for a first assay of pyruvate accumulation. The pyruvate accumulation assays were performed in Verduyn medium under aerobic conditions with cells pre-grown in medium containing the normal thiamine concentration (3.32 μM) (Appendix VII-, Figure 35). The clone that had the highest pyruvate level was selected for further fermentations and confirmation by PCR amplification of *THI2_trp1* was performed to assure that the selected clone had the desired genotype. The confirmation is shown in Figure 18 and the clone 34 was selected for further cultivations.

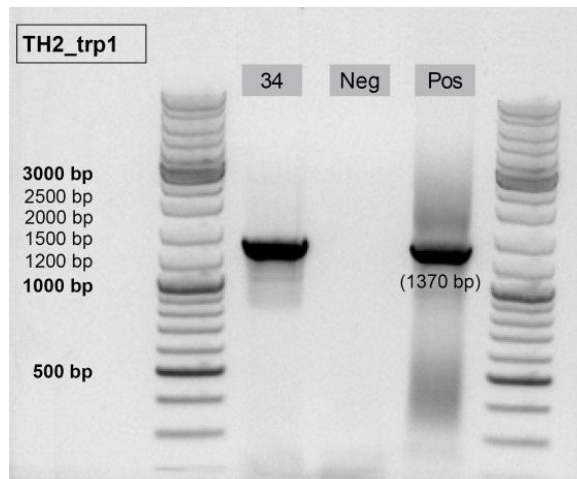


Figure 18- Confirmation of desired genotype through amplification of TH12_trp1 from CEN.PK2-1C+PAMT $\Delta thi2$ clone 34 genomic DNA. The 'Neg' lane represents the amplification of the deletion confirmation fragments from genomic DNA of the control strain, whereas the 'Pos' lane represents the amplification of the deletion cassette. Genomic DNA of *thi2* deleted clone 34 was extracted and TH12_trp1 fragment was amplified. The amplified band possessed the same size as the positive control.

3.2. Assessment of the strain carrying a deletion of *THI2* gene

Pyruvate accumulation was assessed in both synthetic mineral media [101] and phosphate buffer whereas the transamination reactions were conducted only in phosphate buffer.

3.2.1. Pyruvate accumulation during growth

The first fermentations with the *thi2* deleted strain were performed in Verduyn medium [101] containing 20 g/L of glucose. The objective was to assess the effect of thiamine concentration during pre-cultivation growth on pyruvate accumulation during the following cultivation.

Thi2 deleted clone 34 was inoculated in medium containing 0.05, 0.1 and 0.5 μM of thiamine to identify the minimal concentration of thiamine required for growth. Aerobic growth was observed at all levels including in the in medium containing 0.05 μM of thiamine, yet at a much lower rate.

Clone 34 carrying *thi2* deletion was selected and pre-grown together with the control strain having native *THI2*, in medium containing the standard (3.32 μM) and the lowest tested (0.05 μM) thiamine concentration. After obtaining biomass to start the cultivation, cells were transferred to Verduyn medium lacking thiamine but complemented with aminoacids. The clone was tested for both anaerobic (3.2.1.1) and aerobic (3.2.1.2) pyruvate accumulation.

3.2.1.1. Anaerobic pyruvate accumulation after pre-growth with 3.32 μM and 0.05 μM thiamine

The control and *thi2* deleted strain pre-grown in medium containing 3.32 μM thiamine displayed similar fermentation profiles (Figure 19). In contrast, higher pyruvate accumulation was observed for the *thi2* deleted strain when cells were pre-grown with limited (0.05 μM) thiamine concentrations (Figure 20), which confirmed the expected phenotype and highlighted the importance of precultivation conditions on pyruvate accumulation.

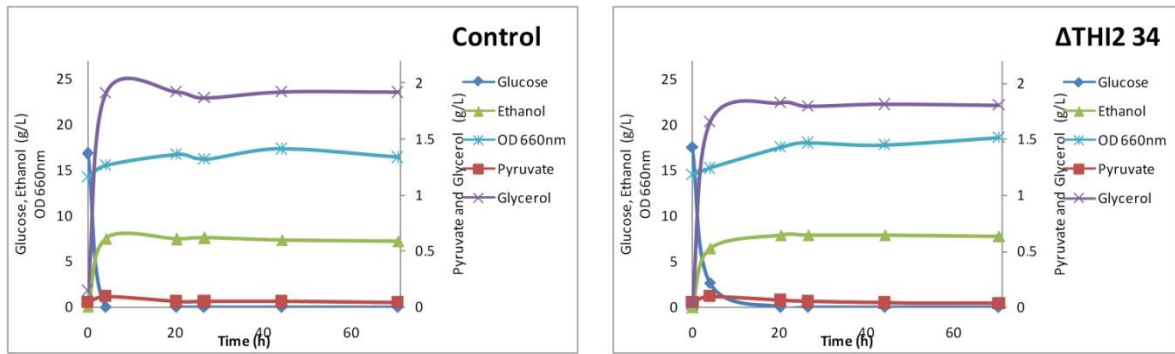


Figure 19- Anaerobic fermentation of CEN.PK2-1C+PAMT $\Delta thi2$ clone 34 and its control in Verduyn medium pre grown in $3.32\mu\text{M}$ thiamine.

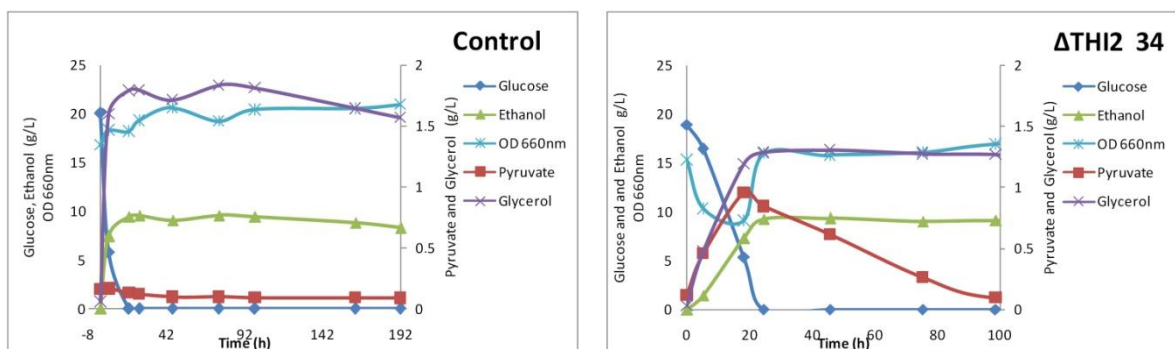


Figure 20- Anaerobic fermentation of CEN.PK2-1C+PAMT $\Delta thi2$ clone 34 and control in Verduyn medium pre grown in $0.05\mu\text{M}$ thiamine.

3.2.1.2. Aerobic pyruvate accumulation after pre-growth with $3.32\mu\text{M}$ and $0.05\mu\text{M}$ thiamine

Aerobic pyruvate accumulation in Verduyn medium with cells pre-grown with $3.32\mu\text{M}$ thiamine showed a different trend than in anaerobic fermentations since some pyruvate accumulation was observed for the deletion strain as shown in Figure 21.

The effect of decreasing the thiamine concentration during the pre-fermentation growth was similar to the one observed in anaerobic fermentations since the pyruvate accumulation was significantly increased in the deletion strain (Figure 22).

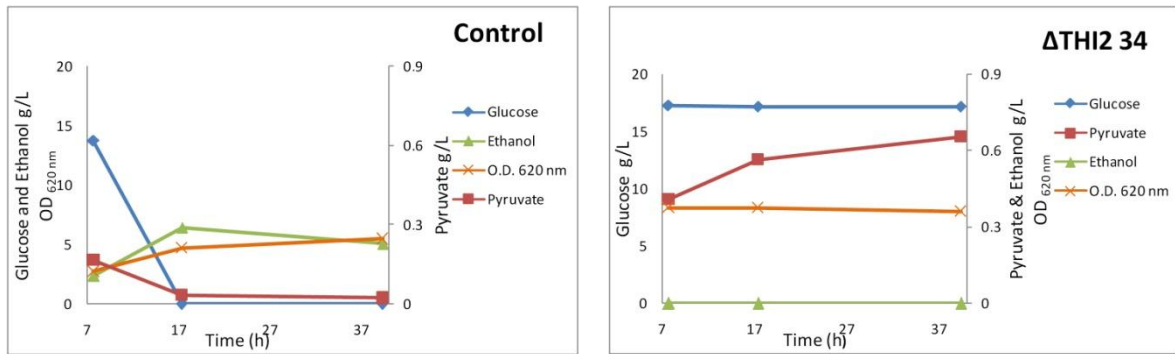


Figure 21- Aerobic cultivation of CEN.PK2-1C+PAMT $\Delta thi2$ clone 34 and its control in Verduyn medium pre grown in 3.32 μM thiamine.

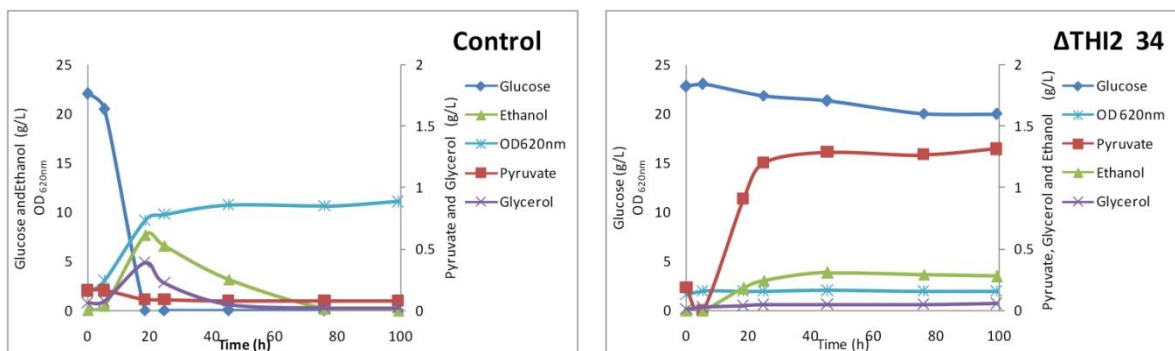


Figure 22- Aerobic cultivation of CEN.PK2-1C+PAMT $\Delta thi2$ clone 34 and its control in Verduyn medium pre grown in 0.05 μM thiamine.

All pyruvate titers and yields of the fermentations/ cultivations in Verduyn medium are summarized in Table 14. The pyruvate yield obtained by the *thi2* deleted clone 34 in aerobic cultivations containing 20 g/L of glucose with cells pre-grown in 3.32 μM was compromised due to problems with the HPLC analysis of the deleted strain samples.

Table 14- Pyruvate titer and yield (g pyruvate/g glucose) for CEN.PK2-1C+PAMT $\Delta thi2$ construct and its control in Verduyn medium, as a function of thiamine concentration during pre-cultivation. The theoretical maximal pyruvate yield (g pyruvate/ g glucose) is 0.98 g/g.

Thiamine in pre-growth (μM)	Aeration	Pyruvate titer (g/L)		Yield g pyruvate/g glucose	
		Control	$\Delta\text{THI2 34}$	Control	$\Delta\text{THI2 34}$
3,32	Aerobic	0,17	0,66	0,01	-*
	Anaerobic	0,09	0,10	<0,01	<0,01
0,05	Aerobic	0,16	1,31	<0,01	0,38
	Anaerobic	0,17	0,96	<0,01	0,07

* Glucose measurements not reliable, due to dilution issues

The comparison of the pyruvate titer for the control strain (Table 14) showed that pyruvate accumulation was not significantly affected by varying the thiamine concentration in the pre-fermentation growth medium in both aerobic and anaerobic conditions.

Aerobic cultivations using cells pre-grown with no-limiting thiamine levels resulted in a 4-fold increased pyruvate accumulation for the $\Delta thi2$ strain clone 34 in comparison to the pyruvate accumulation of the control strain in the same conditions.

Reducing the thiamine level during pre-cultivation, significantly improved pyruvate accumulation by the *thi2* deleted strain under both aerobic and anaerobic cultivations.

The highest pyruvate titer was obtained by *thi2* deleted clone 34 (1.31 g/L) during aerobic cultivations, showing a 2-fold improvement compared to the same strain pre-grown in 3.32 μ M of thiamine.

The effect of varying the thiamine concentration in the pre-fermentation growth medium was more pronounced in anaerobic fermentations since pyruvate accumulation by CEN.PK2-1C+PAMT $\Delta thi2$ 34 was 10-fold improved. Even by having a higher improvement in anaerobic fermentations, the *thi2* deleted strain achieved the same pyruvate titer than in aerobic cultivations when cells were pre-grown in the minimal thiamine concentration.

3.2.2. Pyruvate accumulation during incubation in phosphate buffer

The desired pyruvate accumulative phenotype of the *thi2* deleted strain was confirmed through cultivation in Verduyn medium with cells pre-grown with 0.05 μ M of thiamine. As biocatalyst experiments are usually performed in buffered media that do not allow growth, similar experiments were performed using phosphate buffer and cells pre-grown in 0.05 μ M thiamine. Besides comparing the effect of oxygen during the fermentations, also the effect of varying the glucose concentrations was evaluated.

Each experiment of pyruvate accumulation in phosphate buffer was performed simultaneously with the respective transamination reaction containing cells from the same pre-growth cultivation. Using cells from the same pre-growth cultivation in the two experiments allowed the comparison of pyruvate accumulation and transamination without having the risk that different pre-growth duration would compromise the comparison. However, aerobic and anaerobic experiments were split during the first replica and cells

used for the aerobic experiments were obtained from a different pre-growth cultivation than for the anaerobic experiments. As it will be shown in 3.2.2.1 and 3.3.2, the first experiment of aerobic pyruvate accumulation and transamination in 20 g/L and 50 g/L had neither metabolite formation nor transamination reaction. The lack of pyruvate accumulation and transamination reaction was thought to be due to a too long pre-growth duration in which the cells died. Since the anaerobic experiments were performed with cells from a different pre-growth cultivation no comparison was possible between the two aeration conditions. In order to assess if the reason for the lack of cellular activity during the first aerobic experiments was due to a too long pre-growth duration, enough biomass for all the aerobic and anaerobic experiments was grown and the pre-growth duration was optimized. The pre-growth optimization consisted in following the pre-growth over time through OD_{620nm} measurements. Once the required biomass for all the experiments was obtained the cells were treated as described in 2.4.1 and 2.4.2 and the pyruvate accumulation incubation and transamination reactions were started. The pre-growth duration was reduced by more than 24 hours and by performing all experiments containing cells from the same pre-growth cultivation it was possible to compare pyruvate accumulation and transamination under aerobic and anaerobic conditions.

Both rounds of experiments could therefore not be considered biological replica, since pre-growth duration was optimized between the first and second experiment.

3.2.2.1. Aerobic pyruvate accumulation in phosphate buffer

The effect of glucose concentration during aerobic pyruvate accumulation was screened by inoculating CEN.PK2-1C+PAMT $\Delta thi2$ clone 34 and a control strain in phosphate buffer containing 20 g/L or 50 g/L of glucose under aerobic conditions.

The first experiment resulted in invalid data, as discussed in 3.2.2, since no metabolite formation was observed as shown in Figure 23. The aerobic cultivation containing 20 g/L of glucose had similar profile (data not shown).

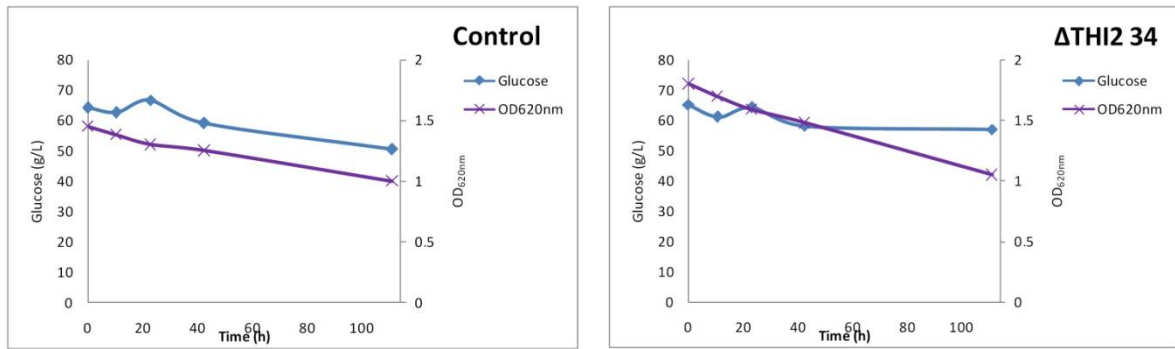


Figure 23- First experiment of CEN.PK2-1C+PAMT $\Delta thi2$ 34 aerobic cultivation in phosphate buffer containing 50 g/L glucose.

A second attempt of aerobic cultivation containing 20 g/L or 50 g/L of glucose was performed after optimizing pre-fermentation growth duration as described in 3.2.2, resulting in the data shown in Figure 24 and Figure 25 respectively. However, the data respectively to the cultivation of the control strain CEN.PK2-1C+PAMT in phosphate buffer containing 20 g/L of glucose was not reliable due to problems during the HPLC analysis.

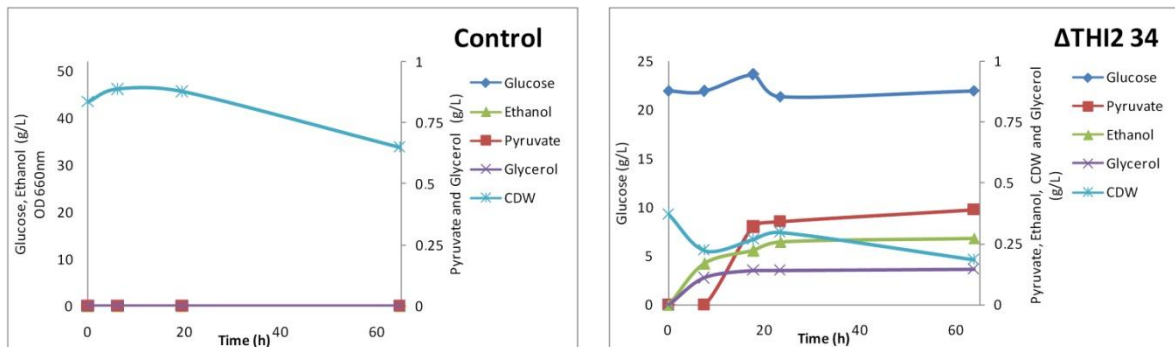


Figure 24- Representative aerobic pyruvate accumulation of CEN.PK2-1C+PAMT $\Delta thi2$ in phosphate buffer containing 20 g/L glucose

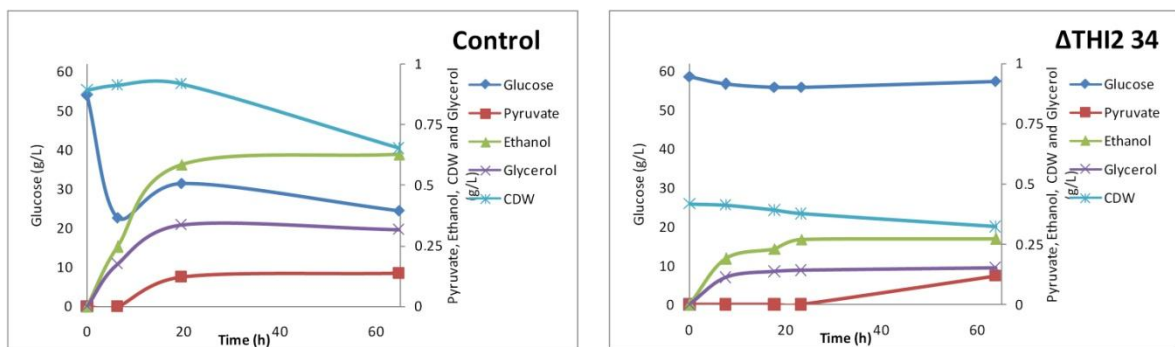


Figure 25- Representative aerobic pyruvate accumulation of CEN.PK2-1C+PAMT $\Delta thi2$ in phosphate buffer containing 50 g/L glucose

Pyruvate titers and yields obtained during aerobic incubation in phosphate buffer are summarized in Table 15.

Table 15- Pyruvate titers and yields obtained in phosphate buffer containing 20 g/L or 50 g/L of glucose under aerobic conditions. Pyruvate accumulation results in 20 g/L of glucose with the control strain were unreliable due to issues in HPLC analysis. The theoretical maximal pyruvate yield (g pyruvate/ g glucose) is 0.98 g/g.

Glucose g/L	Pyruvate titer g/L		Pyruvate yield g pyruvate/g glucose	
	Control	Δ THI2 34	Control	Δ THI2 34
20	-	0.39	-	0.24
50	0.14	0.12	<0.01	0.10

Pyruvate titers and yields for the control strain in phosphate buffer with 20 g/L of glucose were not able to be compared since no reliable results were obtained as shown above. However, a higher pyruvate titer was achieved during aerobic cultivation in phosphate buffer with 20 g/L of glucose than with 50 g/L of glucose by the *thi2* deleted strain.

The desired effect of pyruvate accumulation through the *thi2* deletion was not achieved during aerobic cultivations in phosphate buffer containing 50 g/L of glucose. The pyruvate yield of the *thi2* deleted strain with 50 g/L of glucose however was higher than the control strain.

Comparison of pyruvate titers achieved during aerobic cultivations in Verduyn medium or phosphate buffer showed that pyruvate accumulation was higher during cultivations in Verduyn medium as shown in Figure 26.

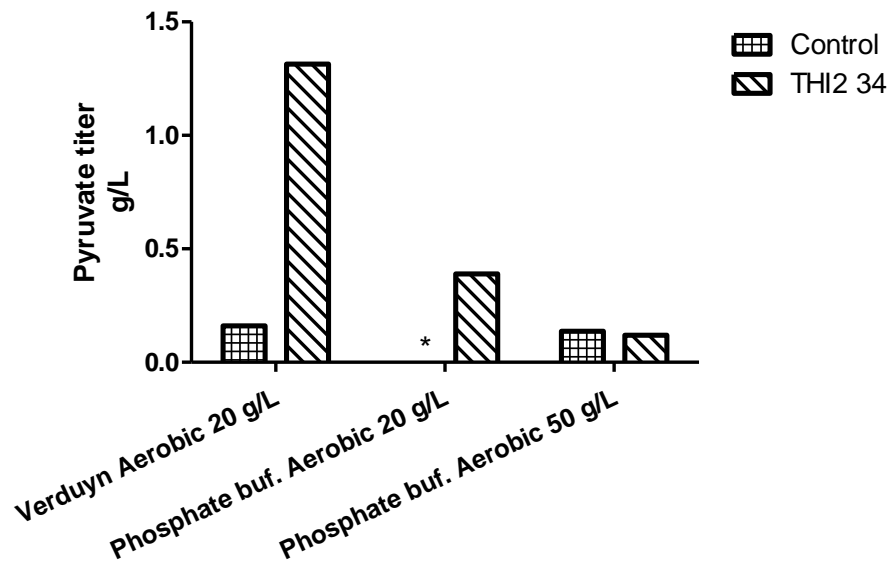


Figure 26- Comparison of pyruvate titers achieved during aerobic pyruvate accumulation in Verduyn medium and phosphate buffer. The * represent the unreliable pyruvate titer result of the control strain in phosphate buffer containing 20 g/L due to HPLC analysis issues.

3.2.2.2. Anaerobic pyruvate accumulation in phosphate buffer

The effect of glucose concentration during anaerobic pyruvate accumulation was screened by inoculating CEN.PK2-1C+PAMT $\Delta thi2$ clone 34 and the control strain in phosphate buffer containing 20 g/L (Figure 27) or 50 g/L of glucose (Figure 28) under anaerobic conditions.

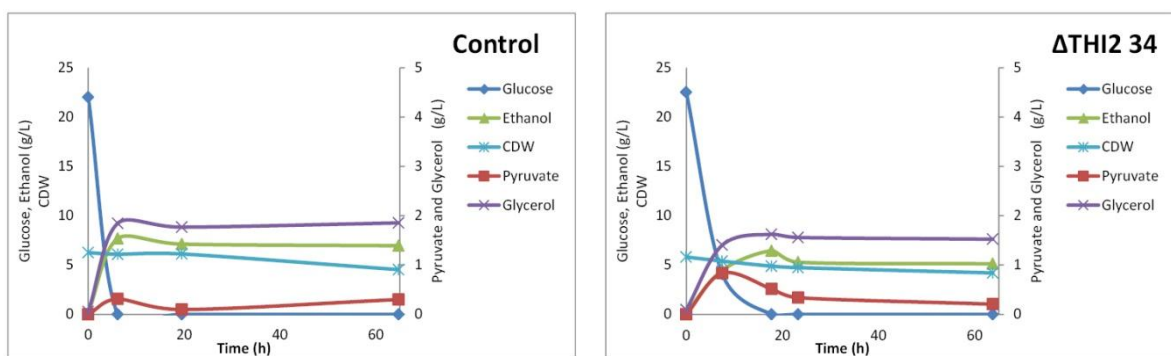


Figure 27- Representative anaerobic pyruvate accumulation of CEN.PK2-1C+PAMT $\Delta thi2$ clone 34 and its control in phosphate buffer containing 20 g/L glucose.

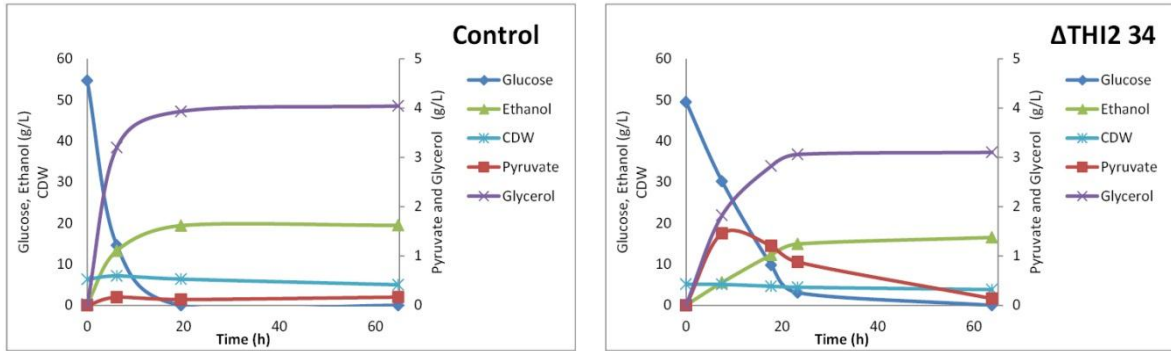


Figure 28- Representative anaerobic pyruvate accumulation of CEN.PK2-1C+PAMT $\Delta thi2$ clone 34 and its control in phosphate buffer containing 50 g/L glucose.

Pyruvate and ethanol titers and yields are summarized respectively in Table 16 and Table 17. Since pre-growth duration was optimized between the two experiments as described in 3.2.2, the results could not be considered as biological replica and were treated separately.

Table 16- Pyruvate titers and yields obtained in phosphate buffer containing 20 g/L or 50 g/L of glucose under anaerobic incubations. Control 1 and $\Delta THI2$ 1 columns represent the first experiment whereas Control 2 and $\Delta THI2$ 2 columns represent the second experiment in which pre-growth duration was optimized as described in 3.2.2. The theoretical maximal pyruvate yield (g pyruvate/ g glucose) is 0.98 g/g.

Glucose g/L	Pyruvate titer g/L				Pyruvate yield g pyruvate/g glucose			
	Control 1	Control 2	$\Delta THI2$ 34 1	$\Delta THI2$ 34 2	Control 1	Control 2	$\Delta THI2$ 34 1	$\Delta THI2$ 34 2
20	0,52	0,31	0,76	0,84	0,026	0,014	0,059	0,045
50	0,53	0,17	0,67	1,46	0,011	<0,01	0,084	0,076

Table 17- Ethanol titers and yields obtained in phosphate buffer containing 20 g/L or 50 g/L of glucose under anaerobic incubations. Control 1 and $\Delta THI2$ 1 columns represent the first experiment whereas Control 2 and $\Delta THI2$ 2 columns represent the second experiment in which pre-growth duration was optimized as described in 3.2.2. The theoretical maximal ethanol yield (g ethanol/ g glucose) is 0.51 g/g.

Glucose g/L	Ethanol titer g/L				Ethanol yield g ethanol/g glucose			
	Control 1	Control 2	$\Delta THI2$ 34 1	$\Delta THI2$ 34 2	Control 1	Control 2	$\Delta THI2$ 34 1	$\Delta THI2$ 34 2
20	6,7	7,7	7,9	6,5	0,33	0,34	0,31	0,23
50	18,6	19,5	9,9	16,5	0,39	0,35	0,34	0,29

CEN.PK2-1C+PAMT $\Delta thi2$ clone 34 demonstrated an improved pyruvate accumulative phenotype of 2.7- and 8.6- fold in phosphate buffer containing, respectively,

20 g/L or 50 g/L of glucose in comparison to the control strain during the incubations in which the pre-growth duration was optimized. Besides the increased pyruvate titer, also the pyruvate yield was improved ~3- and 10- fold in 20 g/L or 50 g/L of glucose.

Ethanol titers and yields in phosphate buffer containing 20 g/L of glucose were similar in both experiments between the control and the $\Delta thi2$ 34 strain. On the contrary, CEN.PK2-1C+PAMT $\Delta thi2$ clone 34 reached a lower ethanol titer than the control strain in phosphate buffer containing 50 g/L in both experiments. However, ethanol yields were similar between the two strains.

The comparison of all anaerobic pyruvate accumulation experiments are summarized in Figure 29.

Comparing the pyruvate titers reached during anaerobic fermentations in phosphate buffer (Figure 29) significant variation between the two experiments of *thi2* deleted strain in phosphate buffer containing 50 g/L of glucose was observed. The significant increase in pyruvate titer during the second experiment demonstrated the importance of pre-growth duration which could be related with an initial higher cellular viability. Yet, biological replicas would be required to confirm the effect of different pre-growth durations.

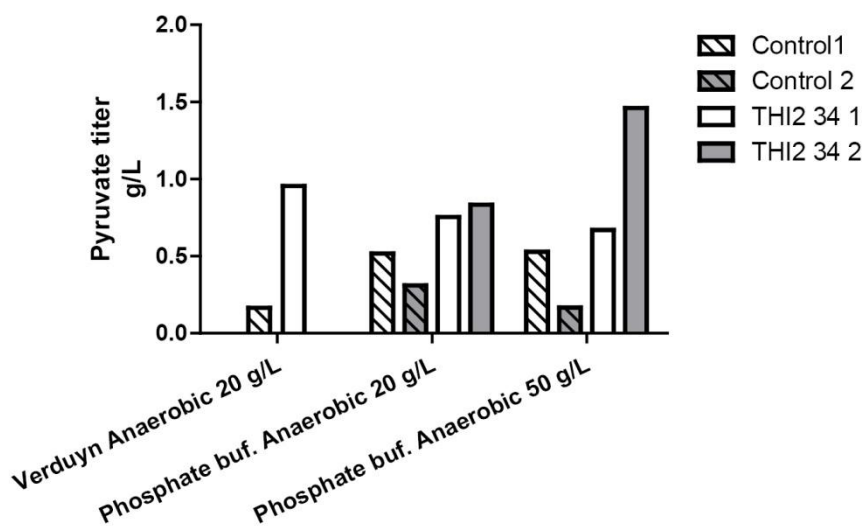


Figure 29- Comparison of pyruvate titers during anaerobic fermentations in Verduyn and phosphate buffer for the control strain and *thi2* deleted clone 34. The grey bars represent the second experiments in which the pre-growth duration was optimized as described in 3.2.2.

3.3. Transamination using the *thi2* deleted strain

After confirming that strains carrying a deletion in *THI2* gene displayed higher pyruvate accumulation than the parental strain, the effect of pyruvate accumulation on the kinetic resolution of *R,S*-PEA was evaluated in phosphate buffer under anaerobic and aerobic conditions with 20 g/L and 50 g/L glucose. The strain CEN.PK2-1C+PAMT $\Delta thi2$ clone 34 was selected for the transamination biocatalysis due to its growth rate and high pyruvate titer.

The second experiments of aerobic and anaerobic transamination incubations were all performed with cells from the same pre-growth cultivation in which the pre-growth duration was optimized as described in 3.2.2.

3.3.1. Anaerobic transamination

The anaerobic transaminations were performed under the same conditions as the pyruvate accumulation fermentations in chapter 3.2.2.2, to be able to relate the pyruvate accumulation directly with the kinetic resolution. A representative reaction profile and the *R,S*-PEA and ACP evolution over time during anaerobic kinetic resolution with 20 g/L or 50 g/L of glucose is shown, respectively, in Figure 30 and Figure 31.

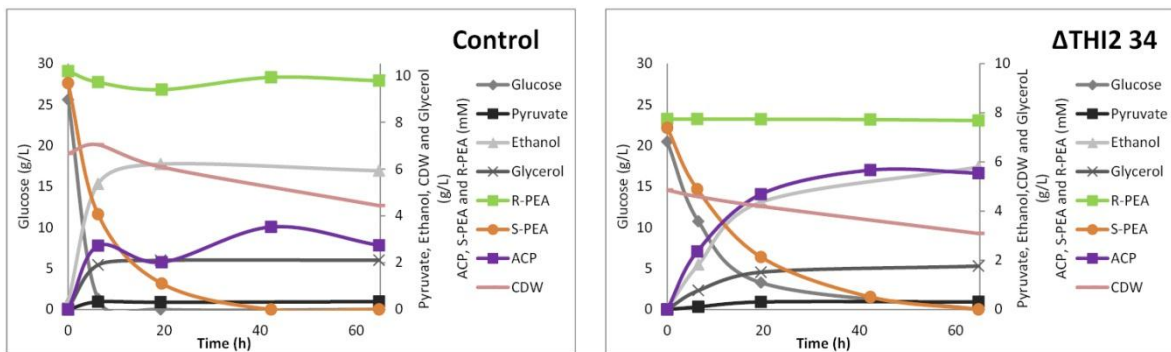


Figure 30-Representative anaerobic kinetic resolution of *R,S*-PEA with CEN.PK2-1C+PAMT $\Delta thi2$ clone 34 and its control strain in phosphate buffer containing 20 g/L glucose. Cells were pre-grown in Verduyn medium containing 20 g/L of glucose and 0.05 μM thiamine.

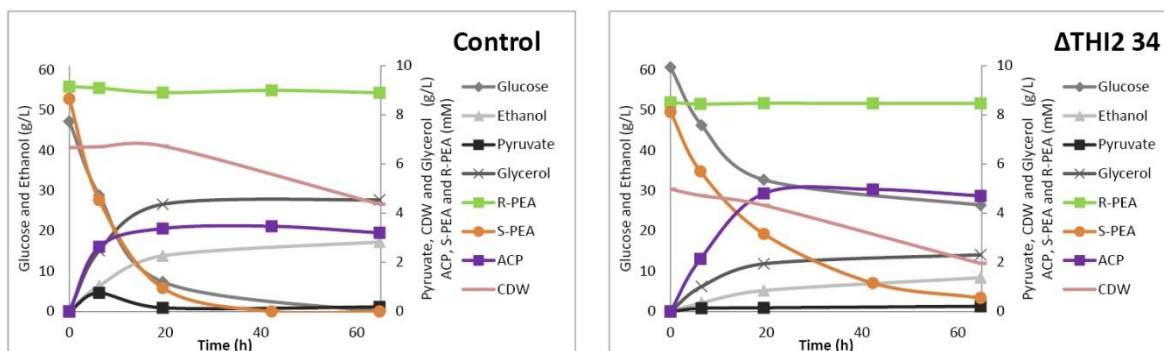


Figure 31- Representative anaerobic kinetic resolution of *R,S*-PEA with CEN.PK2-1C+PAMT $\Delta thi2$ 34 in phosphate buffer containing 50 g/L glucose. Cells were pre-grown in Verduyn medium containing 20 g/L of glucose and 0.05 μ M thiamine.

The conversion rates and enantiometric excess obtained during anaerobic kinetic resolution of *R,S*-PEA with CEN.PK2-1C+PAMT $\Delta thi2$ clone 34 and the control strain in phosphate buffer containing 20 g/L or 50 g/L of glucose are summarized in Table 18. Since pre-growth duration was optimized between the two experiments as described in 3.2.2, the results could not be considered as biological replica and were treated separately.

Table 18- Anaerobic transamination, comparison of conversion and enantiomeric excess in phosphate buffer containing 20 or 50 g/L of glucose. Control 1 and $\Delta THI2$ 1 columns represent the first experiment whereas Control 2 and $\Delta THI2$ 2 columns represent the second experiment in which pre-growth duration was optimized as described in 3.2.2.

Glucose (g/L)	Total conversion (%)				Ee of R-PEA (%)			
	Control 1	Control 2	$\Delta THI2$ 34 1	$\Delta THI2$ 34 2	Control 1	Control 2	$\Delta THI2$ 34 1	$\Delta THI2$ 34 2
20	36,78	51,34	44,07	48,81	57,25	100	78,7	100
50	47,65	49,64	38,71	45,72	89,88	100	63,69	88,49

Taking in account the two experiments, the total conversions achieved by the control strain were slightly higher than *thi2* deleted strain (see Table 18).

Total conversion and enantiomeric excess obtained either by the control or *thi2* deleted strain did not reach interesting values during the first experiments. However, in the second experiment where pre-growth duration was optimized as described in 3.2.2, both parameters were improved for both of the strains. By optimizing the pre-growth duration an enantiomeric excess of 100% was achieved by both strains (except *thi2* deleted strain in 50 g/L of glucose), which means that no *S*-PEA remained in the reaction solution. Yet, the

control strain achieved the *R*-PEA enriched solution faster than the *thi2* deleted strain (Figure 30).

Kinetic resolution of *R,S*-PEA under these conditions was therefore not improved by the deletion of the *THI2* gene.

3.3.2. Aerobic transamination

Aerobic kinetic resolution was performed under the same conditions as in the pyruvate accumulating cultivations described in 3.2.2.1. Despite the lower pyruvate accumulation observed in 3.2.2.1, aerobic transamination was performed in the attempt to observe the effect of oxygen.

Aerobic kinetic resolution of *R,S*-PEA with CEN.PK2-1C+PAMT $\Delta thi2$ clone 34 and the control strain in phosphate buffer containing 20 or 50 g/L of glucose was performed. During the first experiment no metabolite formation or transamination reaction was observed. As described in 3.2.2, such results lead to performing all the experiments with cells obtained from the same pre-growth optimized cultivation.

The results from the second experiment are shown in Figure 32 and Figure 33.

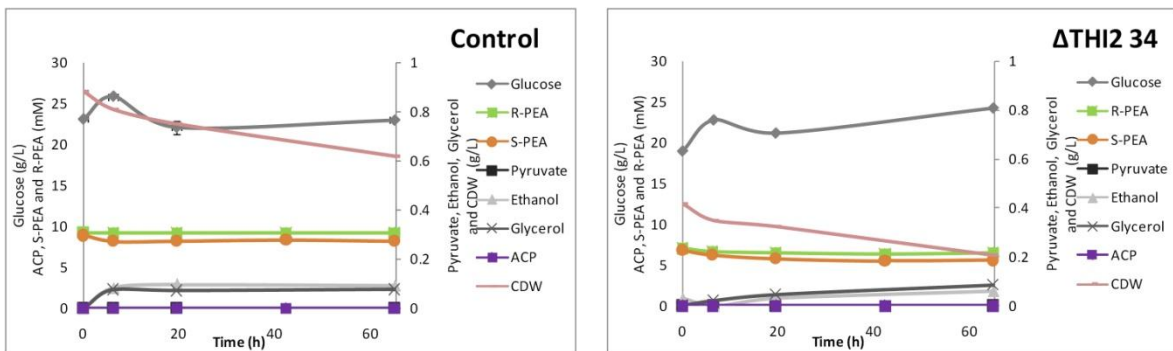


Figure 32- Aerobic kinetic resolution of *R,S*-PEA with CEN.PK2-1C+PAMT $\Delta thi2$ 34 in phosphate buffer containing 20 g/L glucose.

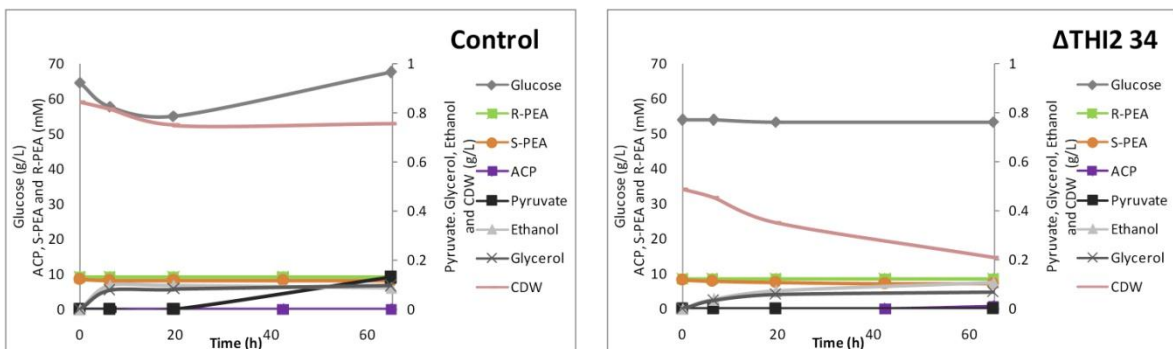


Figure 33- Aerobic kinetic resolution of *R,S*-PEA with CEN.PK2-1C+PAMT $\Delta thi2$ 34 in phosphate buffer containing 50 g/L glucose.

The glucose measurements of the aerobic transaminations were unreliable since glucose concentrations were increasing over time as shown in Figure 32 and Figure 33.

The conversion rates and enantiometric excess obtained during the second experiment of aerobic kinetic resolution of *R,S*-PEA with CEN.PK2-1C+PAMT $\Delta thi2$ 34 and the control strain in phosphate buffer containing 20 g/L or 50 g/L of glucose are summarized in Table 19.

Table 19- Aerobic transamination, comparison of conversion and enantiomeric excess in phosphate buffer containing 20 or 50 g/L of glucose. In this table only the second experiment results were presented since during the first experiment no transamination reaction was observed.

Glucose (g/L)	Total conversion (%)		Ee of <i>R</i> -PEA (%)	
	Neg	$\Delta THI2$ 34	Neg	$\Delta THI2$ 34
20	3.46	3.13	5.80	6.13
50	15.42	8.30	8.76	10.92

Even optimizing the pre-growth cultivation duration, both strains demonstrated low potential for kinetic resolution of *R,S*-PEA and no metabolite formation. These results were similar to the first experiment with cells whose pre-growth cultivation duration was not optimized. As discussed previously in chapter 3.2.2, the hypothesis to explain the results obtained in the first experiment was that the used cells were dead when the reaction started. However, by performing all the second experiments with cells of the same pre-growth cultivation this hypothesis could be declined, since all the second anaerobic experiments containing cells from the pre-growth optimized cultivation were successful and even demonstrated better results than the first experiment. Since all the second experiments in phosphate buffer obtained results except the transamination in aerobic conditions, it is possible to state that the presence of oxygen with *R,S*-PEA has an inhibitory effect on the cells.

4. Discussion

4.1. Strain confirmation and selection

Two strains were constructed to accumulate pyruvate by deletion of PDC structural genes (*PDC1* and *PDC5*) and biosynthetic gene of PDC's cofactor thiamine (*THI2*). The purpose was to improve kinetic resolution of *R,S*-PEA by increasing the amount of the co-substrate pyruvate. In the following sub-chapters the construction of such strains will be discussed.

4.1.1. Construction of the $\Delta thi2$ deleted strain

The desired CEN.PK 2-1C+PAMT $\Delta thi2$ strain was obtained and confirmed by phenotypic, lack of growth in Verduyn medium without thiamine, and genotypic, PCR amplification of the *THI2_trp1* fragment, behavior. The inability of growing in medium without thiamine is related to the enzymes that possess thiamine as co-factor. Besides PDC, other enzymes like acetolactate synthase, transketolase, E1 components of PDH, 2-oxoglutarate dehydrogenase and α -Ketoisocaproate decarboxylase have thiamine as co-factor [103]. PDH and 2-oxoglutarate dehydrogenase catalyze similar reactions, where PDH converts pyruvate into acetyl-CoA and 2-oxoglutarate dehydrogenase converts α -ketoglutarate into succinyl-CoA. Both of the products are important intermediates during the TCA-cycle (Figure 1). By inhibiting the synthesis of succinyl and acetyl-CoA the cell is unable to regenerate co-enzymes aerobically or produce biosynthetic building blocks. Transketolase is another thiamine dependent enzyme which catalyzes the synthesis of erythrose-4-phosphate, an aromatic aminoacid precursor. By inhibiting the activity of transketolase through thiamine auxotrophy, yeast is unable to grow since it cannot produce aromatic aminoacids [104]. Another enzyme which leads to low biomass formation by thiamine auxotrophy is α -acetolactate synthase since it is responsible for the first step in isoleucine and valine biosynthesis [103]. Growing the $\Delta thi2$ strain in medium without thiamine would increase the pyruvate accumulation since even small amounts of this co-factor allow pyruvate consumption by PDC. However, the media required for growing the strain without thiamine would need supplements of all aminoacids and biosynthetic precursors which are connected to thiamine. This media would be possible to prepare for a laboratorial scale yet its application in an industrial scale would be expensive and

operationally ineffective. The minimal concentration of thiamine to obtain biomass was screened to develop a more industrial feasible upstream process. The minimal thiamine concentration that allows biomass formation was 0.05 μM . However, this concentration only allowed obtaining small amounts of biomass per cultivation. This means that in order to obtain the required biomass for the start of the fermentations/cultivations a considerable amount of pre-fermentation growth cultivations was required.

4.1.2. Construction of $\Delta pdc1 \Delta pdc5$ double deleted strain

Another strategy for pyruvate accumulation in *S. cerevisiae* which has been evaluated in this study was a double knock-out of *PDC1* and *PDC5*.

In the first attempt of transformation, the control strain was transformed with each deletion cassette individually or simultaneously. Growth was observed in several transformation plates but only colonies solely transformed with the *PDC5* deletion cassette were successfully confirmed through PCR amplification.

After obtaining the CEN.PK2-1C+PAMT $\Delta pdc5$ strain a single colony was selected and transformed with the $\Delta PDC1$ deletion cassette. The desired strain could not be isolated due to inconclusive PCR results and a high rate of false positive colonies on the transformation plates.

The high rate of colonies that restored the auxotrophic marker without deleting the targeted genes can be explained by homologous recombination between the marker sequence within the deletion cassette and the disrupted marker in the strain (Figure 34). This is possible because the auxotrophic marker in the deletion cassette was amplified from genomic DNA with high similarity to the background strain. The similarity enables a homologous recombination between the marker sequence of the deletion cassette and the disrupted marker gene of the auxotrophic strain. The recombination between the marker sequences results in a strain that grows in media without the supplementation of the aminoacids but does not possess the desired deletion.

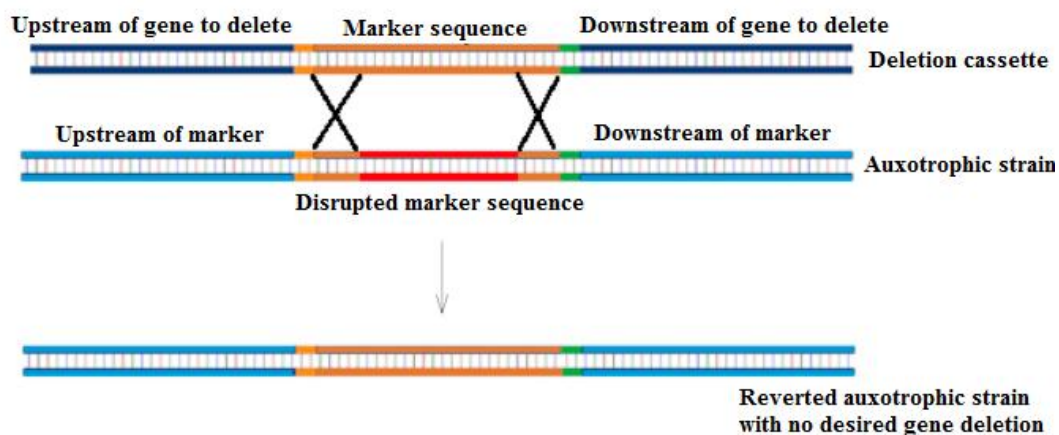


Figure 34- Possible mechanism for false positive colonies in Δ PDC strains. The high similarity between the marker sequence of the deletion cassette and the disrupted marker of the strain allows the homologous recombination between the two marker sequence and restore the expression of the amino acid biosynthetic gene.

However, the most probable recombination should still be the one with the targeted gene since it has longer homologous sequences. At first, transformation plates were prepared with glucose as carbon source which would indirectly select only the false positive strains since the double deleted strains could not grow on glucose. The glucose sensitive phenotype was thought to be due to the inability of synthesizing cytosolic acetyl-CoA which is required for lysine and fatty acid synthesis [58]. In an attempt to overcome such drawback, *Van Maris et al* overexpressed threonine aldolase, which converts threonine to glycine and acetaldehyde, in a Δ PDC strain [105]. The overexpression of threonine aldolase would provide the required acetaldehyde for the production of acetyl-CoA. However, the strain was still unable to grow in high glucose concentrations. Therefore, the reasons for the glucose sensitive phenotype of the Δ PDC strains are still unknown. Attempts to overcome this glucose sensitive phenotype have been focused on directed evolutions followed by the analysis of transcriptome to identify possible genes related to adaptation [68, 73].

Since not so much is known about the glucose sensitive phenotype of PDC deleted strains, the only alternative to increase the probability of isolating a PDC deleted strain was to change glucose by ethanol in the transformation plates. By providing ethanol as the only carbon source, the PDC deleted cells would be able to produce cytosolic acetyl-CoA and thereby grow. However, as expected growth on ethanol plates took some weeks to observe the formation of colonies.

Additionally, to increase the efficiency of selecting the PDC deleted strain the PCR method was changed from colony PCR to genomic DNA extraction followed by PCR amplification. This alternative approach was more time consuming but increased the quality of the PCR amplification by avoiding contamination of potential inhibitors of the DNA polymerase present in the cells. Also to increase the probability of obtaining the desired double deleted strain, the cells after being exposed to the transformation heat shock were incubated in yeast extract peptone (YP) solution during 3 hours. The purpose of the incubation in YP was to regenerate the cell membrane in order to handle the drastic exposure to ethanol.

After improving the transformation and confirmation methods, the desired double deleted strain was obtained as shown in Figure 15 and Figure 16. The dual band from WPDC1 in Figure 15 colony 3, shows the importance of the amplification of WPDC1/WPDC5 fragments. In the specific case of colony 3 it is possible to see that one of the *PDC1 locus* was successfully deleted but that there was still one *locus* with a functional gene. The appearance of two bands was unexpected since haploid strains should only possess a single copy of each gene since they possess only one copy of each chromosome. The existence of two *loci* could be possibly explained by the existence of two *PDC1* gene copies in the same chromosome due to the importance of the *PDC1* gene for the viability of the cell. It is also to notice that if only the amplification of *PDC1_trp1* would be used for strain confirmation the situation discussed above would never be noticed.

All of the selected colonies for PCR strain confirmation were streaked on a new plate. After screening and selecting the colonies containing the double deletions, single colonies from the streaked plate were pre-grown to prepare respective glycerol stocks. Each colony was inoculated in YP containing ethanol in order to obtain biomass required for the fermentations/cultivations. At the same time each colony was inoculated in Verduyn medium containing glucose as carbon source to confirm the glucose sensitive phenotype. However, after 48 hours growth was present in the 250 mL shake flasks. Since no growth was the expected result the DNA of the cells in those cultivations was extracted and PCR amplification of *PDC1_trp1* and WPDC1 was conducted. Surprisingly the PCR demonstrated that the deletions were not present even if those were confirmed before streaking the colonies (Figure 17). The occurrence of pyruvate decarboxylase activity in $\Delta pdc1 \Delta pdc5$ strains and consequent growth in glucose was discussed by Hohman [106].

In this work the growth of $\Delta pdc1 \Delta pdc5$ strains in glucose is explained by the fusion of the *PDC1* promoter with the *PDC6* structural gene. The *PDC6* gene is poorly expressed and its deletion has no effect in pyruvate decarboxylase activity [57]. However, *PDC6* sequence is 84% homologous to *PDC1* showing that the null effect of *PDC6* deletion in PDC activity is due to its low expression level and not inefficient protein activity [103, 107]. It is also reported that the high expression of *PDC1* compared to the other PDC genes is due to its promoter [106]. The fusion between the promoter of *PDC1* and structural gene of *PDC6* would result in a high expression of *PDC6* which by having high structural homology with *PDC1* would lead to the expression of an active PDC.

However, in this case fusion between the *PDC1* promoter and *PDC6* structural gene was not the reason for growth in glucose media since *PDC1* gene was intact leading to the expression of PDC (Figure 17). Reversing a gene knockout in the genomic DNA is uncommon. The loss of the deleted strain can then be explained by contamination during the handling of the strains, by recombination solely between auxotrophic markers as described above or growth of undeleted cells within the colony at the expense of nearby cells. However, the loss of the desired strain just by streaking the colony is still unclear and several attempts to find the desired strain were conducted. These attempts consisted in picking cells from the 'mother' colonies that were streaked and inoculating them in 10 mL of YP ethanol. After overnight growth half of the culture was used to extract the DNA and the other half was directly used for the glycerol stock avoiding the problem of picking a wrong colony from streaked plates. However, the isolation of the desired double knock-out strain was not successful due to problems with PCR amplification since the DNA quality was very low and selection of undeleted colonies from the plate. Nevertheless, it was possible to obtain PCR amplification of certain colonies which revealed intact *PDC1*. As a final attempt the colonies were grown in non-fermentable minimal media instead of an undefined rich media containing ethanol. The purpose was to avoid over-growth of undesired cells since the double deleted strain would grow at the same growth rate as the false positive colonies. The media consisted in YNB without amino acids (6,7 g/L) buffered with succinic acid (10g/L) and supplemented with glycerol (50 g/L), ethanol (20 g/L), glutamic acid (10 g/L) and aspartic acid (10 g/L) as carbon sources [108]. Yet no desired double deleted strain was found from all of the screened colonies.

Despite all the attempts and strategies no double deleted strain was successfully recovered and stored even having previously confirmed three colonies with the desired deletions. Since the main issue for selecting the desired CEN.PK2-1C+PAMT $\Delta pdc1$ $\Delta pdc5$ is the glucose sensitive phenotype, it would be interesting to start the construction of such strain by deleting *MTH1*. Deletion of *MTH1* provides the ability of a PDC deleted strain to grow in glucose containing medium as described in chapter 1.3.1 avoiding growth issues and increase the number of desired colonies compared to the false positives colonies [73].

4.2. Pyruvate Accumulation with CEN.PK2-1C+PAMT $\Delta THI2$

4.2.1. Pyruvate accumulation in Verduyn medium

The first attempts to assess if the obtained CEN.PK2-1C+PAMT $\Delta thi2$ strains possess the desired pyruvate accumulative phenotype were performed in Verduyn medium lacking thiamine. The deleted strain cannot grow in media lacking thiamine which means that a pre-fermentation growth was necessary. The concentration of thiamine during pre-fermentation growth is critical since even small amounts of this vitamin result in an active PDC making the effect of thiamine biosynthetic gene deletion unnoticeable [69]. Several concentrations of thiamine for the pre-fermentation growth medium were screened and the concentration of 0.05 μ M of thiamine was the limit to obtain growth. Anaerobic and aerobic cultivations were carried out with cells pre-grown in Verduyn medium containing either the common thiamine concentration or the minimal concentration. The pyruvate accumulative phenotype of CEN.PK2-1C+PAMT $\Delta thi2$ clone 34 cells pre-grown in common thiamine concentration was only observed in aerobic cultivation. This result was unexpected since pyruvate accumulation should be higher in anaerobic conditions due to a low activity of PDH and PYC combined with the inhibited PDC. The high cellular density with which the anaerobic fermentations started, in contrast to the aerobic cultivations could be the reason for the results observed. Thiamine as a co-factor is not consumed which results in its accumulation inside of the cells. Even after washing the cells with demineralized water the amount of intracellular thiamine accumulated during pre-growth could provide the amount of vitamin to keep a part of the yeast population with an active PDC. This possibility is supported by the ethanol production rate measured during the

pyruvate accumulation fermentations under anaerobic conditions. As shown in Figure 19 the ethanol production rate of the *thi2* deleted strain is similar to the control strain. The similar ethanol production rate demonstrates that no thiamine shortage was present. On the contrary, anaerobic fermentations with the *thi2* deleted cells pre-grown in the minimal thiamine concentration demonstrated increased pyruvate accumulation. This demonstrates the importance of thiamine concentration during pre-fermentation growth.

The highest improvement in pyruvate accumulation by decreasing the thiamine concentration during pre-growth was observed during anaerobic fermentations (10-fold improvement in comparison to cells pre-grown in normal thiamine concentration) as described in 3.2.1.2. Yet, even with a higher improvement in anaerobic fermentations the *thi2* deleted strain reached similar pyruvate titers than in aerobic cultivations. This can be explained by the lower pyruvate accumulation in anaerobic fermentations with cells pre-grown in normal thiamine concentration than in the respective aerobic cultivations. The lower pyruvate accumulation with cells pre-grown in normal thiamine concentration under anaerobic conditions is due to a quick assimilation of pyruvate to convert acetaldehyde into ethanol and regenerate NAD^+ in which for each pyruvate molecule consumed one molecule of NAD^+ is regenerated. In aerobic conditions, the assimilation of pyruvate in the TCA cycle leads to an increased regeneration of NAD^+ per molecule of pyruvate which thereby leads to lower pyruvate consumption. In this way, the *thi2* deleted strain reaches the same pyruvate titer under anaerobic and aerobic conditions with cells pre-grown with the minimal thiamine concentration, but the effect of varying the thiamine concentration during pre-growth is more pronounced in anaerobic than in aerobic conditions, because anaerobically it accumulates less pyruvate with cells pre-grown in normal thiamine concentration.

However, more biological replicas would be needed to prove this hypothesis since these assumptions are based on a single experiment. Since in aerobic cultivations the initial cellular density was much lower this phenomenon would not occur leading to a partial pyruvate accumulative phenotype.

4.2.2. Pyruvate accumulation in phosphate buffer

As it was proven that the desired pyruvate accumulating phenotype was possible, incubations were performed in phosphate buffer to assess if the desired phenotype was also present in the transamination solution. Incubations in phosphate buffer lacking *R,S*-PEA allowed measuring the pyruvate accumulation and directly relate its effect during the transamination reactions. Phosphate buffer does not provide the co-factors and salts required for yeast growth as Verduyn medium. However, the development of a biocatalytic process in this solution is in an economical and industrial point of view more profitable due to its low preparation cost and also providing simpler and faster downstream processes.

The first experiments of pyruvate accumulation in phosphate buffer were performed with cells whose pre-growth cultivation were between 48-54 hours to assure that the cells were in mid-stationary phase and obtain the maximum biomass amount per cultivation. However, the first aerobic incubations did not present any metabolite formation which was thought to be due to the use of dead cells since the pre-growth cultivation could be too long. To assess such hypothesis and obtain a reference to compare if the cells were dead, pre-growth duration was optimized and biomass was obtained to start all the experiments with the same pre-grown cells, as described in 3.2.2.

The pyruvate accumulation phenotype was present in both anaerobic incubations with the *thi2* deleted strain in phosphate buffer as shown in Table 16. During the second experiment, higher pyruvate titers and yields (both 1.7-fold improved) were achieved by the *thi2* deleted strain in phosphate buffer containing 50 g/L of glucose in comparison to the incubation in 20 g/L of glucose with the same strain. The reason could be a higher glycolytic flux creating an increase overflow in the pyruvate branch point. The obtained pyruvate titers did not reach the values previously reported by *Xu et al.* since in this work the maximum pyruvate titer reached was 8.21 g/L compared to the 1.46 g/L of pyruvate accumulated in this thesis. However, the variance can be explained due to a more complex fermentation media since it contained NH_4Cl , KH_2PO_4 , $\text{MgSO}_4 \cdot 7\text{H}_2\text{O}$, urea and 0.04 μM of thiamine such as an optimized carbon-nitrogen ration [69]. By having thiamine during the pyruvate accumulation fermentation the cellular viability is increased since cytosolic acetyl-CoA is produced leading to generation of biosynthetic precursors. This leads to an increased number of cells with a higher viability resulting in higher carbon flow and

consequently higher pyruvate titers. However, the approach of having the minimal thiamine concentration during the pyruvate accumulation fermentation was not followed in this study since the preparation of media containing a specific concentration of thiamine is impractical and expensive for industrial purposes. Another drawback of providing thiamine during fermentations to accumulate pyruvate is the possibility to loose carbon to biomass, resulting in lower yields.

The *thi2* deletion should have a direct effect in ethanol titers and yields since through inactivation of PDC no acetaldehyde is formed to be consumed by ADH. Ethanol titers were mainly lower for the *thi2* deleted strain in comparison to the control strain, especially in incubations containing 50 g/L of glucose (Table 17). Even producing lower ethanol titers in fermentations containing 50 g/L of glucose, the deleted *thi2* strain obtained yield values similar to the ones reached by the control strain (see Table 17). By achieving the same ethanol yield even producing less ethanol than the control strain, the *thi2* deleted strain would have to re-direct the glucose consumption mainly for ethanol production and avoid consumption for other cellular requirements. This can be explained by the effect of thiamine auxotrophy in an overall view which is the lower biomass formation. The control strain enables the activity of several enzymes related to biomass formation by production of thiamine which would thereby lead to the consumption of glucose for biomass synthesis. However, the *thi2* deleted strain does not have thiamine to maintain those enzymes active and thereby the glucose would be mainly consumed in ethanol formation. This can be based on the slower glucose consumption by the *thi2* deleted strain in Figure 28 which shows the lower glucose demand.

Comparing with the values reported by *Xu et al* [69], the ethanol titers and yield obtained by the *thi2* deleted strain in this work were, respectively, 2.8- and 1.6-fold higher. However, the different conditions in which pyruvate was accumulated by *Xu et al* could explain the different ethanol titers. *Xu et al* performed the pyruvate accumulation under aerobic conditions with less biomass concentration (2.24 OD_{620nm}). In aerobic conditions, glucose is consumed through respiration and, depending on the extracellular glucose concentration, partially consumed for ethanol production. By consuming glucose to fuel both of these pathways, the ethanol titers and yields are lower.

Independent of the glucose concentration, pyruvate accumulation by *thi2* deleted strain in phosphate buffer during aerobic cultivations, did not reach the titers obtained

during anaerobic fermentations (Table 15 and Table 16). This was unexpected since high pyruvate titers were achieved by *Xu et al* in aerobic conditions. Additionally, high pyruvate titers were observed during aerobic cultivations in Verduyn medium as discussed in 4.2.1, which would suggest that pyruvate accumulation would occur also in phosphate buffer. Performing transamination reactions in Verduyn medium lacking thiamine would be interesting since pyruvate accumulation observed in Verduyn medium during aerobic cultivations was much higher than in phosphate buffer.

4.3. Pyruvate accumulation effect in kinetic resolution of amines

Total conversion and enantiometric excess of R-PEA were the two parameters analyzed during the kinetic resolution of *R,S*-PEA to evaluate the effect of the pyruvate accumulation. The total conversion shows the reaction rate of the transamination reaction by relating the total initial amount with the total final amount of amine. The theoretical maximum value for total conversion is 50 %, which would mean that all of the *S*-PEA was converted to ACP. The enantiometric excess is related to the purpose of the reaction which is to obtain a solution only containing *R*-PEA. The desired result is an enantiometric excess of >99% which would be a solution only containing *R*-PEA. Though, due to intrinsic problems during an industrial process it is difficult to reach an enantiometric excess of >99%. However, only amines for pharmaceutical applications require such high enantiomeric excess, which is mainly obtained through downstream purifications.

During aerobic transaminations neither total conversion nor enantiometric excess demonstrated a good reaction rate or the obtainment of a commercial valuable enantiometric enriched amine solution. In the first experiment where the pre-growth duration was not optimized, no metabolite formation neither variation in the *R,S*-PEA concentration was observed. Such result was thought to be due to the use of dead cells since the pre-growth duration could be too long. To assess such hypothesis the pre-growth duration was optimized as described in 3.2.2 and all the second experiments were performed with cells from the same pre-growth cultivation. All the second anaerobic experiments with the pre-growth duration optimized cells resulted in improved results in comparison to the first experiment. However, the aerobic kinetic resolution with the same cells demonstrated some residual cellular activity as shown in Figure 32 and Figure 33. This demonstrates that the lack of metabolite formation and transamination reaction in

aerobic conditions is not due to cellular death during the pre-growth cultivations, since cells of the same pre-growth cultivation demonstrated pyruvate accumulation and transaminase activity under anaerobic conditions. However, since such assumptions were based on one experiment more replicas are required. A more accurate assessment would consist of viability assays during the transamination incubations.

Better results were obtained during anaerobic transamination reactions which were also expected since higher pyruvate titers were obtained during the pyruvate accumulation incubations in phosphate buffer. It is possible to see that biocatalysis with the *thi2* deleted strain resulted in higher ACP concentrations in comparison to the control strain, as shown in Figure 30 and Figure 31. The high ACP concentrations should mean better transamination rates however the total conversion and enantiometric excess did not show improvements in comparison to the control strain. The higher ACP values obtained by the *thi2* deleted strain can be explained by differences observed during the organic extraction step. During organic extraction the samples from the control strain possessed a smeary phase between the aqueous and organic phase which complicates extraction resulting in lower volumes recovered. Additional centrifugations were performed to remove the smeary phase and even with some improvements the volume recovered was lower than in the *thi2* deleted samples. The existence of the smeary phase could be due to a higher number of proteins since the control strain by producing biosynthetic precursors can lead to increase protein expression. This assumption can be grounded by the increase of the smeary phase over the sampling time. Also the high volatility of ACP could lead to lower concentrations in the control strain since control samples required additional centrifugations.

Kinetic resolution with control strain reached the *R*-PEA enriched solution 2.7-fold faster than the *thi2* deleted strain during the second experiment as shown in Figure 30 and Figure 31. This parameter is also important for an industrial process since this would represent higher productivities. It is also to notice that the *thi2* deleted strain only reached high enantiomeric excess during the second experiment demonstrating the importance of pre-growth cultivation duration.

Anaerobic kinetic resolution with 50 g/L of glucose catalyzed by the *thi2* deleted strain showed lower total conversion and enantiometric excess in comparison to the reactions performed in 20 g/L with the same strain. The decrease of kinetic resolution in

phosphate buffer containing 50 g/L by the *thi2* deleted strain was not expected since pyruvate accumulation was higher in phosphate buffer.

Nevertheless, the obtained values showed that the control strain was not improved by deletion of *thi2* and that it reached the *R*-PEA enriched solution faster than the constructed strain. The higher transamination biocatalysis observed by the control strain can be explained by its pyruvate accumulation shown in Table 16. The pyruvate pool measured during the second anaerobic pyruvate accumulation containing 20 g/L of glucose represents an extracellular pyruvate concentration of 0.31 g/L (3.52 mM). Taking into account that stoichiometric amounts of pyruvate are required for kinetic resolution and that the maximum *S*-PEA concentration to be converted is 12.5 mM, shows that the maximum pyruvate concentration measured is by itself already around a fourth of the total pyruvate required. This demonstrates that the control strain could possess the requirements to convert the 12.5 mM of *S*-PEA in an efficient way. Another observation that grounds the possibility that the control strain is already efficient in converting 12.5 mM of *S*-PEA is the minimal pyruvate accumulation observed during the biocatalysis. Pyruvate titers of 0.3 g/L and 0.7 g/L were measured during the second kinetic resolution reactions in phosphate buffer containing 20 g/L and 50 g/L of glucose respectively. By measuring extracellular pyruvate during transaminations, it implies that the cells are saturated in pyruvate and that they possess the required pyruvate for the transaminase activity and for metabolic pathways. The lack of pyruvate shortage in the control strain is also proven by ethanol titers. During the second transamination reactions the ethanol titer achieved was 6.2 g/L and 17.2 g/L in respectively 20 g/L and 50 g/L of glucose whereas in pyruvate accumulation fermentations the ethanol titers were 6.5 g/L and 16.5 g/L respectively. By having similar ethanol titers it is possible to state that no pyruvate shortage by the control strain is present in the kinetic resolution of *R,S*-PEA and thereby no improvement with the *thi2* deletion could be observed. The metabolism of the control strain is more active than the *thi2* deleted strain resulting in higher protein expression during pre-fermentation growth. The transaminase expression could thereby also be increased during pre-fermentation growth leading to a faster reaction rate in comparison to the *thi2* deleted strain as shown in Figure 30 and Figure 31. The quantification of transaminase expression by analyzing the transcriptome and the evaluation of cellular viability by flow cytometry or serial plating would assess if this hypothesis is correct.

A possible alternative to observe the effect of *thi2* deletion in kinetic resolution using transaminases would be increasing the amine concentration to a value in which the control strain would show a shortage in pyruvate. The additional pyruvate accumulated by the *thi2* deleted strain would in this way convert *S*-PEA that the control strain could not. Another advantage of such approach is the production of a more concentrated enriched amine solution by the *thi2* deleted strain since the initial *R*-PEA concentration would also be higher. However, the screening of high PEA concentrations would be limited by its toxicity to the cells.

5. Conclusions

The construction of the two desired strains was successful and confirmed through PCR. However, CEN.PK2-1C+PAMT $\Delta pdc1 \Delta pdc5$ was not possible to construct due to possible homologous recombination between the disrupted marker sequences of the strain and the marker sequence of the deletion cassette. Also issues during colony restreaking could explain the isolation of undeleted colonies.

The first attempt to assess pyruvate accumulation of the *thi2* deleted strain was in Verduyn medium where the effect of thiamine concentration during pre-fermentation growth was also assessed. Improvements by reducing the thiamine concentration during pre-growth was observed since pyruvate accumulation of *thi2* deleted strain increased 2- and 10-fold in, respectively, aerobic and anaerobic fermentations in Verduyn medium containing 20 g/L of glucose.

Having the desired pyruvate accumulative phenotype of the *thi2* deleted strain confirmed, fermentations and kinetic resolution were carried out in phosphate buffer. The maximum pyruvate titer of 1.46 g/L was achieved by CEN.PK2-1C+PAMT $\Delta thi2$ 34 in phosphate buffer containing 50 g/L in comparison to the 0.17 g/L accumulated by the control strain under the same conditions.

The kinetic resolution of *R,S*-PEA was not significantly improved by the *thi2* deletion. The total conversion and enantiomeric excess were similar between the control and the *thi2* deleted strains. The similar results can be explained by a native sufficient pyruvate accumulation by the control strain. The lack of pyruvate shortage can be grounded by the pyruvate accumulation and ethanol titers achieved by the control strain during the transaminations. Another parameter in which the control strain showed better results was the time required to obtain the amine enriched solution. The control strain achieved high enantiomeric excess faster than the *thi2* deleted strain. The higher reaction rate of the control strain can be explained by a more active metabolism due to an active PDC which leads to the production of biosynthetic precursors. The expression of transaminase could indirectly be increased during pre-fermentation growth leading to the faster conversion observed during the reactions.

Through this thesis the improvement of pyruvate accumulation was achieved by deleting the *thi2* but since the Δ PDC strain was not successfully isolated both of the initial

approaches could not be compared. The kinetic resolution of *R,S*-PEA was not improved by the *thi2* deletion. However, the results suggested that the lack of improvements were not due to intrinsic problems with the constructed strains but to the use of an inadequate reaction set up. Further investigations are required to improve the kinetic resolution with the *thi2* deleted strain.

6. Future Work

According to the obtained results, additional biological replicas of the fermentations with the optimized pre-growth cultivation duration should be performed to increase the accuracy of the results.

Since the desired CEN.PK2-1C+PAMT $\Delta pdc1 \Delta pdc5$ was not isolated, a different approach could be to begin the strain construction by deleting *MTH1* in order to overcome the glucose sensitive phenotype and facilitate the strain selection.

During the kinetic resolution of *R,S*-PEA the cellular viability and expression of transaminase should be followed to understand their relation with the deletion of *THI2*. The cellular viability could be followed by taking time point samples, stain them with Calcein AM, which is a dye that only stain viable cells and analyze those samples with flow cytometry. An alternative approach could consist in serial dilution plating of time point samples and counting the number of CFU's over time. The expression of transaminase could be followed by real time PCR since it quantifies the amount of mRNA of a specific gene.

As discussed in chapter 4.3, the lack of improvement during kinetic resolution of *R,S*-PEA by the *thi2* deleted strain can be due to an amine concentration which is low enough for the control strain to convert it in an efficient way. Higher amine concentrations should therefore be screened to assess if by increasing the amine concentration the *thi2* deleted strain demonstrates the advantage of higher pyruvate accumulation in comparison to the control strain.

7. References

- [1] D. Samuel, "Investigation of ancient Egyptian baking and brewing methods by correlative microscopy," *Science*, pp. 488-490, 1996.
- [2] J. A. Barnett, "Beginnings of microbiology and biochemistry: the contribution of yeast research," *Microbiology-Sgm*, pp. 557-567, 2003.
- [3] S. E. Milner and A. R. Maguire, "Recent trends in whole cell and isolated enzymes in enantioselective synthesis," *Arkivoc*, pp. 321-382, 2012.
- [4] C. de Carvalho, "Enzymatic and whole cell catalysis: Finding new strategies for old processes," *Biotechnology Advances*, pp. 75-83, 2011.
- [5] B. Pscheidt and A. Glieder, "Yeast cell factories for fine chemical and API production," *Microbial Cell Factories*, 2008.
- [6] R. Kohler, "The background to Eduard Buchner's discovery of cell-free fermentation," *Journal of the History of Biology*, pp. 35-61, 1971.
- [7] H. J. Muller, "Further studies on the nature and causes of gene mutations," *Proceedings of the Sixth International Congress of Genetics, Ithaca, New York.*, pp. 213-255, 1932.
- [8] J. E. Bailey, "Toward a science of Metabolic Engineering " *Science*, pp. 1668-1675, 1991.
- [9] S. Anderson, C. Bermanmarks, J. Miller, D. Estell, K. Stafford, J. Seymour, D. Light, W. Rastetter, and R. Lazarus, "A novel process for L-ascorbate synthesis - production of 2-keto-L-gulonate by a recombinant *Erwinia-Herbicola*," *Abstracts of Papers of the American Chemical Society*, pp. 71, 1985.
- [10] J. Nielsen, "Metabolic engineering," *Applied Microbiology and Biotechnology*, pp. 263-283, 2001.
- [11] M. Patek, J. Holatko, T. Busche, J. Kalinowski, and J. Nesvera, "Corynebacterium glutamicum promoters: a practical approach," *Microbial Biotechnology*, pp. 103-117, 2013.
- [12] J. A. Dietrich, D. L. Shis, A. Alikhani, and J. D. Keasling, "Transcription Factor-Based Screens and Synthetic Selections for Microbial Small-Molecule Biosynthesis," *Acs Synthetic Biology*, pp. 47-58, 2013.
- [13] J. M. Willey, L. M. Sherwood, and C. J. Woolverton, *Prescott/Harley/Klein's Microbiology: McGraw-Hill Science/Engineering/Math*; 7 edition, 2008.
- [14] I. Stefanini, L. Dapporto, J. L. Legras, A. Calabretta, M. Di Paola, C. De Filippo, R. Viola, P. Capretti, M. Polsinelli, S. Turillazzi, and D. Cavalieri, "Role of social wasps in *Saccharomyces cerevisiae* ecology and evolution," *Proceedings of the National Academy of Sciences of the United States of America*, pp. 13398-13403, 2012.
- [15] H. Feldmann, *Yeast: molecular and cell biology*. Weinheim, Germany: Wiley-VCH, 2010.
- [16] B. G. Curran and V. Bugeja, "Basic Investigations in *Saccharomyces cerevisiae*," in *Yeast Protocol.*, pp. 1-13, 2006.
- [17] R. A. J. Darby, S. P. Cartwright, M. V. Dilworth, and R. M. Bill, "Which yeast species shall I choose? *Saccharomyces cerevisiae* versus *Pichia pastoris* (review)," *Methods in molecular biology (Clifton, N.J.)*, pp. 11-23, 2012.
- [18] N. Bonander, C. Ferndahl, P. Mostad, M. D. B. Wilks, C. Chang, L. Showe, L. Gustafsson, C. Larsson, and R. M. Bill, "Transcriptome analysis of a respiratory

- Saccharomyces cerevisiae strain suggests the expression of its phenotype is glucose insensitive and predominantly controlled by Hap4, Cat8 and Mig1," *Bmc Genomics* 2008.
- [19] J. M. Thomson, E. A. Gaucher, M. F. Burgan, D. W. De Kee, T. Li, J. P. Aris, and S. A. Benner, "Resurrecting ancestral alcohol dehydrogenases from yeast," *Nature Genetics*, pp. 630-635, 2005.
- [20] S. G. Oliver, "From DNA sequence to biological function," *Nature*, pp. 597-600, 1996.
- [21] N. S. Parachin, M. Carlquist, and M. F. Gorwa-Grauslund, "Comparison of engineered *Saccharomyces cerevisiae* and engineered *Escherichia coli* for the production of an optically pure keto alcohol," *Applied Microbiology and Biotechnology*, pp. 487-497, 2009.
- [22] B. N. Zhou, A. S. Gopalan, F. VanMiddlesworth, W. R. Shieh, and C. J. Sih, "Stereochemical control of yeast reductions. 1. Asymmetric synthesis of L-carnitine," *Journal of the American Chemical Society*, pp. 5925-5926, 1983.
- [23] J. Ehrler, F. Giovannini, B. Lamatsch, and D. Seebach, "Stereoselectivity of yeast reductions - an improved procedure for the preparation of ethyl (S)-3-hydroxybutanoate and (S)-2-hydroxymethylbutanoate," *Chimia*, pp. 172-173, 1986.
- [24] K. Nakamura, Y. Kawai, and A. Ohno, "Stereochemical control in microbial reduction .13. A novel method to synthesize (L)-beta-hydroxyl esters by the reduction with bakers-yeast," *Tetrahedron Letters*, pp. 267-270, 1990.
- [25] L. Y. Jayasinghe, A. J. Smallridge, and M. A. Trehwella, "The yeast mediated reduction of ethyl acetoacetate in petroleum ether," *Tetrahedron Letters*, pp. 3949-3950, 1993.
- [26] H. Pfruender, R. Jones, and D. Weuster-Botz, "Water immiscible ionic liquids as solvents for whole cell biocatalysis," *Journal of Biotechnology*, pp. 182-190, 2006.
- [27] P. F. Smith and D. Hendlin, "Mechanism of phenylacetylcarbinol synthesis by yeast," *Journal of Bacteriology*, pp. 440-445, 1953.
- [28] R. Csuk and B. I. Glanzer, "Bakers-yeast mediated transformations in organic-chemistry," *Chemical Reviews*, pp. 49-97, 1991.
- [29] S. Servi, "Baker yeast as a reagent in organic-synthesis," *Synthesis-Stuttgart*, pp. 1-25, 1990.
- [30] H. G. W. Leuenberger, W. Boguth, E. Widmer, and R. Zell, "Synthesis of optically-active natural carotenoids and structurally related compounds .1. Synthesis of chiral key compound (4R,6R)-4-hydroxy-2,2,6-trimethylcyclohexanone," *Helvetica Chimica Acta*, pp. 1832-1849, 1976.
- [31] Y. Kawai, Y. Inaba, and N. Tokitoh, "Asymmetric reduction of nitroalkenes with baker's yeast," *Tetrahedron-Asymmetry*, pp. 309-318, 2001.
- [32] J. Beecher, I. Brackenridge, S. M. Roberts, J. Tang, and A. J. Willetts, "Oxidation of methyl p-tolyl sulfide with bakers-yeast - Preparation of a synthon of the mevinic acid-type hypocholesteremic agents," *Journal of the Chemical Society-Perkin Transactions I*, pp. 1641-1643, 1995.
- [33] P. H. Buist, D. M. Marecak, E. T. Partington, and P. Skala, "Enantioselective sulfoxidation of a fatty-acid analog by bakers-yeast," *Journal of Organic Chemistry*, pp. 5667-5669, 1990.
- [34] B. M. Nestl, A. Bodlener, R. Stuermer, B. Hauer, W. Kroutil, and K. Faber, "Biocatalytic racemization of synthetically important functionalized alpha-

- hydroxyketones using microbial cells," *Tetrahedron-Asymmetry*, pp. 1465-1474, 2007.
- [35] D. H. G. Crout, H. Dalton, D. W. Hutchinson, and M. Miyagoshi, "Studies on pyruvate decarboxylase - acyloin formation from aliphatic, aromatic and heterocyclic aldehydes," *Journal of the Chemical Society-Perkin Transactions 1*, pp. 1329-1334, 1991.
- [36] B. Gasser and D. Mattanovich, "Antibody production with yeasts and filamentous fungi: on the road to large scale?," *Biotechnology Letters*, pp. 201-212, 2007.
- [37] L. Evans, M. Hughes, J. Waters, J. Cameron, N. Dodsworth, D. Tooth, A. Greenfield, and D. Sleep, "The production, characterisation and enhanced pharmacokinetics of scFv-albumin fusions expressed in *Saccharomyces cerevisiae*," *Protein Expression and Purification*, pp. 113-124, 2010.
- [38] O. Joubert, R. Nehme, M. Bidet, and I. Mus-Veteau, "Heterologous Expression of Human Membrane Receptors in the Yeast *Saccharomyces cerevisiae*," in *Heterologous Expression of Membrane Proteins: Methods and Protocols.*, pp. 87-103, 2010.
- [39] J. P. van Dijken, J. Bauer, L. Brambilla, P. Duboc, J. M. Francois, C. Gancedo, M. L. F. Giuseppin, J. J. Heijnen, M. Hoare, H. C. Lange, E. A. Madden, P. Niederberger, J. Nielsen, J. L. Parrou, T. Petit, D. Porro, M. Reuss, N. van Riel, M. Rizzi, H. Y. Steensma, C. T. Verrips, J. Vindelov, and J. T. Pronk, "An interlaboratory comparison of physiological and genetic properties of four *Saccharomyces cerevisiae* strains," *Enzyme and Microbial Technology*, pp. 706-714, 2000.
- [40] P. Houston, P. J. Simon, and J. R. Broach, "The *Saccharomyces cerevisiae* recombination enhancer biases recombination during interchromosomal mating-type switching but not in interchromosomal homologous recombination," *Genetics*, pp. 1187-1197, 2004.
- [41] A. Rogowska-Wrzesinska, P. M. Larsen, A. Blomberg, A. Gorg, P. Roepstorff, J. Norbeck, and S. J. Fey, "Comparison of the proteomes of three yeast wild type strains: CEN.PK2, FY1679 and W303," *Comparative and Functional Genomics*, pp. 207-225, 2001.
- [42] EUROSCARF. (31-7-2013). *CEN.PK2 wild type reference strains used in the German functional analysis project and EUROFAN I* Available: <http://web.uni-frankfurt.de/fb15/mikro/euroscarf/data/cen.html>
- [43] M. Rose and F. Winston, "Identification of a Ty insertion within the coding sequence of the *S-cerevisiae* URA3 gene," *Molecular & General Genetics*, pp. 557-560, 1984.
- [44] P. J. Flynn and R. J. Reece, "Activation of transcription by metabolic intermediates of the pyrimidine biosynthetic pathway," *Molecular and Cellular Biology*, pp. 882-888, 1999.
- [45] S. Chabelskaya, V. Gryzina, S. Moskalenko, C. Le Goff, and G. Zhouravleva, "Inactivation of NMD increases viability of sup45 nonsense mutants in *Saccharomyces cerevisiae*," *Bmc Molecular Biology*, 2007.
- [46] G. H. Braus, "Aromatic amino-acid biosynthesis in the yeast *Saccharomyces-cerevisiae* - A model system for the regulation of a eukaryotic biosynthetic-pathway," *Microbiological Reviews*, pp. 349-370, 1991.

- [47] A. Hinnen, J. B. Hicks, and G. R. Fink, "Transformation of yeast," *Proceedings of the National Academy of Sciences of the United States of America*, pp. 1929-1933, 1978.
- [48] R. F. Gaber and M. R. Culbertson, "Frameshift suppression in *Saccharomyces cerevisiae*. 4. New suppressors among spontaneous co-revertants of the group II HIS4-206 and LEU2-3 frameshift mutations," *Genetics*, pp. 345-367, 1982.
- [49] S. Scherer and R. W. Davis, "Replacement of the chromosome segments with altered DNA sequences constructed invitro," *Proceedings of the National Academy of Sciences of the United States of America*, pp. 4951-4955, 1979.
- [50] P. Alifano, R. Fani, P. Lio, A. Lazcano, M. Bazzicalupo, M. S. Carlomagno, and C. B. Bruni, "Histidine biosynthetic pathway and genes: Structure, regulation, and evolution," *Microbiological Reviews*, pp. 44-&, 1996.
- [51] M. Jules, V. Guillou, J. Francois, and J. L. Parrou, "Two distinct pathways for trehalose assimilation in the yeast *Saccharomyces cerevisiae*," *Applied and Environmental Microbiology*, pp. 2771-2778, 2004.
- [52] M. Carlson and D. Botstein, "Organization of the SUC gene family in *Saccharomyces*," *Molecular and Cellular Biology*, pp. 351-359, 1983.
- [53] J. T. Pronk, H. Y. Steensma, and J. P. vanDijken, "Pyruvate metabolism in *Saccharomyces cerevisiae*," *Yeast*, pp. 1607-1633, 1996.
- [54] D. K. Bricker, E. B. Taylor, J. C. Schell, T. Orsak, A. Boutron, Y. C. Chen, J. E. Cox, C. M. Cardon, J. G. Van Vranken, N. Dephoure, C. Redin, S. Boudina, S. P. Gygi, M. Brivet, C. S. Thummel, and J. Rutter, "A Mitochondrial Pyruvate Carrier Required for Pyruvate Uptake in Yeast, *Drosophila*, and Humans," *Science*, pp. 96-100, 2012.
- [55] S. Jitrapakdee, M. St Maurice, I. Rayment, W. W. Cleland, J. C. Wallace, and P. V. Attwood, "Structure, mechanism and regulation of pyruvate carboxylase," *Biochemical Journal*, pp. 369-387, 008.
- [56] H. Holzer and H. W. Goedde, "Zwei wege von pyruvat zu acetyl-coenzym-A in hefe," *Biochemische Zeitschrift*, pp. 175-191, 1957.
- [57] M. T. Flikweert, L. VanderZanden, W. Janssen, H. Y. Steensma, J. P. VanDijken, and J. T. Pronk, "Pyruvate decarboxylase: An indispensable enzyme for growth of *Saccharomyces cerevisiae* on glucose," *Yeast*, pp. 247-257, 1996.
- [58] M. T. Flikweert, M. de Swaaf, J. P. van Dijken, and J. T. Pronk, "Growth requirements of pyruvate-decarboxylase-negative *Saccharomyces cerevisiae*," *Fems Microbiology Letters*, pp. 73-79, 1999.
- [59] H. G. Crabtree, "Observations on the carbohydrate metabolism of tumours," *Biochemical Journal*, pp. 536-545, 1929.
- [60] H. Ronne, "Glucose repression in Fungi," *Trends in Genetics*, pp. 12-17, 1995.
- [61] O. Kappeli, "Regulation of carbon metabolism in *Saccharomyces-cerevisiae* and related yeasts," *Advances in Microbial Physiology*, pp. 181-209, 1986.
- [62] J. P. Barford and R. J. Hall, "Examination of the Crabtree effect in *Saccharomyces-cerevisiae* - Role of respiratory adaptation," *Journal of General Microbiology*, pp. 267-275, 1979.
- [63] M. Webb, "Pyruvate accumulation in growth-inhibited cultures of *Aerobacter aerogenes*," *Biochemical Journal*, pp. 375, 1968.
- [64] D. Kalman, C. M. Colker, I. Wilets, J. B. Roufs, and J. Antonio, "The effects of pyruvate supplementation on body composition in overweight individuals," *Nutrition*, pp. 337-340, 1999.

- [65] T. Yonehara and R. Miyata, "Fermentative production of pyruvate from glucose by *Torulopsis-glabrata*," *Journal of Fermentation and Bioengineering*, pp. 155-159, 1994.
- [66] Q. H. Wang, P. He, D. J. Lu, A. Shen, and N. Jiang, "Metabolic engineering of *Torulopsis glabrata* for improved pyruvate production," *Enzyme and Microbial Technology*, pp. 832-839, 2005.
- [67] H. Vanurk, D. Schipper, G. J. Breedveld, P. R. Mak, W. A. Scheffers, and J. P. Vandijken, "Localization and kinetics of pyruvate-metabolizing enzymes in relation to aerobic alcoholic fermentation in *Saccharomyces-cerevisiae* CBS-8066 and *Candida-utilis* CBS-621," *Biochimica Et Biophysica Acta*, pp. 78-86, 1989.
- [68] A. J. A. van Maris, J. M. A. Geertman, A. Vermeulen, M. K. Groothuizen, A. A. Winkler, M. D. W. Piper, J. P. van Dijken, and J. T. Pronk, "Directed evolution of pyruvate decarboxylase-negative *Saccharomyces cerevisiae*, yielding a C-2-independent, glucose-tolerant, and pyruvate-hyperproducing yeast," *Applied and Environmental Microbiology*, pp. 159-166, 2004.
- [69] G. Q. Xu, Q. Hua, N. J. Duan, L. M. Liu, and J. Chen, "Regulation of thiamine synthesis in *Saccharomyces cerevisiae* for improved pyruvate production," *Yeast*, pp. 209-217, 2012.
- [70] H. Vanurk, E. Postma, W. A. Scheffers, and J. P. Vandijken, "Glucose-transport in Crabtree-positive and Crabtree-negative yeasts," *Journal of General Microbiology*, pp. 2399-2406, 1989.
- [71] K. Nosaka, "Recent progress in understanding thiamin biosynthesis and its genetic regulation in *Saccharomyces cerevisiae*," *Applied Microbiology and Biotechnology*, pp. 30-40, 2006.
- [72] M. T. Flikweert, J. P. vanDijken, and J. T. Pronk, "Metabolic responses of pyruvate decarboxylase-negative *Saccharomyces cerevisiae* to glucose excess," *Applied and Environmental Microbiology*, pp. 3399-3404, 1997.
- [73] B. Oud, C. L. Flores, C. Gancedo, X. Y. Zhang, J. Trueheart, J. M. Daran, J. T. Pronk, and A. J. A. van Maris, "An internal deletion in MTH1 enables growth on glucose of pyruvate-decarboxylase negative, non-fermentative *Saccharomyces cerevisiae*," *Microbial Cell Factories*, 2012.
- [74] J. M. Gancedo, "The early steps of glucose signalling in yeast," *Fems Microbiology Reviews*, pp. 673-704, 2008.
- [75] M. E. Franks, G. R. Macpherson, and W. D. Figg, "Thalidomide," *Lancet*, pp. 1802-1811, 2004.
- [76] M. Eichelbaum, B. Testa, and A. Somogyi, "Stereochemical aspects of drug action and disposition," in *Stereochemical aspects of drug action and disposition.*, 2003.
- [77] I. Agranat, H. Caner, and A. Caldwell, "Putting chirality to work: The strategy of chiral switches," *Nature Reviews Drug Discovery*, pp. 753-768, 2002.
- [78] A. M. Rouhi, "Chiral business," *Chemical & Engineering News*, pp. 45, 2003.
- [79] Research Impact, *Chiral Chemicals*, 2012.
- [80] M. Carlquist, C.-J. Wallentin, K. Wärnmark, and M. F. Gorwa-Grauslund, "Genetically engineered *Saccharomyces cerevisiae* for kinetic resolution of racemic bicyclo[3.3.1]nonane-2,6-dione," *Tetrahedron: Asymmetry*, pp. 2293-2295, 2008.
- [81] M. Carlquist, C. Olsson, B. Bergdahl, E. W. J. van Niel, M. F. Gorwa-Grauslund, and T. Frejd, "Kinetic resolution of racemic 5,6-epoxy-bicyclo[2.2.1]heptane-2-one using genetically engineered *Saccharomyces cerevisiae*," *Journal of Molecular Catalysis B: Enzymatic*, pp. 98-102, 2009.

- [82] H. S. Bea, Y. M. Seo, M. H. Cha, B. G. Kim, and H. Yun, "Kinetic Resolution of alpha-methylbenzylamine by Recombinant *Pichia pastoris* Expressing omega-transaminase," *Biotechnology and Bioprocess Engineering*, pp. 429-434, 2010.
- [83] J. Royer, "Chiral Amine Synthesis. Methods, Developments and Applications. Herausgegeben von Thomas C. Nugent," *Angewandte Chemie*, pp. 8013-8013, 2010.
- [84] M. Breuer, K. Ditrich, T. Habicher, B. Hauer, M. Kessler, R. Sturmer, and T. Zelinski, "Industrial methods for the production of optically active intermediates," *Angewandte Chemie-International Edition*, pp. 788-824, 2004.
- [85] M. S. Malik, E. S. Park, and J. S. Shin, "Features and technical applications of omega-transaminases," *Applied Microbiology and Biotechnology*, pp. 1163-1171, 2012.
- [86] I. Karame, M. Jahjah, A. Messaoudi, M. L. Tommasino, and M. Lemaire, "New ruthenium catalysts containing chiral Schiff bases for the asymmetric hydrogenation of acetophenone," *Tetrahedron-Asymmetry*, pp. 1569-1581, 2004.
- [87] H. Yun and B. G. Kim, "Asymmetric Synthesis of (S)-alpha-Methylbenzylamine by Recombinant *Escherichia coli* Co-Expressing Omega-Transaminase and Acetolactate Synthase," *Bioscience Biotechnology and Biochemistry*, pp. 3030-3033, 2008.
- [88] G. Matcham, D. Stirling, and Z. Zeitlin, "Enantiomeric enrichment and stereoselective synthesis of chiral amines," 1990.
- [89] M. D. Toney, "Reaction specificity in pyridoxal phosphate enzymes," *Archives of Biochemistry and Biophysics*, pp. 279-287, 2005.
- [90] H. Yun, S. Lim, B. K. Cho, and B. G. Kim, "omega-amino acid : pyruvate transaminase from *Alcaligenes denitrificans* Y2k-2: a new catalyst for kinetic resolution of beta-amino acids and amines," *Applied and Environmental Microbiology*, pp. 2529-2534, 2004.
- [91] J. P. Vandijken and W. A. Scheffers, "Redox balances in the metabolism of sugars by yeasts," *Fems Microbiology Reviews*, pp. 199-224, 1986.
- [92] B. M. Bakker, K. M. Overkamp, A. J. A. van Maris, P. Kotter, M. A. H. Luttik, J. P. van Dijken, and J. T. Pronk, "Stoichiometry and compartmentation of NADH metabolism in *Saccharomyces cerevisiae*," *Fems Microbiology Reviews*, pp. 15-37, 2001.
- [93] M. D. Truppo, N. J. Turner, and J. D. Rozzell, "Efficient kinetic resolution of racemic amines using a transaminase in combination with an amino acid oxidase," *Chemical Communications*, pp. 2127-2129, 2009.
- [94] D. Koszelewski, I. Lavandera, D. Clay, D. Rozzell, and W. Kroutil, "Asymmetric Synthesis of Optically Pure Pharmacologically Relevant Amines Employing omega-Transaminases," *Advanced Synthesis & Catalysis*, pp. 2761-2766, 2008.
- [95] H. S. Bea, S. H. Lee, and H. Yun, "Asymmetric Synthesis of (R)-3-fluoroalanine from 3-fluoropyruvate Using Omega-transaminase," *Biotechnology and Bioprocess Engineering*, pp. 291-296, 2011.
- [96] Y. Q. Lang, H. Kisaka, R. Sugiyama, K. Nomura, A. Morita, T. Watanabe, Y. Tanaka, S. Yazawa, and T. Miwa, "Functional loss of pAMT results in biosynthesis of capsinoids, capsaicinoid analogs, in *Capsicum annuum* cv. CH-19 Sweet," *Plant Journal*, pp. 953-961, 2009.
- [97] M. D. Abraham-Juarez, M. D. Rocha-Granados, M. G. Lopez, R. F. Rivera-Bustamante, and N. Ochoa-Alejo, "Virus-induced silencing of Comt, pAmt and

- Kas genes results in a reduction of capsaicinoid accumulation in chili pepper fruits," *Planta*, pp. 681-695, 2008.
- [98] N. Weber, A. Ismail, M. F. Gorwa-Grauslund, and M. Carlquist, "Functional validation and biocatalytic application of vanillin aminotransferase (VAMT) from *Capsicum chinense*," *Manuscript*, 2013.
- [99] J. Sambrook and D. D. W. Russell, *Molecular Cloning: A Laboratory Manual*: Cold Spring Harbor Laboratory Press, 2001.
- [100] J. T. Pronk, "Auxotrophic yeast strains in fundamental and applied research," *Applied and Environmental Microbiology*, pp. 2095-2100, 2002.
- [101] C. Verduyn, E. Postma, W. A. Scheffers, and J. P. Vandijken, "Effect of benzoic acid on metabolic fluxes in yeasts- A continuous-culture study on the regulation of respiration and alcoholic fermentation," *Yeast*, pp. 501-517, 1992.
- [102] R. D. Gietz and R. H. Schiestl, "High-efficiency yeast transformation using the LiAc/SS carrier DNA/PEG method," *Nature Protocols*, pp. 31-34, 2007.
- [103] S. Hohmann and P. A. Meacock, "Thiamin metabolism and thiamin diphosphate-dependent enzymes in the yeast *Saccharomyces cerevisiae*: genetic regulation," *Biochimica Et Biophysica Acta-Protein Structure and Molecular Enzymology*, pp. 201-219, 1998.
- [104] Y. Lindqvist and G. Schneider, "Thiamin diphosphate dependent enzymes - Transketolase, pyruvate oxidase and pyruvate decarboxylase," *Current Opinion in Structural Biology*, pp. 896-901, 1993.
- [105] A. J. A. van Maris, M. A. H. Luttik, A. A. Winkler, J. P. van Dijken, and J. T. Pronk, "Overproduction of threonine aldolase circumvents the biosynthetic role of pyruvate decarboxylase in glucose-limited chemostat cultures of *Saccharomyces cerevisiae*," *Applied and Environmental Microbiology*, pp. 2094-2099, 2003.
- [106] S. Hohmann, "PDC6, a weakly expressed pyruvate decarboxylase gene from yeast, is activated when fused spontaneously under the control of the PDC1 promoter," *Current Genetics*, pp. 373-378, 1991.
- [107] S. Hohmann, "Characterization of PDC6, a 3rd structural gene for pyruvate decarboxylase in *Saccharomyces-cerevisiae*," *Journal of Bacteriology*, pp. 7963-7969, 1991.
- [108] K. Karhumaa, B. Q. Wu, and M. C. Kielland-Brandt, "Conditions With High Intracellular Glucose Inhibit Sensing Through Glucose Sensor Snf3 in *Saccharomyces cerevisiae*," *Journal of Cellular Biochemistry*, pp. 920-925, 2010.

8. Appendix

I- PCR Programs

	Desired Fragment	Deletion Fragments	
Cycles	Steps	Temperature (°C)	Duration (s)
1	Initial Denaturation	98	30
30	Denaturation	98	10
	Annealing	65-50	30
	Extension	72	15(60*)
1	Final Extension	72	600

*PDC1_trp1, PDC5_ura3 and THI2_trp1

	Desired Fragment	Overlap Extension PCR Cassettes	Deletion
Cycles	Steps	Temperature (°C)	Duration (s)
1	Initial Denaturation	98	30
16	Denaturation	98	10
	Annealing	68-60	30
	Extension	72	60
Primers are added to PCR mix			
1	Initial Denaturation	98	30
20	Denaturation	98	10
	Annealing	63-55	30
	Extension	72	60
1	Final Extension	72	600

	Desired Fragment	Deletion Confirmation of PDC1 PDC1_trp1 fragment		Deletion Confirmation of PDC1 WPDC1 fragment	
Cycles	Steps	Temperature (°C)	Duration (s)	Temperature (°C)	Duration (s)
1	Initial Denaturation	98	180	98	180
	Denaturation	98	10	98	10
30	Annealing	54-51	30	54-51	30
	Extension	72	60	72	80
1	Final Extension	72	300	72	300

	Desired Fragment	Deletion Confirmation of PDC5 PDC5_ura3 fragment		Deletion Confirmation of PDC5 WPDC5 fragment	
Cycles	Steps	Temperature (°C)	Duration (s)	Temperature (°C)	Duration (s)
1	Initial Denaturation	98	180	98	180
	Denaturation	98	10	98	10
30	Annealing	54,6	30	52	30
	Extension	72	50	72	80
1	Final Extension	72	300	72	300

	Desired Fragment	Deletion Confirmation of THI2 THI2_trp1 fragment		Deletion Confirmation of THI2 WTHI2 fragment	
Cycles	Steps	Temperature (°C)	Duration (s)	Temperature (°C)	Duration (s)
1	Initial Denaturation	98	180	98	180
	Denaturation	98	10	98	10
30	Annealing	54-51	30	54-51	30
	Extension	72	55	72	70
1	Final Extension	72	300	72	300

II- DNA sequences of PDC1, PDC5 and THI2 from CEN.PK 113-7D

PDC1

CTTATTGCTTAGCGTTGGTAGCAGCAGTCAACTTAGCTTGTTCAACCAAGTTTT
 GTGGAGCATCGAAGACTGGCAACATNNNCTCAATCATTCTGATCTTAGAGTTGTCTGTT
 GAAAGACTTGTCTTGGGTCAACTTGTCCCATTACCGGTGGTAGCGACTCTGTGGGTTT
 CGTAGTCCTTAGCACCGAAAGTTGGCAACAAGGATAGGTGGTCCCAACCTTGAATTTT
 GTTGTATTGAGCCTTTGGACCGTGAATCAACTTTTCAATGGTGTAAACCATCGTTGTTCA
 AGACGAACAAGTATGGCTTCAAGCCCCATCTGATCATGGTGGAGATTTCTTGAACAGT
 CAATTGCAAAGAACCGTCACCAATGAATAAGATAACTCTCTTCTTTGGATCAATTTCTT
 CAGCAGCGAAAGCAGCACCCAAGGTAGCACCAGTGGTGAACCAATGGAACCCATA
 AGACTTGAGAGATACCGTAGGTGTTGTTTGGGAAAGTGGTTTGGTTGATACCGAAAGC
 GGAGGTACCGTTTTAGCAATGACAACATCACCTTCTTGCAAGAAGTTACCCAATTGG
 TTCCACATCCATTCTTGCTTCAATGGGGTAGAAGCTGGGACAGCAGCGTTAGCTGGAG
 TTCTAGCTGGGACAGCAACTGGCTTGTAAACCCTTAGCGGCGTCAGCAATATTGGTCAA
 CAACTTTTGCAAACGAATTTCAATTTGGACACCTGGGAAAGTGGCGTTTCTGATCTTCA
 TGTGGTCGGAGTGGAATTCGACAATGTTCTTGGTCTTGTAAAGAGTAAGAGAAAGAACC
 GGTGTTGAAATCAGACAACAAAGCACCGACAGACAAAATCAAGTCAGCAGATTCAAC
 GGCTTCCTTAACTTCTGGCTTGGACAAGGTACCGACGTAACACCACCGTATCTTGGG
 TGTTGTTTCGTCATGGAACCTTACCCATTGGGGTGACGAAAGCTGGGAATTGAGTCA
 AGTCAATCAACTTCTTAGTTTTAGCCTTGACGTCGTGTCTGGAACAACAAGCATCAGC
 CAAGATAACTGGGTTCTTAGCATCCTTGACCAAAGCCAAGATGGTGTCAATGACTTCC
 TTTTCGGATTCAGCATCGTTTGGCTTCAAAGACATGTCAATTGGAGTTTGCAACAACCT
 AGCTGGGACGTTCAAGTCGACCAAGTTAGCTGGCAAACCTAAGTAGACTGGTCTTTGG
 GTGACGTAAGTGGTTCTGATACATCTGTCAATTTAGCTGGGGCGGTAGCAATGTCAG
 TGATCATAGCAGTGGTTTTCAGAAATGTTGGCAGACATTCTGTGAAAACAGTGAAGTC
 ACCGTTACCCAAGGTGTGGTGCAACAACAATTGCTTAGCTTGAGAAGAGATGGATGGG
 ACACCAACAACGTGCAAAAACCCGACGTGTTACGCGTAAGAACCAGCAATACCGTTC
 AAAGCAGACAATTCACCGACACCGAAGGTGGTGATGATACAAGACATAACCTTGATA
 CGAGCGTAACCATCAGCGGCGTAAGCAGCGTTCAATTCGTTGGCGTTACCAGCCCATC
 TCATACCTTCAACTTCGTAGATCTTGTCCAACAAGGACAAGTTGAAGTCACCTGGCAA
 ACCGAAAACGGTGTTAACGTTGACTTGCTTTAATCTTTCGAACAATATTTACCCAAA
 GTAATTTTCAGACA

PDC5

CAAGAAGAACAAAATGTCTGAAATAACCTTAGGTAATATTTATTTGAAAGAT
 TGAGCCAAGTCAACTGTAACACCGTCTTCGGTTTGCCAGGTGACTTTAACTTGTCTCTT
 TTGGATAAGCTTTATGAAGTCAAAGGTATGAGATGGGCTGGTAACGCTAACGAATTGA
 ACGCTGCCTATGCTGCTGATGGTTACGCTCGTATCAAGGGTATGTCCTGTATTATTACC
 ACCTTCGGTGTTGGTGAATTGTCTGCTTTGAATGGTATTGCCGGTTCTTACGCTGAACA
 TGTCGGTGTTTTGCACGTTGTTGGTGTTCATCCATCTCTTCTCAAGCTAAGCAATTGTT
 GTTGCATCATACTTGGGTAACGGTGACTTCACTGTTTTCCACAGAATGTCTGCCAACA
 TTTCTGAAACCACTGCCATGATCACTGATATTGCTAACGCTCCAGCTGAAATTGACAG
 ATGTATCAGAACCACCTACACTACCCAAAGACCAGTCTACTTGGGTTTGCCAGCTAAC
 TTGGTTGACTTGAACGTCCCAGCCAAGTTATTGGAAACTCCAATTGACTTGTCTTTGAA
 GCCAAACGACGCTGAAGCTGAAGCTGAAGTTGTTAGAAGTGTGTTGAATTGATCAAG
 GATGCTAAGAACCAGTTATCTTGGCTGATGCTTGTGCTTCTAGACATGATGTCAAGG

CTGAAACTAAGAAGTTGATGGACTTGACTCAATTCCCAGTTTACGTCACCCCAATGGG
 TAAGGGTGCTATTGACGAACAACACCCAAGATACGGTGGTGTTTACGTTGGTACCTTG
 TCTAGACCAGAAGTTAAGAAGGCTGTAGAATCTGCTGATTTGATATTGTCTATCGGTG
 CTTTGTGTCTGATTTCAATACCGGTTCTTTCTCTTACTCCTACAAGACCAAAAATATC
 GTTGAATTCCACTCTGACCACATCAAGATCAGAAACGCCACCTCCCAGGTGTTCAA
 TGAAATTTGCCTTGCAAAAATTGTTGGATGCTATTCCAGAAGTCGTCAAGGACTACAA
 ACCTGTTGCTGTCCCAGCTAGAGTTCCAATTACCAAGTCTACTCCAGCTAACACTCCAA
 TGAAGCAAGAATGGATGTGGAACCATTTGGGTAACTTCTTGAGAGAAGGTGATATTGT
 TATTGCTGAAACCGGTACTTCCGCCTTCGGTATTAACCAAACTACTTTCCCAACAGATG
 TATACGCTATCGTCCAAGTCTTGTGGGGTTCATTGGTTTCACAGTCGGCGCTCTATTG
 GGTGCTACTATGGCCGCTGAAGAACTTGATCCAAAGAAGAGAGTTATTTTATTATTG
 GTGACGGTTCTCTACAATTGACTGTTCAAGAAATCTCTACCATGATTAGATGGGGTTTG
 AAGCCATACATTTTTGTCTTGAATAACAACGGTTACACCATTGAAAAATTGATTCACG
 GTCCCTCATGCCGAATATAATGAAATTCAAGGTTGGGACCACTTGGCCTTATTGCCAAC
 TTTTGGTGCTAGAACTACGAAACCCACAGAGTTGCTACCACTGGTGAATGGGAAAAG
 TTGACTCAAGACAAGGACTTCCAAGACAACCTCTAAGATYAGAATGATTGARGTTATGT
 TGCCAGTCTTTGATGCTCCACAAAACCTTGGTTAAACAAGCTCAATTGACTGCCGCTACT
 AACGCTAAACAATAA

THI2

CTAGTCCTGCATGGCATATACATCCTTGTA AAAATTGTTGATTACACTTCAGTTG
 TAGCTGCCAGTACCGCAGTTGGGAACATGAAAGTGTGGTATCTTGACATGAGCAAAGT
 TGTTGCAATATTGTATCTTTCCAACTATTCCTAGGCGCTCCGTGACCAAGACATGTAA
 CTCCGACGTAAGCTCGTCCTGATAGGGATCCTCGAATAAGTCGGCATTCCCTAGTAAT
 CCATTACAATGGTACAGAACGTCTAAATCTTGTGTATTGTTTATGATAAAGTTGACCAG
 CGGATACATCGAAAATCTCAATAGCTTTTGTCTGGAGAAACCACACTCTTAGAAGCTTT
 GTCAAGTTGGGGCAGGTATATCCATGAATGATGACCAGCATTGTTATAGCTATGGATT
 GCCAATCGACACAACCTCAACGAGCGATGCACTCTTTGAACAGGCACGAGGCCATATT
 GATGTCCGGGTCGTCAATTATTTCCCAAGGAAGCGTATGAATTCCGTGGTCAACGAG
 TTCCTCATCTTATTGATGAACCACGTCGTGTATTCTTGTCTGCGTTCAATATCATGTTCCCG
 TAGCAATTAACCATAGGATCCCGAAAATTTTGCCTTGGATAATATCGATCAAAGAGG
 TGCTGTCTTCTGGCGGGGATGACAGCGCTGCAGTAGTGGTTTCCTCTGCTGACGACATC
 GAATGACCCGGCGACGGCAGCTGATCTGTAAGAGCAGAGGTAACCTGCAGCCGGATTG
 GCCCTGAAAACCTGAGTAAGGCCCGTGTGGAGCAATTGAGGTTGACCACAGATATGT
 CGTTTTCCACCATATTAAGCAATTCGTCCAACCTTCTTGTCTATGCGCTTTTGAGTATAAT
 CTCTATTTGTCATGCTACCAAAGACAGAGGCCACAGCGTTATTGTATATCTTCAATCTC
 CGTACGCTTATGGTGAATGTATTATCGTTAGGAAGCGTAGTTTCCTTACTTGCCTCGTG
 CACGCTGTCTTCGCAGTCACTTGTCTGGGGGTGATAGTTGTCTAAAATGGGTCAATTTGTT
 TAAACCTTGATTTTGTAGATTTTCTGGCACAATGGTTTCGATTTTCGATTTGCGAGCCTGT
 AATGAACTGATCAGTGAATGCTTGCCTACTTTGTAGATGTTCTCCTCTAACACATAAG
 TCTGATATCGTAACTACAATTATCTCCATGTTTGGCACACAGTGAACAGATTGGTCTAT
 TCTCGTCGCATCTGCGTTTCTTGAATCTGCATGCCAGCAGCCAGTAAATGTCCTCCCC
 TTGGTGGGGGGCACTTTGGAGGATGACGCTACTTTCTTGTCTCTGCTGCCTCTTACT
 ATTGATCAT

III- DNA sequences of Up- and Downstream of PDC1, PDC5 and THI2 in CEN.PK 113-7D

PDC1

Upstream

AAAAACTAATACGTAAACCTGCATTAAGGTAAGATTATATCAGAAAATGTGTT
GCAAGAAATGCATTATGCAATTTTTTGATTATGACAATCTCTCGAAAGAAATTCATAT
GATGAGACTTGAATAATGCAGCGGCGCTTGCTAAAAGAACTTGTATATAAGAGCTGCC
ATTCTCGATCAATATACTGTAGTAAGTCCTTTCCTCTCTTTCTTATTACACTATTTTAC
ATAATCAATCTCAAAGAGAACAACAATAATAA

Downstream

GCTAATTAACATAAACTCATGATTCAACGTTTGTGTATTTTTTTACTTTTGAAG
GTTATAGATGTTTAGGTAATAATTGGCATAGATATAGTTTTAGTATAATAAATTTCTG
ATTTGGTTTTAAATATCAACTATTTTTTTTTCACATATGTTCTTGTAACTTTTCTGTC
CTGTCTTCCAGGTTAAAGATTAGCTTCTAATATTTTAGGTGGTTTATTATTTAATTTTAT
GCTGATTAATTTATTTACTTTTCGTATTCGGTTTTGTACCTTTAGCTATGATCTTAGCTAA
TTGAAGAGGGTGGTGTGATCTTTAACCATACCTTATTATCTTTCAGCTGCTTACCATTTT
CTTATATTGATTTTTAGCGAAAGATTTTTATTCAACAAGCTTTTTTTATCCTTAATGCTCG
AATACTACAACAAAACAAAAACATTAACAGTTTTTTAATTTTGTGAACAACTGAAT
TACAAGGCCTTACATCTTATTTAGAATATATTAAGAAACAGAGGCCAACATGCCTTCT
TAATTATATTGATATGGACCTCTGTCTTCTTAAAACGGGTTTTTGTTCGATGAAAAA
TCACCAGTAGAGCACCATATATGAATTTACAATCATTGTAGGGAAAAGAAAACCTTGT
CTGCTTCGCCAATTGATTTCAATTTCTTTTTTTCCTTTGTTTTT

PDC5

Upstream

AAAAACTAATACGTAAACCTGCATTAAGGTAAGATTATATCAGAAAATGTGTT
GCAAGAAATGCATTATGCAATTTTTTGATTATGACAATCTCTCGAAAGAAATTCATAT
GATGAGACTTGAATAATGCAGCGGCGCTTGCTAAAAGAACTTGTATATAAGAGCTGCC
ATTCTCGATCAATATACTGTAGTAAGTCCTTTCCTCTCTTTCTTATTACACTATTTTAC
ATAATCAATCTCAAAGAGAACAACAATAATAA

Downstream

GCTAATTAACATAAACTCATGATTCAACGTTTGTGTATTTTTTTACTTTTGAAG
GTTATAGATGTTTAGGTAATAATTGGCATAGATATAGTTTTAGTATAATAAATTTCTG
ATTTGGTTTTAAATATCAACTATTTTTTTTTCACATATGTTCTTGTAACTTTTCTGTC
CTGTCTTCCAGGTTAAAGATTAGCTTCTAATATTTTAGGTGGTTTATTATTTAATTTTAT
GCTGATTAATTTATTTACTTTTCGTATTCGGTTTTGTACCTTTAGCTATGATCTTAGCTAA
TTGAAGAGGGTGGTGTGATCTTTAACCATACCTTATTATCTTTCAGCTGCTTACCATTTT
CTTATATTGATTTTTAGCGAAAGATTTTTATTCAACAAGCTTTTTTTATCCTTAATGCTCG
AATACTACAACAAAACAAAAACATTAACAGTTTTTTAATTTTGTGAACAACTGAAT
TACAAGGCCTTACATCTTATTTAGAATATATTAAGAAACAGAGGCCAACATGCCTTCT
TAATTATATTGATATGGACCTCTGTCTTCTTAAAACGGGTTTTTGTTCGATGAAAAA
TCACCAGTAGAGCACCATATATGAATTTACAATCATTGTAGGGAAAAGAAAACCTTGT
CTGCTTCGCCAATTGATTTCAATTTCTTTTTTTCCTTTGTTTTT

THI2

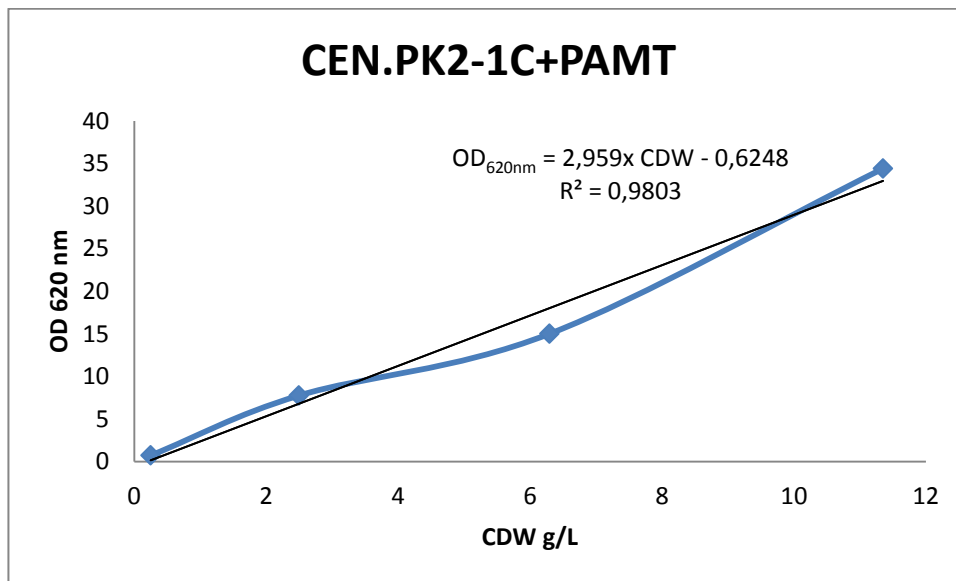
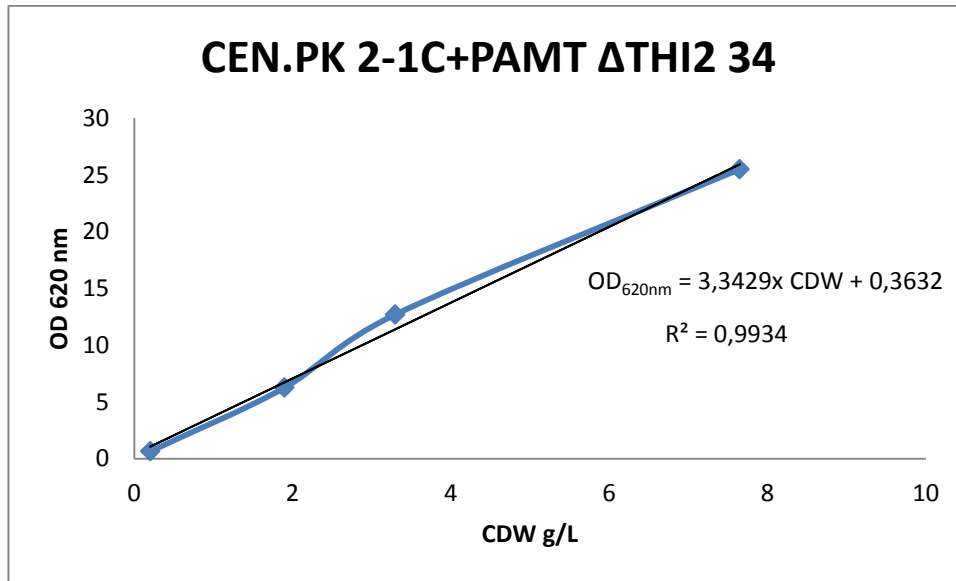
Upstream

TTGGTTCTAGTGCGGATATATATATAGGCTATATATATACGTGGTGAAATGAAA
TGAAAACGCTTTTAAAGTGTGCAGAAATTGTTATAGCTCTAACCCGTAGTATTAGTTCC
CCATATAATTCCGACCGAGAAAGGTGCACCCACTTGTGCATACAAATTGTACATATATA

CGTGTGCATTCGTAATGTCTGCCCATTTCTGCTATTCTGTATACACCCGCAGA
 GTACTGCAATTTGACTGTATTACCAATGTCAGCAAATTTTCTGTCTTCGAAG
 AGTAAAAAATTGTA CTTGGCGGATAATGCCTTTAGCGGCTTAACTGTGCC
 TCCATGGAAAAATCAGTCAAGATATCCACATGTGTTTTTAGTAAACAAATT
 TTGGGACCTAATGCTTCAACTAACTCCAGTAATTCCTTGGTGGTACGAACAT
 CCAATGAAGCACACAAGTTTGTGTTGCTTTTCGTGCATGATATTAATAGCTT
 GGCAGCAACAGGACTAGGATGAGTAGCAGCACGTTCCCTTATATGTAGCTTT
 CGACATGATTTATCTTCGTTTCCTGCATGTTTTTGTTCGTGCAGTTGGGTTA
 AGAATACTGGGCAATTTTCATGTTTCTTCAACACTACATATGCGTATATATAC
 CAATCTAAGTCTGTGCTCCTTCCTTCGTTCTTCCTTCTGTTCCGGAGATTACCG
 AATCAAAAAAATTTCAAAGAAACCGAAATCAAAAAAAGAATAAAAAA
 AATGATGAATTGAA

V- Primer list

Name	Sequence (5'-3')	Length	Tm °C (Santa Lucia)
PDC1_DS_f	TAATCAAGGATACCTCTTTTTTTTCTTGTTTC	34	57
PDC1_DS_r	TATATATATAGTAATGTCGGCGATTAACTCTAATTATTAGTTAAAGTTTATAAG	57	57
PDC1_TRP1_f	TAATAATTAGAGATTAAATCGCCGACATTACTATATATAATATAGGAAGCATTAAATAG	61	59
PDC1_TRP1_r	CAAAATAACACAGTCAAATCAATCAAAAACAACACTCAACCCTATCTCG	49	63
PDC1_US_f	GGGTTGAGTGTTGTTTTGATTGATTTGACTGTGTTATTTTGC	43	63
PDC1_US_r	GTGGCATTGCAAAAATGCATAACCTATG	28	57
PDC5_US_f	AAAACTAATACGTAAACCTGCATTAAGGTAAG	30	55
PDC5_US_r	ATTATATCAGTTATTACCCTATTGTATTGTGTTGTTCTCTTTGAGATTG	50	60
PDC5_URA3_f	CACAATACAATAAGGGTAATAACTGATATAATTAATGAAGCTC	45	57
PDC5_URA3_r	CATGAGTTTTATGTTAATTAGCTTCAATTCATCATTTTTTTTTTATTCTTTTTTTTGG	57	60
PDC5_DS_f	TAAAAAATAATGATGAATTGAAGCTAATTAACATAAAACTCATGATTCAAC	52	59
PDC5_DS_r	AAATGAAATCAATTGGCGAAGCAGAACAAG	37	58
THI2_DS_f	TCACCCTGGCAGATAGGAAACCCTATCTC	29	60.5
THI2_DS_r	ATATATATAGTAATGTCGGCTTATTGAGCCTCCCTTCACTC	42	61
THI2_TRP1_f	GAAGGCTCAATAAGCCGACATTACTATATATAATATAGGAAGCATTAAATAG	54	60
THI2_TRP1_r	CTATATATATATCCGCACTAGAACCAAAAACAACACTCAACCCTATCTCG	49	63
THI2_US_f	AGATAGGGTTGAGTGTTGTTTTGGTTCTAGTGC GGATATATATATAGG	48	63
THI2_US_r	ATGTACAATTTGTATGACAAGTGGGTGCAC	30	58

VI-OD_{620nm}/Cell Dry weight regression curve

VII- Fermentations/Cultivations profiles

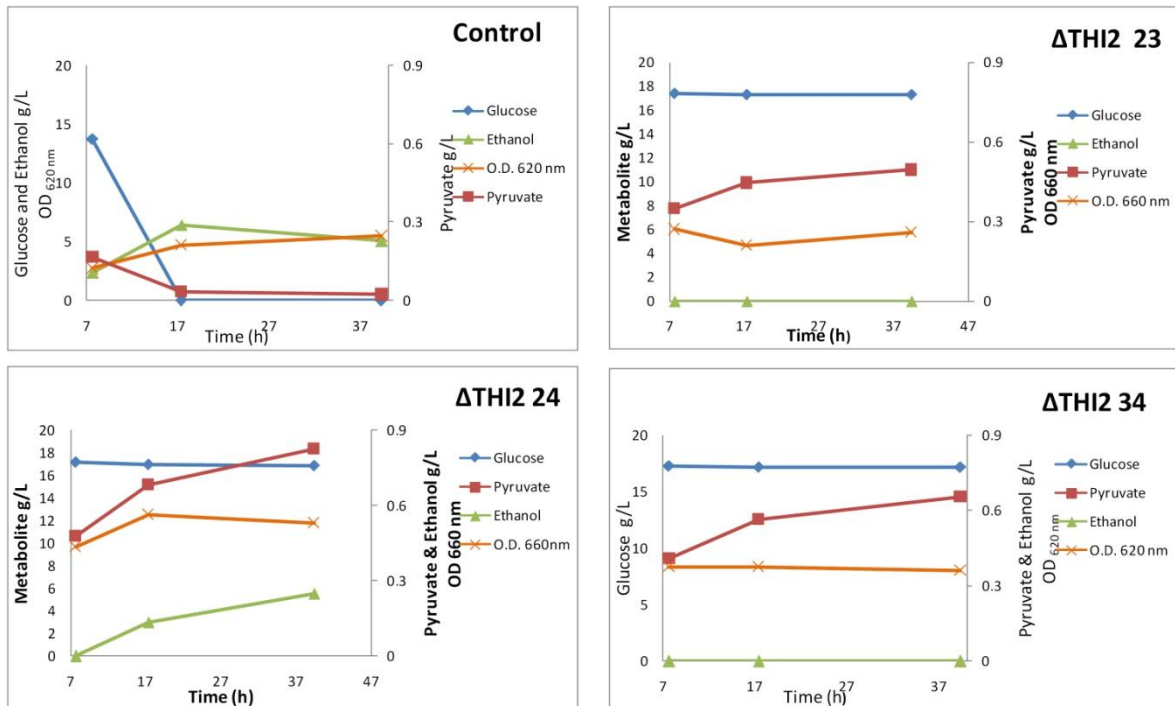


Figure 35- Aerobic cultivation of Δ THI2 colonies in Verduyn medium pre-grown in medium containing 3,32 μ M thiamine.

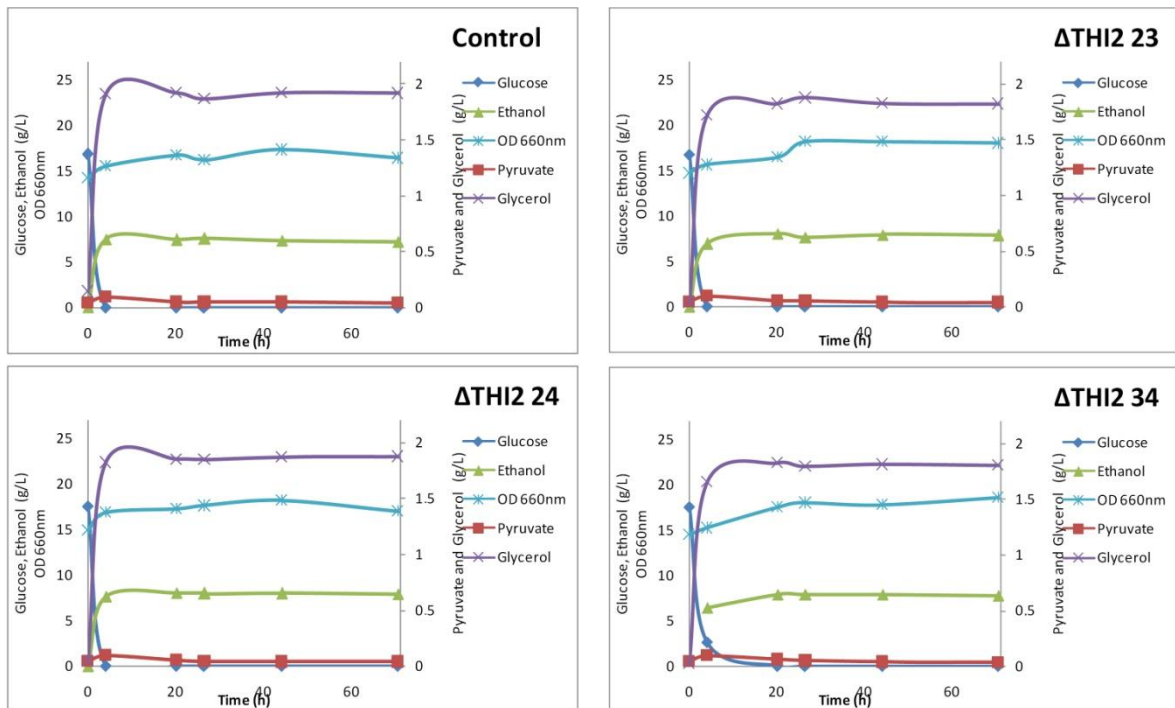


Figure 36- Anaerobic fermentation of Δ THI2 colonies in Verduyn medium pre-grown in medium containing 3,32 μ M thiamine.

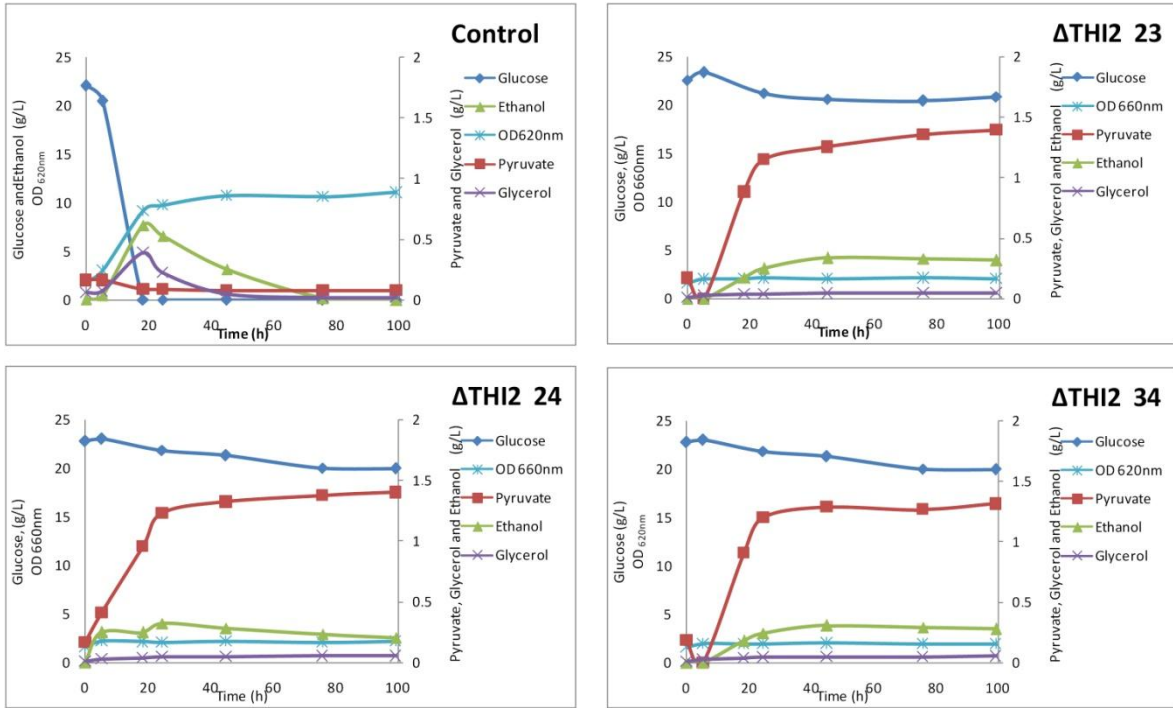


Figure 37- Aerobic cultivation of Δ THI2 colonies in Verdun medium pre-grown in medium containing 0,05 μ M of thiamine.

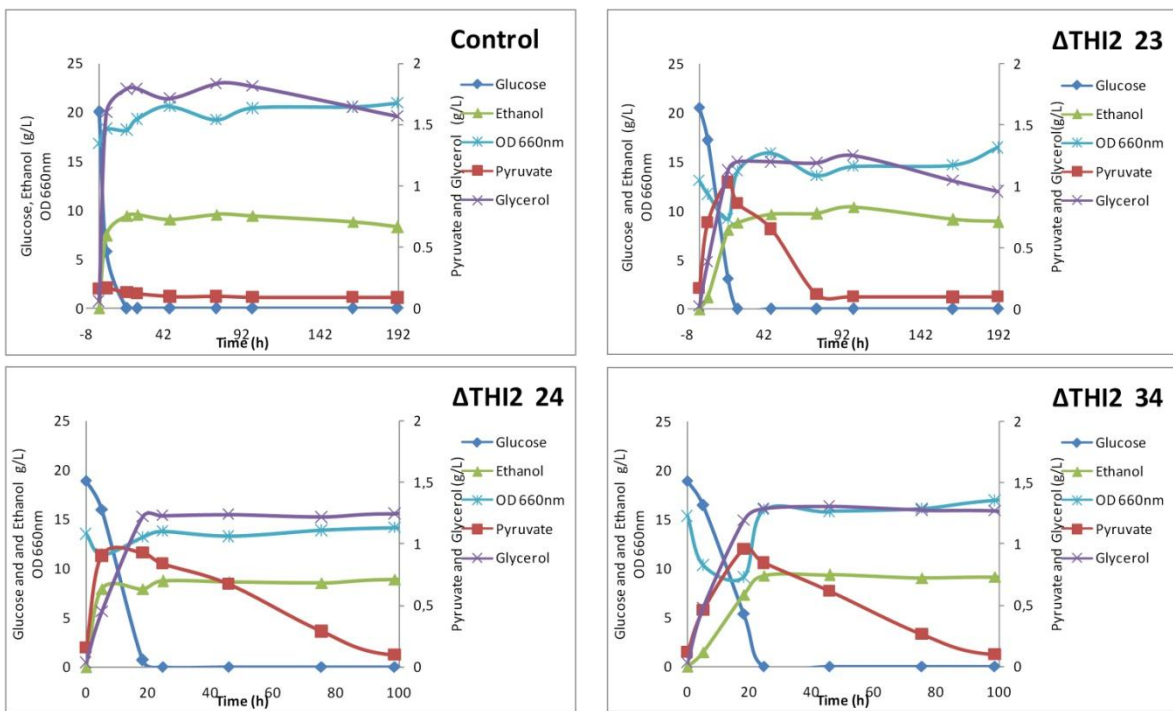


Figure 38- Anaerobic fermentation of Δ THI2 colonies in Verdun medium pre-grown in medium containing 0,05 μ M of thiamine.